The impact of energy availability and substrate complexity on anaerobic microbial communities in marine sediment

Thesis by

Sujung Lim

In Partial Fulfillment of the Requirements for the

degree of

Doctor of Philosophy

CALIFORNIA INSTITUTE OF TECHNOLOGY

Pasadena, California

2024

(Defended 12 March 2024)

Sujung Lim
ORCID: 0000-0001-6040-729X

ACKNOWLEDGEMENTS

My greatest thanks to past and present Orphan lab members who have made my journey at Caltech so memorable through so many late nights in lab, onboard, outside. I have found my interactions with you all not just to be incredibly intellectually fulfilling, but also just plain fun. There are too many names to list here but I'd like to call out the people who have provided edits, draft review, and manuscript assistance — especially Ranjani Murali, Daan Speth, Alon Philosoph, and Dan Utter — you have been critical to helping me put the content in my head (and lab notebook) onto the page. Thank you as well to Nathan Dalleska for the entertaining conversation and troubleshooting help during the many hours of instrument time I've spent at the WEL. Special thanks to my advisor, Victoria Orphan, who has provided me with so many incredible opportunities to go out into the field and, through much insightful commentary, was fundamental to my ability to grow as a scientist. Thank you to Alex Sessions for being a great voice of reason, letting me audit your wonderfully informative Organic Geochemistry class, and additionally chairing my committee. I would also like to thank Jared Leadbetter for many enlightening conversations about microbes, music, and driving; TAing Microbial Physiology was a great experience. And thank you to Woody Fischer for leading Geobiology Reading Group and your enthusiasm for all things geobiological. Additional, and no smaller number of, thanks go to my family and friends — both at Caltech and farther afield — who have supported me throughout my time as a graduate student. Thank you. I wouldn't be here without all of you.

ABSTRACT

This thesis probes the interplay of organic matter complexity (Chapters 1 and 2) and local redox gradients (Chapter 3) with the community structure and function of the anaerobic marine sediment microbiome. Deep marine sediments, despite being generally organic-poor, harbor a vast diversity of microorganisms that are critical to the global nutrient cycle. Transient nutrient inputs such as whale falls result in hotspots of microbial community activity in an environment that normally processes heavily degraded organic material from the upper ocean. These organic loading events result in transitions down redox gradients and dynamic shifts in the local energy availability of the microbial communities. Through in situ seafloor and laboratory microcosm experiments, we provide insights into the impact of energy availability and carbon complexity on maintaining hierarchical and complex community interactions, community activity, and systematic and functional diversity.

TABLE OF CONTENTS

LIST OF ILLUSTRATIONS AND/OR TABLES

Chapter 1 *Page*

Chapter 2 *Page*

Chapter 3 *Page*

Introduction

Marine sediments are critical to global nutrient cycling and harbor a diverse, numerically abundant microbiome. Sudden carbon loading events, e.g., whale falls or plankton blooms, cause perturbations to the sediment microbiome and can result in dynamic geochemical shifts. Because they are as widely distributed as the oceans above them, the marine sediment ecosystem response can have global-scale effects ranging from shifts in oceanic productivity to changes in greenhouse gas production. Volumetrically, most of the marine subsurface is anoxic due to the rapid exhaustion of oxygen in the water column or upper sediments. Thus, anaerobic processes carried out by subsurface microbial communities largely determine the fate of carbon in marine sediments. This thesis explores the response of the sediment microbial community to anaerobic energy gradients, either as a factor of carbon complexity (Chapter 1 and 2) or energy availability in the respiratory substrate (Chapter 3), and puts these findings into context with regard to ecological theory.

The seafloor is not static. Marine sediments are subject to changes in the depositional environment by factors such as riverine input, turbulent flow, upwelling, and others (Arzayus & Canuel, 2005; Caffrey et al., 2010; Dagg et al., 2004) resulting in dynamic shifts in energy availability on multiple timescales from diel to seasonal to annual. Organic material input to the typically electron donor-poor, dark, cold conditions results in a transition from the oxic environment at the sediment-water interface to electron acceptors of a lower midpoint potential. Anaerobic processes then become responsible for carbon degradation, driven by

the energy available in the organic matter degradation coupled to the respiration of terminal electron acceptors such as the sulfate and nitrate in seawater. The contribution of these anaerobic processes, such as sulfate reduction, to carbon mineralization in sediments is estimated to be, per mass of carbon, quantitatively equivalent to the contribution of the much higher energy aerobic metabolism (Canfield, 1989; Jørgensen, 1982).

Methanogenic archaea and sulfate-reducing bacteria are important terminal members in the anaerobic degradation of organic matter in the marine regime despite their use of relatively poor, low potential electron acceptors such as carbon dioxide or sulfate. In the absence of sulfate, some sulfate reducers and taxonomically related organisms in the phylum Desulfobacterota also form syntrophic partnerships with methanogenic archaea. They do so by producing substrates such as hydrogen and formate that would normally be oxidized coupled with sulfate reduction. These syntrophies are only energetically feasible if hydrogen and formate are kept at low enough concentrations (Bryant, 1979; Hoehler et al., 1998). Methanogenic archaea have a high affinity for hydrogen and are able to maintain that low — near 40 nM — concentration (Schink, 1997), which allows the net metabolic reaction to proceed. An additional level of complexity is added to these trophic interactions in that neither methanogens nor sulfate reducers are known to utilize complex organic substrates: the former is only able to use methylated compounds, acetate, or carbon dioxide, and the latter is usually restricted to small fatty acids and primary alcohols (Schink, 1997). Thus, in the context of the complex forms of allochthonous carbon reaching the sediment, these terminal respirers are reliant on upstream processes of carbon degradation, usually via

fermentative heterotrophs, to degrade complex carbon into useful reductants. These include simpler carbon substrates that are available to downstream primary or secondary syntrophic members or to terminal respirers. However, the succession of metabolic handoffs between the primary and terminal members in these communities can be complex and not just tied to the direct processing of carbon. For example, the stimulation of primary degraders through sulfate reducer-mediated production of secondary metabolites such as thioredoxins has been observed to occur in an anaerobic chitin-degrading consortium (Pel & Gottschal, 1989).

Such interactions between microbial community members — syntrophy or other metabolic cascades and nutrient auxotrophy — contribute to the maintenance of community structure, here defined as the combination of the alpha diversity of taxonomic units and diversity of functions. While alpha diversity metrics such as species richness or evenness are insufficient as predictors of overall top-down community function, e.g., the degradation of input complex organic matter, they are nonetheless useful in conjunction with other assessments of community structure such as co-occurrence network analysis (Fuhrman, 2009; Shade, 2017). Quantifying community structure is also useful as a means to move beyond descriptive observations towards tracking communities' responses to natural or artificial perturbation, on a variety of timescales (Brown et al., 2024; Friedman et al., 2017; Fuhrman, 2009).

In the past, the microbial aspect of the post-disturbance community response was assumed to be trivial so was omitted from resource models studying ecological disturbances (after Allison & Martiny, 2008). However, more recent work has shown microbial community

composition and the distribution of functions are both sensitive to disturbance. Given their importance in nutrient cycling, it is critical to assess their ability to withstand changes to their environment ("resistance") and to recover back to the initial state ("resilience") (Chaer et al., 2009; Griffiths & Philippot, 2013; S.-H. Lee et al., 2017; Turkarslan et al., 2017). Moreover, the ability of the sediment microbiome to recover from perturbation is particularly relevant given increased anthropogenic impacts (Nogales et al., 2011). Some factors that have been suggested to contribute to community resistance and resilience include functional redundancy, the maintenance of the rare biosphere, and interactions — positive and negative — between members (Girvan et al., 2005; Griffiths & Philippot, 2013; Jousset et al., 2017). Many of these factors are interrelated; for example, a species abundance distribution with a long tail indicates many discrete rare members, which also is coincident with higher species richness. High functional redundancy (defined here as certain broad functions, e.g., the terminal respiratory process or primary degradation of complex polymers, occurring in multiple community members) can additionally be overlaid onto alpha diversity metrics to assess its role in metering the community response. While increased diversity has been shown to contribute to community stability due to the wider distribution of functions in some systems (Girvan et al., 2005; Xun et al., 2021), the relationship of community interactions to ecosystem stability after a disturbance event is not as clear.

Whale falls are a standout example of a disturbance to the seafloor community. Nearly 70,000 whales are estimated to die every year, and their density causes them to sink rapidly through the water column to rest on the seafloor, where they cause rapid successional events

in the local macrofaunal and microbial ecology. Their massive size provides an incredible influx of organic material to the local seafloor environment corresponding to as much as 2000 years of marine snow (C. R. Smith & Baco, 2003). This huge carbon pulse rapidly results in local anoxia at the sediment bed and, post-scavenger, the "sulphophilic" phase begins (C. R. Smith & Baco, 2003). This is characterized by the proliferation of sulfate-reducing bacteria producing sulfide which can then be utilized by sulfide-oxidizers at the sediment-water interface and can manifest macroscopically as a mat. After the initial release of organic matter to the sediment, the more recalcitrant lipid-rich bones of the whale are degraded by the polychaete worm *Osedax* in conjunction with bacterial endosymbionts (Goffredi et al., 2005). This slower release of carbon to the surrounding sediment results in subsequent shifts in community structure that last for years to decades (Goffredi & Orphan, 2010). A diverse suite of sulfate-reducers, both those capable of complete oxidation of their substrates to carbon dioxide and those incomplete oxidizers that stop the catabolic process at acetate, have been demonstrated to actively respond to these influxes of oxidizable carbon (Goffredi & Orphan, 2010). Additionally, other low energy terminal respirers that proliferate in these systems include methanogenic clades such as *Methanogenium* and *Methanococcoides*, microbes which are at low abundance in background sediments (Goffredi et al., 2008). Even after the majority of the available carbon has been utilized, the large bones still remain and act as a reef system that can recruit assemblages of macrobenthos such as amphipods or other arthropods. Despite a previous report suggesting that no trace of the carcass would remain after a decade due to biotic degradation and the sedimentation rate

(Lundsten et al., 2010), it is clear that the bones still remained nearly two decades post-emplacement. This reef system can further allow for the localized input of organic material such as chitin from arthropod molts and excreta directly to the seafloor.

Chitin represents another important form of carbon input in the ocean, as it is among the most abundant biopolymers produced in the oceans, with 10^{10} metric tons produced annually by diatoms, molluscs, and crustaceans (Durkin et al., 2009; Gooday, 1990; Souza et al., 2011). It consists of cross-linked N-acetylglucosamine moieties and is a major component of marine snow (Bochdansky & Herndl, 1992). It is insoluble and moderately recalcitrant, but does not bioaccumulate due to complete mineralization in the water column and in sediment (Poulicek & Jeuniaux, 1991). In conjunction with the massive amount that is produced annually, chitin's nearly complete turnover — it does not accrue in marine sediment — renders it an important contributor to marine nitrogen cycles. While aerobic chitin degradation can be mediated by a single organism (e.g., Osawa & Koga, 1995), its complex nature requires trophic interactions for complete degradation in anaerobic, low-energy environments. These metabolic interdependencies are then hypothesized to contribute to the maintenance of community structure in anaerobic sediments.

In this work, we examined the response to organic carbon complexity and terminal electron acceptor manipulation on anaerobic microbial community structure and activity at a former whale fall site (Lundsten et al., 2010). Though it had been decades since the initial organic loading event, the community still retained the "memory" of the priming effect. In order to assess the effect of the complexity of organic carbon, we used the insoluble polymer chitin

and its soluble monomer N-acetylglucosamine in our in situ and laboratory whale fall sediment incubation experiments. The stimulation of the activity of low-potential respirers such as methanogens and sulfate-reducing bacteria in response to complex carbon has been previously reported from diverse environments including freshwater sediments, anaerobic digesters, the human gut microbiome, and acid mine drainage (Chassard et al., 2010; Rodrigues et al., 2019; Rojas et al., 2021; Xu et al., 2024). Chapters 1 and 3 provide further support for the stimulation of methanogens — here in permanently cold, deep sea sediments — by complex carbon as assessed by functional potential and taxonomic signal. These chapters additionally discuss the competitive and cooperative interactions of these low-potential respirers with other community members.

Previous work studying the impact of complex organic loading on environmental systems has been restricted to aerobic incubations, freshwater environments, or the pelagic water column (Bienhold et al., 2012; Q. Chen et al., 2022; Hoffmann et al., 2017; Rodrigues et al., 2019; Rojas et al., 2021; Wörner & Pester, 2019). Anaerobic deep sea sediments are less well studied, despite their importance, representing nearly 2/3 of the planet's surface. Chapter 2 of this thesis addresses this gap, comparing and contrasting the patterns of activity and community structure seen over time in both in situ and ex situ microcosm incubations. These parallel incubations were amended with activity tracers and chitin or GlcNAc, enabling a better understanding of the impact of incubation in the laboratory versus on the deep sea floor.

The major microbial ecosystem responses addressed in this thesis involve shifts in community structure and function investigated in terms of community composition, the distribution of members, and distribution of functions; all of these facets are expected to be modified by environmental conditions and may be interrelated. For example, microbial community composition is thought to be tuned by the three axes of dispersal, drift, and selection (Fuhrman, 2009; Milke et al., 2022; Philippot et al., 2021; Vellend, 2010). These stochastic and deterministic influences additionally feedback to intermicrobial interactions within the community, resulting in further changes to e.g., functional distribution or diversity. Disentangling the drivers of microbial ecosystem functioning is further complicated by the uncertainty surrounding the applicability of concepts from classical ecology to microbial ecology. Studies addressing such questions and attempting to discern overarching themes from the many, frequently contradictory, disparate single-treatment effects have recently proliferated (Chaer et al., 2009; Finke & Snyder, 2008; Girvan et al., 2005; Goldford et al., 2018; Konopka et al., 2015; Marsland et al., 2019; Shade, 2018). These studies often address more tractable systems, e.g., defined cocultures, resource modeling, or aerobic environments; we supplement the current body of knowledge through our highly replicated anaerobic and psychrophilic microcosm approach (Chapters 1 and 3). These microcosms were inoculated by serial dilutions of marine sediment, which was expected to result in the winnowing of the community to, perhaps, a minimized set of core functions. Instead, we observed a maintenance of complex interactions that highlights the irreducibility of the community, in contrast to prior reports in soil that have shown a dilution-based decrease in members

carrying out specialized metabolic functions (McClure et al., 2020; Xun et al., 2021). This trend could be due to particle association, consistent with other spatially heterogeneous systems (Probandt et al., 2018), and would not necessarily be observable in planktonic culture or in defined coculture microcosms.

During the anaerobic degradation process, marine sediments are thought to go down the "thermodynamic ladder" of available electron acceptors in order of decreasing midpoint potential from nitrate to CO_2 (Bethke et al., 2011; LaRowe & Van Cappellen, 2011). These shifting environmental redox conditions necessarily result in differential free energy present in the system, and transitions between these gradients have been shown to promote dynamic changes in both the microbial community and the geochemical environment (Blodau & Knorr, 2006; Dick et al., 2019; Graw et al., 2018). Additionally, insoluble electron acceptors such as Fe_2O_3 or MnO_2 have energetics that are driven by surface area and the activity of their soluble reduction products (LaRowe & Van Cappellen, 2011); here, the inherent spatial structure of an insoluble substrate can contribute to community structure through niche partitioning.

Through addressing the specific ecological and ecophysiological underpinnings surrounding the community response to energy availability, this thesis hopes to provide insight into the nature of the anaerobic marine sediment biosphere and the factors that contribute to the maintenance of microbial community structure in these low-energy environments.

Chapter 1

ACTIVITY AND DIVERSITY OF SULFATE AND METHANE-BASED PATHWAYS OF ANAEROBIC CARBON RESPIRATION IN MARINE SEDIMENTS IS CORRELATED WITH CARBON COMPLEXITY

Sujung Lim[1], Ranjani Murali[2], Daan R. Speth[2§], Rachel E. Szabo[3], Otto X. Cordero[3], Victoria J. Orphan[1,2]

[1] Division of Geological and Planetary Sciences, Caltech, Pasadena, CA 91125
[2] Division of Biology and Biological Engineering, Caltech, Pasadena, CA 91125
[3] Department of Civil and Environmental Engineering, Massachusetts Institute of Technology, Cambridge, MA 02139
[§] present address: Division of Microbial Ecology, Centre for Microbiology and Environmental Systems Science, University of Vienna, Vienna, Austria

ABSTRACT

Sulfate reduction is estimated to account for half of the organic carbon respiration in anoxic organic-rich ocean sediments; however, sulfate reducing bacteria tend to only be able to oxidize simple carbon compounds such as primary alcohols or small fatty acids. Much of the organic input to the seafloor is complex, resulting in trophic interactions between groups of terminal respirers such as sulfate reducing microorganisms and primary degraders that can catalyze the first step of complex organic carbon remineralization. To determine how these trophic interactions structure the sediment microbiome, we used chitin, an abundant complex biopolymer, and its monomer N-acetylglucosamine as substrates in highly replicated multi-month time course microcosm experiments in serial dilution to independently track the effect

on the initial sediment inoculum. By using geochemical analysis of metabolites with 16S rRNA gene amplicon and metagenomic sequencing, we demonstrate the impact of carbon complexity on community metabolic processes, community structure, and the maintenance of functional redundancy. Here, complex carbon promotes the dynamic turnover, diversity, and maintenance of rare community members, especially terminal respirers, that then assemble in robust functional guilds.

INTRODUCTION

As much as half of organic matter biotically degraded in marine sediments is estimated to occur through sulfate reduction. With estimated fluxes of up to 11 Tmol sulfate reduced per year, biological sulfate reduction represents the dominant respiratory process in global ocean sediments (Bowles et al., 2014; Canfield, 1989). Microbial ecological surveys indicate that sulfate-reducing microorganisms dominate organic-rich sediments with as much as 85% abundance (Jochum et al., 2017; Leloup et al., 2009; Sahm et al., 1999). The conventional understanding is that organic matter breakdown in anaerobic systems is coupled to a downward cascade through redox gradients as available oxidants are depleted in thermodynamic order (Graw et al., 2018). In the oceans, sulfate is the dominant anaerobic terminal electron acceptor; once it is exhausted, methanogenesis is the next major respiratory process.

However, organic matter present in sediments is frequently complex, polymeric, and/or aromatic and is not degradable by the vast majority of sulfate-reducing microbes or methanogens. These low-energy respirers then need to rely on upstream processes such as

exoenzyme production by fermenting heterotrophs that can yield the simple fatty acids and alcohols needed for their growth.

The aminopolysaccharide chitin ($[C_8H_{15}NO_6]_n$) is an important constituent of complex particulate organic matter in marine environments. As one of the most abundant biopolymers in the ocean, it is a major contributor to global carbon and nitrogen cycles with an estimated annual production of over 10^{13} kg (Souza et al., 2011). The carapaces of copepods, crabs, and shrimp are commonly recognized as the major donor sources of chitin in the ocean, but its production encompasses all trophic levels as it is also synthesized by phototrophic diatoms (Durkin et al., 2009; Gooday, 1990). Chitin has been found to be a major component of marine snow, with much of it mineralized aerobically during transit to the seafloor through the oxic water column (Aluwihare et al., 2005; Jiang et al., 2022). As such, most environmental microcosm studies have examined the impact of chitin on aerobic communities (Hoffmann et al., 2017; Kanzog et al., 2008). Less is known about anaerobic degradation of chitin in marine sediment; in deep sea productivity hotspots like whale falls, crustaceans and other macrofauna with chitinous exoskeletons tend to congregate (C. R. Smith & Baco, 2003), resulting in localized deposition of chitin to the seafloor.

Anaerobic chitin degradation studies in the laboratory have identified the following major steps. Primary chitin degraders, likely fermenters in anaerobic environments, produce exoenzymes allowing the initial cleavage of the chitin polymer to oligomeric forms (Beier & Bertilsson, 2013). Chitin cleavage is followed by degradation of oligomers, including the monomer N-acetylglucosamine (GlcNAc), by primary and secondary chitin degraders.

Because GlcNAc is part of the bacterial cell wall, genes for its assimilation and utilization are widespread in prokaryotes. In anaerobic environments, secondary degraders produce organic acids and primary alcohols which are available to the terminal respirers, in this case, either sulfate reducers or methanogens (Jørgensen, 1982; Pelikan et al., 2021). Marine sediment ecosystems represent one of the most taxonomically diverse after terrestrial soils, providing many potential interactions within their microbial communities (Probandt et al., 2018; Shaffer et al., 2022; Thompson et al., 2017). These interactions, as observed through the lens of the relationship between microbial community structure and net biogeochemical activity, appear to be promoted more by functional groups than taxonomic membership (Goldford et al., 2018; Louca et al., 2018; Matthews et al., 2021; Tully et al., 2018). This suggests that different species that share function could readily substitute for each other within an ecosystem ("functional redundancy"), making it less likely that communities degrading chitin and GlcNAc are composed of a fixed set of core taxa. 16S rRNA gene-based diversity surveys and metagenomic analysis indicate a high level of predicted functional redundancy among sulfate-reducing bacteria and methanogens in marine sediments (Kleindienst et al., 2012; Leloup et al., 2009; Y. Zhang et al., 2017). The contribution of functional redundancy to the maintenance of community structure and performance in anaerobic deep sea microbial communities that necessarily require higher order interactions for complete degradation of complex organic matter is still unclear, however. Prior work suggests that a diffuse correlation network that contains multiple layers of nodes (members) and edges (interactions) may contribute to driving the relationship

between this assessment of community interactions and the overall community response (Embree et al., 2015; Philippot et al., 2021).

Moreover, rare biosphere members — those that are less than 0.1% abundance — can have an outsized impact, providing key metabolic functions and allowing communities to remain resistant to perturbations while being maintained stably in their local environment (Fuhrman, 2009; Lennon & Jones, 2011; Pascoal et al., 2021; Sogin et al., 2006). For example, while sulfate-reducing bacteria are abundant in marine sediments, they are often scarce in terrestrial freshwater systems. Despite this scarcity, they are responsible for high rates of sulfate reduction and carbon mineralization. In freshwater peatland systems, specific taxa of sulfate reducing bacteria contribute as much as 10.8% of the sulfate reduction rate despite only being at 0.006% native relative abundance (Hausmann et al., 2016; Jousset et al., 2017; Pester et al., 2010). Therefore, considering the apparent functional redundancy of multiple rare taxa of sulfate reducers or other terminal respirers may have important implications on overall ecosystem function and, more broadly, environmental impact.

Here, we tested the impact of organic matter complexity on marine sediment microbial communities over time, using microcosm incubations established using serially diluted deep sea sediment from a former whale fall site. The design of our seven-month experiment enabled us to examine the fundamental roles of community structure and functional redundancy in metabolic guilds during the breakdown of the complex polymer chitin and its constituent monomer GlcNAc. Community surveys within these microcosms provided us a readout on the abundance and diversity of key metabolic guilds while simultaneously

allowing us to observe the effect of a dilution-based falloff of rare biosphere members on community performance. Because the inoculum was sourced from an older whale fall site (emplacement in October 2004), the host microbial communities were primed with a large pulse of organic material in the past; the microbial response to organic loading can nonetheless persist over many years (Braby et al., 2007; Goffredi & Orphan, 2010). To reflect the low-temperature, low-energy regime on the seafloor, this experiment was carried out under psychrophilic and anaerobic conditions. Nondestructive sampling over a timecourse provided us the ability to follow the trajectory of metabolic potential and geochemical changes over the degradation of differentially complex carbon substrates. These microcosms were highly replicated, allowing us to disentangle stochastic effects caused by sediment heterogeneity from an actual signal of community structure.

RESULTS

To examine the microbial community potential for the anaerobic degradation of the insoluble polymer chitin and its monomer GlcNAc, we established replicated microcosm experiments using serially diluted sediment inoculum from a 6-9 cm depth horizon at a previously described whale fall site in the Monterey Submarine Canyon, CA, USA at 1018 m water depth ('Whale 1018'; Braby et al., 2007). These incubations were conducted anoxically at 10 °C in 96-well plates with eight dilution steps and twelve replicates per amendment (chitin, GlcNAc, and no amendment). The initial dilution step of the inoculum was a tenfold dilution of a 1:1 sediment slurry resulting in sediment dilutions from $5x10^{-2}$ to $5x10^{-9}$. This study

focused on a subset of dilutions and replicates following preliminary unpublished data indicating metabolic transitions at intermediate levels of dilution; all 12 replicates from $5x10^{-5}$ to $5x10^{-7}$ and four replicates from $5x10^{-8}$ (henceforth described as dilution 1 to dilution 4 in order of ascending dilution) were analyzed (Fig. 1). We assessed the effect of treatment, incubation time, and dilution on microbial community structure and function by 1) measurement of respiration of the provided substrate, 2) 16S rRNA gene sequence-based analysis of the change in community membership and structure, and 3) metabolic gene mining of metagenomic sequences to assess the functional redundancy of sulfate-reducing bacteria and methanogenic archaea.

1. Geochemical proxies for microbial GlcNAc and chitin degradation

1.1 Metabolite production and sulfate drawdown in incubations allude to temporal and substrate-dependent dynamics in the carbon breakdown process

Chitin is an insoluble polymer, making it difficult to measure the top-down process of chitin degradation directly. We instead followed the accumulation of ammonium and acetate, the previously reported breakdown products of chitin and monomer GlcNAc, as a proxy for their degradation (Beier & Bertilsson, 2013; Jiang et al., 2022). According to the following predicted stoichiometry of three moles acetate, one mole ammonium, and eight reducing equivalents, GlcNAc oxidation is assumed to be coupled with equimolar amounts of sulfate reduction as the terminal respiratory process in these incubations. This results in

the theoretical production of three moles acetate per mole ammonium and a loss of one mole sulfate per overall community reaction (hypothesized total reaction, Eqn. 1).

$$C_8H_{15}NO_6 + 2H_2O + SO_4^{2-} \rightarrow 3CH_3COO^- + NH_4^+ + 3H^+ + 2HCO_3^- + HS^- \quad (1)$$

Using this idealized equation, we tracked the progression of chitin or GlcNAc oxidation with increasing dilution of the initial sediment inoculum over the course of seven months; the 3:1 acetate:ammonium ratio is expected to change over time as secondary processes (e.g., acetate oxidation) occur. Indeed, we observed accumulation of these products in our incubations at a greater concentration than was seen in the context geochemistry of the source inoculum (Supp. Fig 1).

Ammonium utilization in these incubations is expected to be largely tied to anabolism and drawdown occurs at a lower rate than catabolism of the other GlcNAc metabolic product, acetate. For this reason, the carbon degradation activity of the GlcNAc and chitin-amended samples can be proxied by ammonium accumulation. We chose an activity threshold based on accumulation of the hypothesized metabolites acetate or ammonium above 0.5 mM or the utilization of sulfate below a measured concentration of 4.2 mM using the inflection points of metabolite concentration in an empirical cumulative density function plot (Supp. Fig. 2). In GlcNAc treatments, 60% of samples in dilutions 1-4 (69/115) met this activity threshold; these had a mean acetate:ammonium ratio that increased to above the expected stoichiometry across dilutions for the first two time points (one month: 2.52:1, SD 1.6, n=37; three months: 3.63:1, SD 2.15, n=21) (Fig. 2a, middle row). This average ratio decreased back to 2.52:1 (SD 1.650) after seven months (n=29); a decrease likely attributed to acetate utilization.

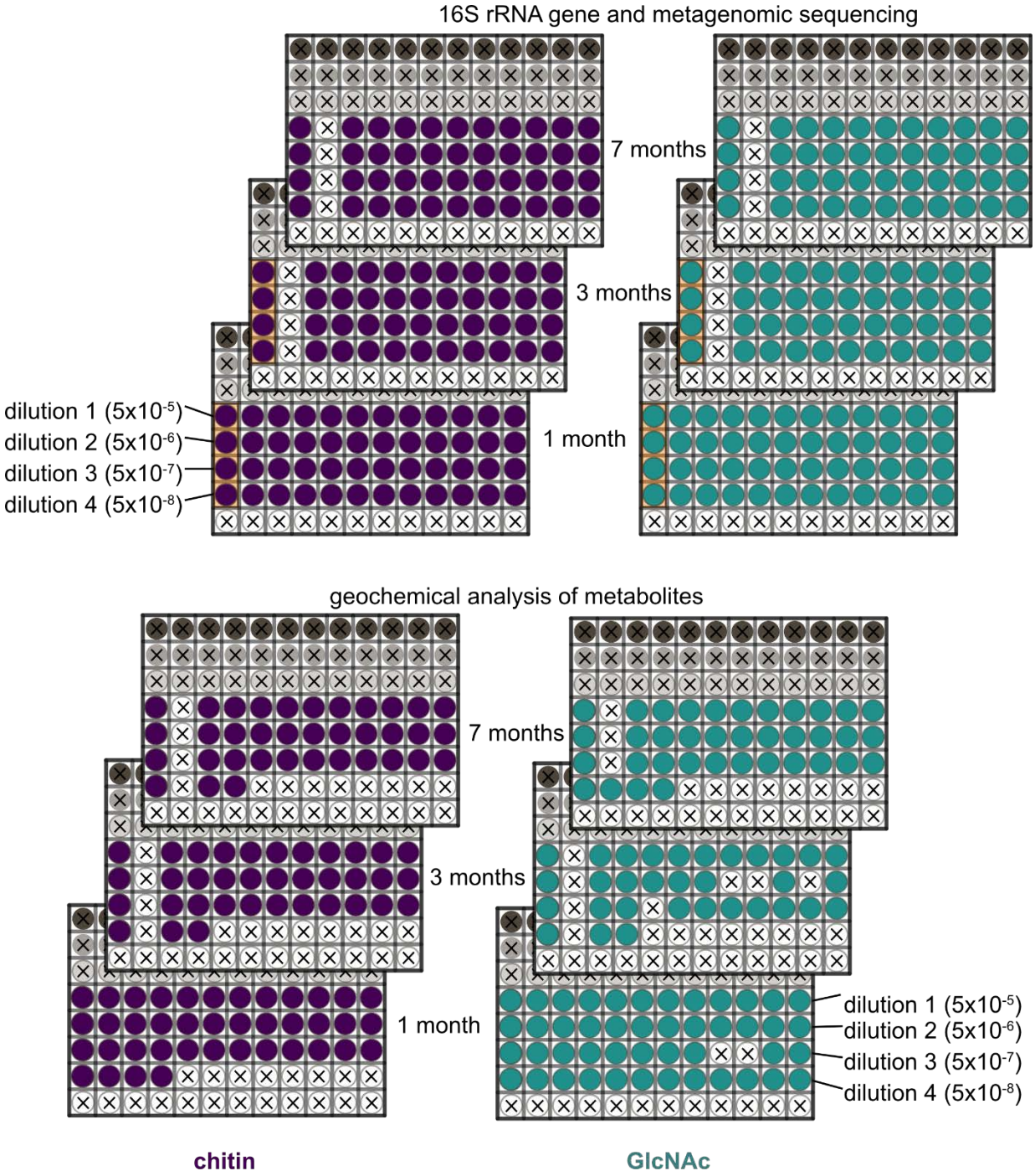

Figure 1. Experimental diagram and sampling processing scheme for 16S rRNA gene amplicon sequencing (top, filled wells), metagenomic sequencing (top, orange highlights), and geochemical analysis of metabolites acetate, ammonium, and sulfate (bottom, filled wells).

Notably, some GlcNAc-amended replicates (n=3) showed active carbon metabolism uncoupled to a stoichiometric amount of sulfate drawdown by the final time point with millimolar amounts of ammonium accumulation and a lack of total sulfate utilization (Fig. 2a, middle row, right). Although sulfate was largely exhausted in most active wells by three months, acetate continued to decrease until seven months (Fig. 2b), suggesting a syntrophic or methanogenic sink. Serial dilution of the starting sediment had a significant impact on activity in the GlcNAc incubations. While ~19% of all measured wells consumed 50% or greater (>2.5 mM) sulfate by the first month, the distribution of sulfate drawdown was skewed to lower dilutions. Specifically, by the final time point, 11/15 of the replicates with the most diluted inoculum (dilutions 3 and 4) did not show significant sulfate loss (Fig. 2b). This was suggestive of either loss of active sulfate reducers or, alternatively, other taxa required for GlcNAc utilization at high sediment dilution.

Chitin-amended incubations contained fewer active samples, with 50% of samples meeting our activity threshold; these active incubations were heavily weighted to the two lowest dilutions ($5x10^{-5}$, $5x10^{-6}$) and additionally exhibited a strong shift in the ratio of metabolic products over time (Fig. 2a, top row). At the earliest time point, the average acetate:ammonium ratio for active samples was 2.21:1 (SD 2.20, n=29), indicating either early acetate consumption or an alternative pathway (Fig. 2a, top row, left). The high standard deviation reflected the variability within these microcosms with some samples that accumulated low concentrations of ammonium (<1 mM) with higher relative levels of acetate. In contrast, all 19 microcosm incubations that accumulated moderate to high

amounts of ammonium (>1 mM) produced significantly more ammonium relative to acetate than the predicted 3:1 stoichiometric ratio (average acetate:ammonium = 1.05:1, SD 0.31). Very high amounts of ammonium were produced from chitin and appeared decoupled from sulfate reduction. In contrast to GlcNAc incubations, there was little to no sulfate drawdown within the first month, with sulfate drawdown increasing in the three-month time point. By the 7-month time point, at least 14 out of 40 incubations exhibited > 0.5 mM sulfate utilization. This time lag in sulfate reducing activity was consistent with limited accessibility and slower degradation of the insoluble polymeric electron donor. 83% of samples from dilutions 1 and 2 (10/12) with greater than 5 mM ammonium used less than 1 mM sulfate (Fig. 2a, top row, left). These temporal activity patterns suggest the potential involvement of additional processes beyond simple cleavage to the GlcNAc monomer and subsequent secondary oxidation; for example, production of nonionic metabolites such as ethanol (proposed metabolic reaction, Eqn. 2) in lieu of acetate. Acetate drawdown by other community members or acetoclastic methanogens could also explain the deviation from the predicted 3:1 stoichiometry. We did not test for ethanol but small fatty acid metabolites such as propionate or butyrate were not detected in the microcosms.

$$[GlcNAc]_n \rightarrow GlcNAc + 4H_2O \rightarrow CH_3COO^- + NH_4^+ + 2CH_3CH_2OH + 2H^+ + 2HCO_3^- \quad (2)$$

In the last two time points, the acetate:ammonium ratio in active chitin-amended incubations increased to near or above the expected value. By three months, these incubations reached a ratio of 4.43:1 (SD 2.95, n=14), which finally decreased to near 3:1 at seven months (3.75:1, SD 3.18, n=15) (Figure 2a, top row). Ammonium also was utilized to a greater extent than

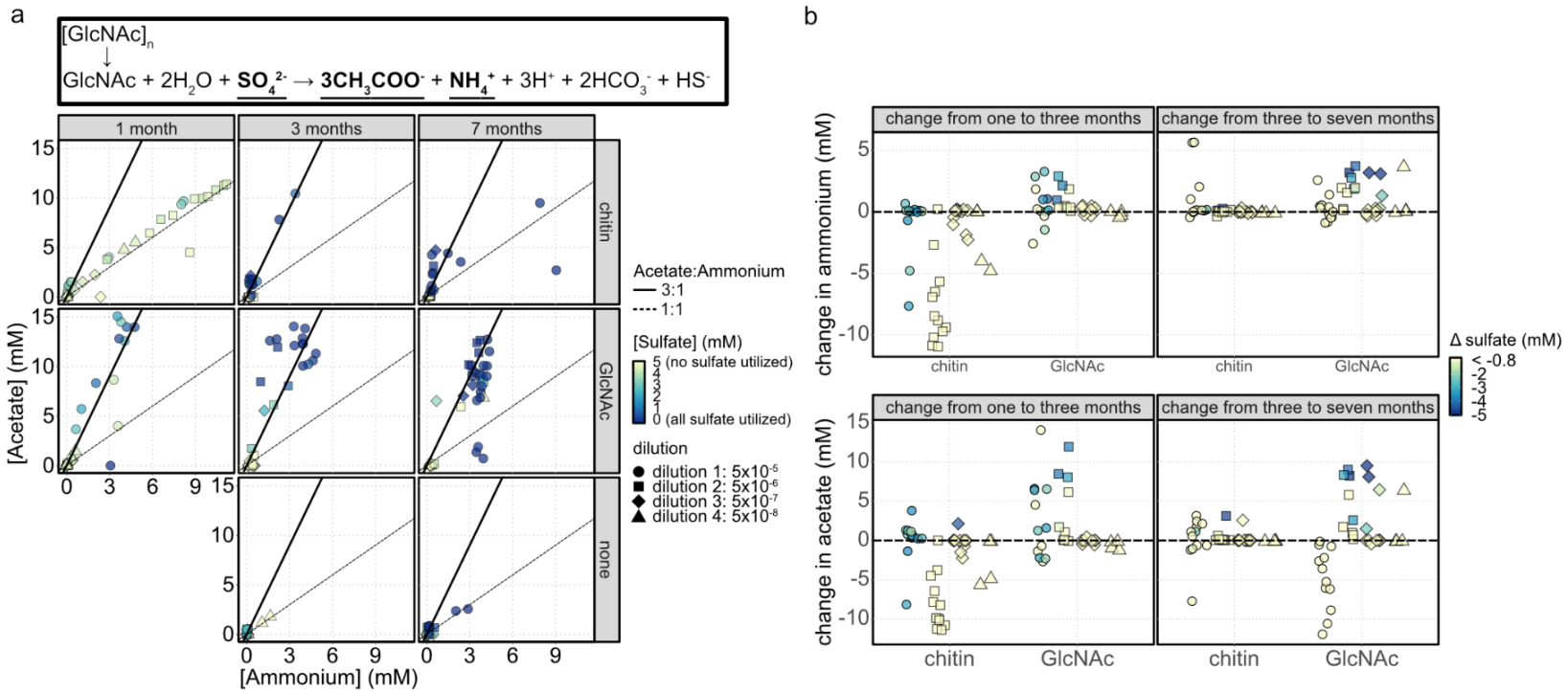

Figure 2. Patterns in metabolic output in 96-well incubations. (a) The bulk ratio of metabolic end products of a subset of dilutions (represented by point shape) and replicates demonstrates a temporal shift in the stoichiometric balance between ammonium and acetate. Catabolic processes would affect sulfate (color) and acetate concentration. The 3:1 line (solid line) denotes the ratio of acetate to ammonium if all of the carbon substrate is fermented or oxidized to acetate according to the hypothetical reaction, listed above and in equation 1. Early chitin-degrading incubations exhibit an equimolar amount of excreted ammonium and acetate (dashed line) The initial metabolite concentration in the media was 0 mM for acetate and ammonium, and 5 mM for sulfate. (b) Difference plots of acetate and ammonium concentration displaying change in metabolites between the first two (one month to three months) and last two (three months to seven months) time points over dilution (shape). The horizontal line represents no change between time points, and shading represents differential sulfate concentration between the time points beginning at our activity threshold of 0.8 mM sulfate utilization.

expected between the three- and seven-month time points (Fig. 2b, top) and this drawdown could have contributed to the elevated acetate:ammonium ratios we observed. Both GlcNAc- and chitin-amended incubation sets were highly active in the last six months of the experiment. These activity patterns were in agreement with the overall trend of sulfate drawdown; with the exception of two samples in the GlcNAc treatment, the maximum extent of acetate and ammonium accumulation occurred with complete to near-complete sulfate utilization in both amendments (Fig. 2a).

Incubations that were not supplied an external carbon source showed some evidence of metabolic activity with endogenous organic carbon degraded to acetate and ammonium even after a three-month incubation and even at the highest dilution (dilution 4) (Fig. 2a, bottom row), where very little carryover of sediment from the initial inoculum is expected. The samples using endogenous carbon rather than supplied GlcNAc or chitin did not produce acetate or ammonium at values close to the 3:1 predicted stoichiometry for GlcNAc degradation. The degradation of this endogenous carbon is coupled to sulfate drawdown only at the final time point, with both samples accumulating above-average ammonium (0.23 mM) and completely consuming sulfate.

1.2. Dilution has a pronounced effect on the metabolic response to the GlcNAc- and chitin-amended incubations

We observed a strong shift in activity related to sediment dilution when tracking the trajectory of each GlcNAc treatment replicate over time from dilutions 1-4. The lowest

measured dilution ($5x10^{-5}$) exhibited strong acetate drawdown while higher dilutions accumulated up to 10 mM acetate between the three and seven-month time points. The trajectory of ammonium concentration per replicate was more heterogeneous but on average ammonium concentration increased over the last two time points (Fig. 2b, top), consistent with continued degradation of the provided substrate.

In chitin-amended incubations, sulfate reducers in the high dilution samples appeared to have only a modest amount of activity. This is in contrast with the initially highly active acetate and ammonium production followed by an eventual drawdown; this rise and fall behavior occurred in all dilutions except dilution 1 ($5x10^{-5}$) between the first two time points (1-3 months). Both metabolites then accumulated between the last two time points (3-7 months), indicating a shift in community behavior at three months (Fig. 2b**)**. Chitin treatments exhibited sporadic heterogeneous "jackpots" of microbial activity at higher dilutions with the resulting ammonium and acetate then metabolized over time; four out of the twelve dilution 3 samples produced either measured metabolite above the threshold 0.25 mM concentration by the first time point; by the final time point, only one replicate has accumulated acetate or ammonium (4.7 mM acetate, 0.6 mM ammonium). That single replicate at dilution 3 ($5x10^{-7}$) with high metabolite accumulation did so in conjunction with nearly complete sulfate utilization. A different pattern emerged at dilution 4, where there was high ammonium and acetate production (>4 mM) decoupled to sulfate utilization in two of the four measured samples at the one-month time point. Both metabolites were utilized in these samples by 7 months.

2 The stabilizing effect of complex carbon on community composition

2.1 The relationship between active carbon utilization and community composition over time

The heterogeneity in metabolic activity between dilutions and complexity of the amended carbon source provided an opportunity to examine the potential relationships between microbial activity and community composition. Genus-level agglomeration of the 16S rRNA gene sequence data simplified downstream analysis while still providing good completeness of sampling (Supp. Fig 2). Nonmetric multidimensional scaling analysis (NMDS) indicated that GlcNAc- and chitin-degrading communities become more dissimilar over time before finally converging at seven months. These data agree with the analysis of similarities between treatments (ANOSIM) (Supp. Table 1) which demonstrated a per-treatment dissimilarity in active incubations which reaches a maximum at three months before decreasing at the final time point. As expected, acetate and ammonium accumulation contributed to between-treatment dissimilarities, especially at early time points (**Fig. 3**).

When we assessed the dissimilarity of all treatments combined, a trend consistent with that seen in the metabolic output was observed. The one-month chitin incubations at all dilutions exhibited greater dissimilarity from all other time points and incubations, consistent with the unusual acetate:ammonium ratios (Supp. Fig 4). While these samples clustered together and were distant from other treatments, by the seven-month time point all treatments had converged (Fig. 3).

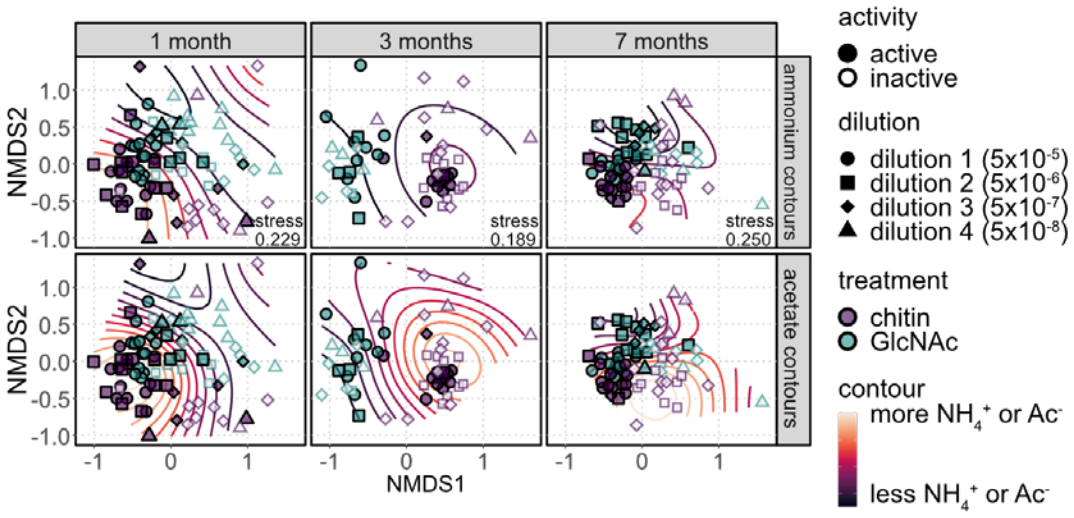

Figure 3. Community dissimilarity using nonmetric multidimensional dissimilarity analysis (NMDS). Only samples with geochemistry data are included in this analysis, and metabolite abundance is contoured on the plots ($p<0.005$). The accumulation of both acetate and ammonium contributes to the dissimilarity between samples and varies at each time point. Meanwhile, per-treatment community dissimilarity converges over time. Contour lines follow ammonium (top) and acetate (bottom) concentrations, with yellow corresponding to greater metabolite concentration. Active samples are indicated by filled symbols, with activity thresholded to at least 0.5 mM accumulated ammonium or acetate, or at most 4.2 mM sulfate.

This difference was also observed in ANOSIM analysis of the active replicates with statistically significant dissimilarity between chitin and GlcNAc communities increasing from 0.1875 at one month to 0.611 at three months (Supp. Table 1). The seven-month value (-0.035) was insignificant. Follow-up similarity percentage (SIMPER) analysis on significant ANOSIM analyses demonstrated that the top 30% taxa with significant ($p<0.05$) contributions to dissimilarity between chitin and GlcNAc treatments at the one month time point were *Psychromonas*, Desulfomonadales family Sva1033, and *Pontiella* (formerly Kiritimatiellales family R76-B128; Van Vliet et al., 2020); at the three month time point

these were *Desulfoconvexum*, *Carboxylicivirga*, an unassigned member of the class Bacteroidia, and *Marinifilum* (Supp. Files). All of the major contributors to dissimilarity at both time points were largely psychrophiles consistent with the deep sea source inoculum and incubation temperature. These taxa were on average more abundant in GlcNAc treatments in the last two time points. The above taxa with the possible exception of Sva1033 and *Desulfoconvexum* are also groups which contain heterotrophic bacteria that have the potential to degrade not only mono- and disaccharides but, surprisingly, also polysaccharides of varying complexity. The metabolic potential and ecological roles for these genera were inferred from cultivated species and environmental surveys (Enke et al., 2019; Mountfort et al., 1998; Na et al., 2009; Van Vliet et al., 2020; Wunder et al., 2021; Yang et al., 2014).

Given the strong influence of carbon degradation activity on community dissimilarity, we analyzed the effect of metabolic activity on indicator taxa (De Cáceres et al., 2010) by binning samples based on activity (e.g., accumulation of at least 0.5 mM acetate or ammonium, or at most 4.2 mM sulfate remaining) and determined the taxa significantly associated ($p<0.05$) with active replicates for each treatment and time point. Over twice the number of taxa were associated with active microcosms from the chitin treatments (24) than those incubated with the monomer GlcNAc (10). Taxa associated with activity differed between the one-, three-, and seven-month time points, as well (Supp. Fig. 5). Seven genera were identified as highly correlated with active GlcNAc treatments at the one-month time point, including potential sulfate-reducing taxa Desulfocapsaceae and *Desulforhopalus*, and putative saccharide utilizers *Spirochaeta* and *Marinifilum* (Harwood & Canale-Parola, 1983;

Na et al., 2009). The nearest cultured *Spirochaeta* species hit found via BLAST against the NCBI nucleotide collection was the marine monosaccharide-utilizing spirochete *Spirochaeta isovalerica* (Harwood & Canale-Parola, 1983). No indicator taxa were identified at the three-month time point in these active GlcNAc treatments, and at the seven-month time point, substantially fewer indicator genera were identified versus the first time point. Only three genera were associated with that final time point:*Desulfoconvexum*, a member of the Bacteroidetes BD2-2 family, and *Marinifilum*.

This trend differed from the chitin treatments, which did not have any identified indicator taxa at the first time point, and seven identified in incubations after three months. These included putative sulfate reducers *Desulfobacterium* and *Desulfoconvexum*, the potential saccharide-utilizing Firmicutes Christensenellaceae and Peptostreptococcales-Tissierellales (Klouche et al., 2007; Liu et al., 2021), and the putative sulfonated saccharide-utilizing Verrucomicrobia, *Pontiella* (Van Vliet et al., 2020). The member of the Peptostreptococcales-Tissierellales belonged to an uncultured cold seep-associated genus that branched closely with the disaccharide-utilizing genus *Geosporobacter* (Klouche et al., 2007). At the final, seven-month time point, there were 17 taxa associated with active chitin-amended treatments (Supp. Fig. 5). The taxa that were most associated with activity included putative heterotrophs *Sediminispirochaeta*, a member of the Bacteroidetes BD2-2 family, *Carboxylicivirga*, and an uncultured member of the Spirochaetaceae, and, notably, the methanogenic genera *Methanogenium* and *Methanococcoides*. Of the predicted sulfate-reducing taxa, *Desulfobacterium* species are known to be capable of acetate oxidation (Bak

& Widdel, 1986), while *Desulforhopalus* and *Desulfoconvexum* are both considered incomplete oxidizers using fatty acids or primary alcohols rather than acetate (Isaksen & Teske, 1996; Könneke et al., 2013). Moreover, the two methanogen genera associated with the final time point from active chitin microcosms were expected to have differing niches and were not observed in GlcNAc microcosms. While *Methanococcoides* was associated with noncompetitive methylotrophic substrates and thus expected to potentially be coincident with sulfate reducers, *Methanogenium* was thought to be hydrogenotrophic (Akinyemi et al., 2019; L'Haridon et al., 2014; Romesser et al., 1979).

2.2 Effect of carbon complexity and dilution on community structure and association networks

Chitin amendments supported higher levels of microbial diversity, especially at the lower dilutions, compared with GlcNAc amendments in the first three months. By the final, seven-month time point, however, the species richness converged between chitin and GlcNAc treatments (Fig. 4a; Supp. Table 2). GlcNAc amendments exhibited a precipitous decrease in richness and unique taxa between the first two time points followed by a rebound at the last two time points (Fig. 4b). Taxonomic richness was maintained at the same magnitude in chitin-amended incubations as in the input sediment inoculum (data not shown); these chitin-amended incubations additionally exhibited a modest change in richness over the course of the experiment. This change masked a dynamic gain and loss of taxa in the incubations over time. There was gain and loss of genera at roughly equal magnitude during both the first two

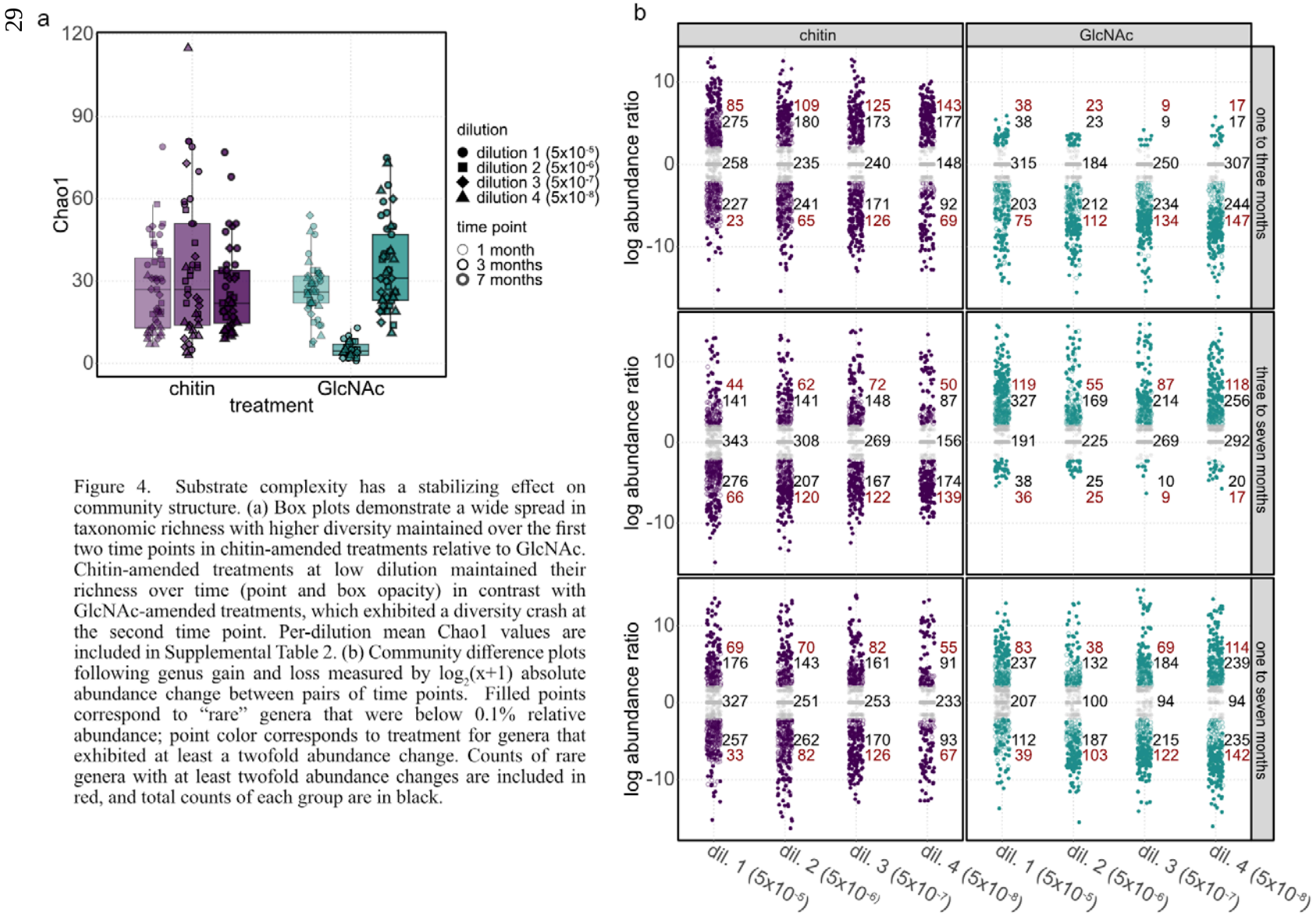

Figure 4. Substrate complexity has a stabilizing effect on community structure. (a) Box plots demonstrate a wide spread in taxonomic richness with higher diversity maintained over the first two time points in chitin-amended treatments relative to GlcNAc. Chitin-amended treatments at low dilution maintained their richness over time (point and box opacity) in contrast with GlcNAc-amended treatments, which exhibited a diversity crash at the second time point. Per-dilution mean Chao1 values are included in Supplemental Table 2. (b) Community difference plots following genus gain and loss measured by $\log_2(x+1)$ absolute abundance change between pairs of time points. Filled points correspond to "rare" genera that were below 0.1% relative abundance; point color corresponds to treatment for genera that exhibited at least a twofold abundance change. Counts of rare genera with at least twofold abundance changes are included in red, and total counts of each group are in black.

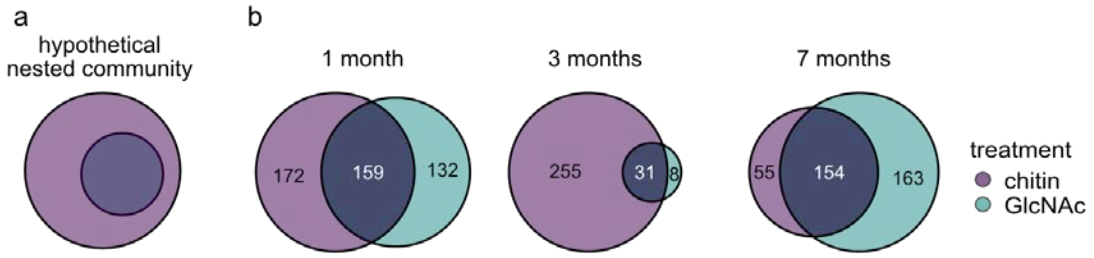

Figure 5. Communities amended with the monomer are not compositionally nested within polymer-amended communities. (a) A hypothetical nested community would have communities carrying out downstream metabolic processes such as GlcNAc degradation be a subset of chitin degradation. (b) Euler diagrams demonstrating GlcNAc-amended community members found in all replicates and dilutions at each time point are not nested within chitin-amended communities.

replicates, and, corresponding with NMDS analysis, the communities at the first and final time points were dissimilar. Notably, many of the genera gained between these time point pairs proliferated from an originally rare state below 0.1% relative abundance (Fig. 4b, Supp. Fig. 6). The increased diversity in early chitin amendments suggested that polymer degrading communities may be a superset of the monomer degrading communities. When we assessed the pool of shared genera within each treatment in a conservative estimate of the "core microbiome", we did not observe compositional nesting between GlcNAc and chitin microcosm communities (Fig. 5). This was contrary to the expectation that the community composition in these incubations might parallel the nestedness of the GlcNAc and chitin degradation processes.

Given the role of sulfate reduction as the major respiratory process in these incubations, we expected some correlation with sulfate reduction activity to community structure. However, the lack of sulfate reduction activity was not correlated to overall diversity in any treatment (Supp. Table 3). Further, despite the hypothesis that sulfate reducing taxa presence would be

correlated with sulfate drawdown, high dilution incubations (dilutions 3 and 4) with low to no sulfate utilization still maintained DNA evidence of putative sulfate reducing taxa which were not diluted out. Although most sulfate drawdown in the chitin treatment was constrained to dilution 1 (Fig. 2b), sulfate reducing taxa were detected even in the highest dilution (dilution 4, $5x10^{-8}$) (Supp. Fig. 7; Supp. Files). Moreover, methanogenic taxa were below detection in the original inoculum, yet rose in relative abundance even at the highest dilutions in response to both carbon sources (Supp. Fig. 7).

To determine whether microcosms with the highest activity contained common interaction patterns between distinct community members, we generated co-occurrence networks using the active incubations for each carbon amendment, dilution, and time point. All statistically significant networks ($p<0.005$, threshold 0.5) contained putative sulfate reducing taxa consistent with the sulfate reduction activity observed. An exception to this was the early time point for the active chitin incubation where inclusion of sulfate reducing taxa in the network preceded observed sulfate drawdown. Moreover, in all but two dilution/time point pairs of this set, chitin incubations each contained a higher number of discrete clusters than GlcNAc treatments (Fig. 6b) consistent with the greater overall diversity observed in these incubations. Further, occurrence of the hydrogenotrophic methanogen *Methanogenium* in correlation networks was often associated with putative incomplete acetate oxidizing sulfate reducers (e.g., *Desulfoconvexum*) in active incubations (Supp. Files). Other methanogenic genera such as methylotrophic *Methanococcoides* and *Methanosarcina* were also

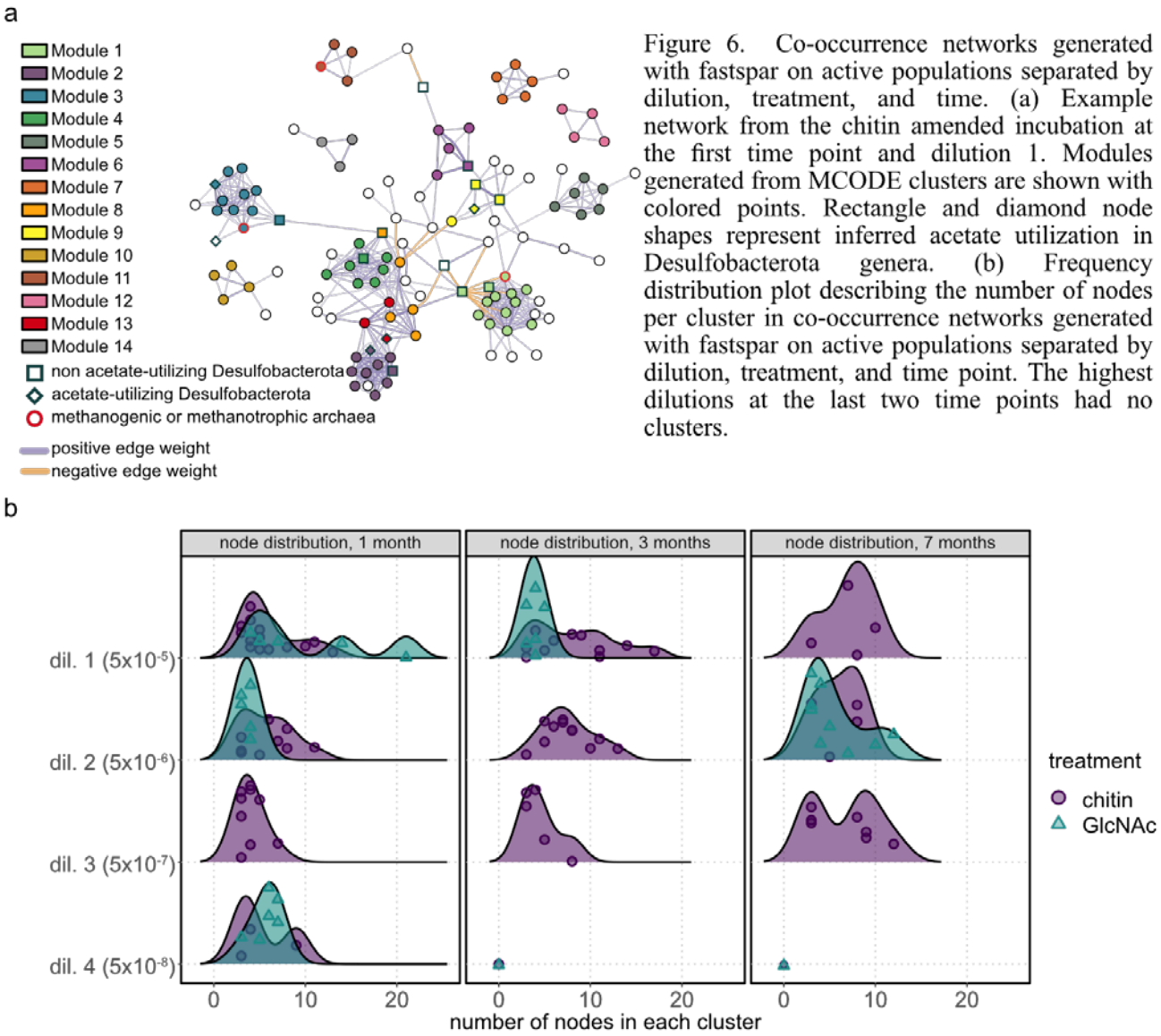

Figure 6. Co-occurrence networks generated with fastspar on active populations separated by dilution, treatment, and time. (a) Example network from the chitin amended incubation at the first time point and dilution 1. Modules generated from MCODE clusters are shown with colored points. Rectangle and diamond node shapes represent inferred acetate utilization in Desulfobacterota genera. (b) Frequency distribution plot describing the number of nodes per cluster in co-occurrence networks generated with fastspar on active populations separated by dilution, treatment, and time point. The highest dilutions at the last two time points had no clusters.

present in correlation networks for nearly all dilutions of chitin-treated incubations, suggesting the presence of viable methanogens in situ and potential interactions with other community members.

3 The effect of carbon amendment on the functional redundancy of metabolic genes

3.1 High diversity of sulfate reducing taxa supported polymer chitin amendments over the monomer GlcNAc

The dynamism in community data recorded by 16S rRNA gene amplicon sequencing was also independently supported by diversity and abundance of key genes for sulfate reduction (*dsrA*) and methanogenesis (*mcrA*) in metagenomic data. At the one and three-month time points, we sequenced the metagenome of one of the 12 replicate samples from each serial dilution representing four metagenomes per treatment and per time point and sixteen metagenomes total (eight per treatment). The *dsrA* gene, a subunit of sulfite reductase, encodes the final step of sulfate reduction and is present in all putative sulfate reducers and some sulfur oxidizers with a high degree of homology (Wagner et al., 2005). Identifying *dsrA* reads in the metagenome provided an assessment of within guild diversity and possible functional redundancy across coexisting sulfate reducing populations. We recovered *dsrA* from all treatments and dilutions; all four dilutions experienced a proliferation of phylogenetically distinct *dsrA* over the first two time points which was enhanced in chitin incubations (n=65) vs. in GlcNAc incubations (n=55) (Fig. 7). There were more *dsrA* genes

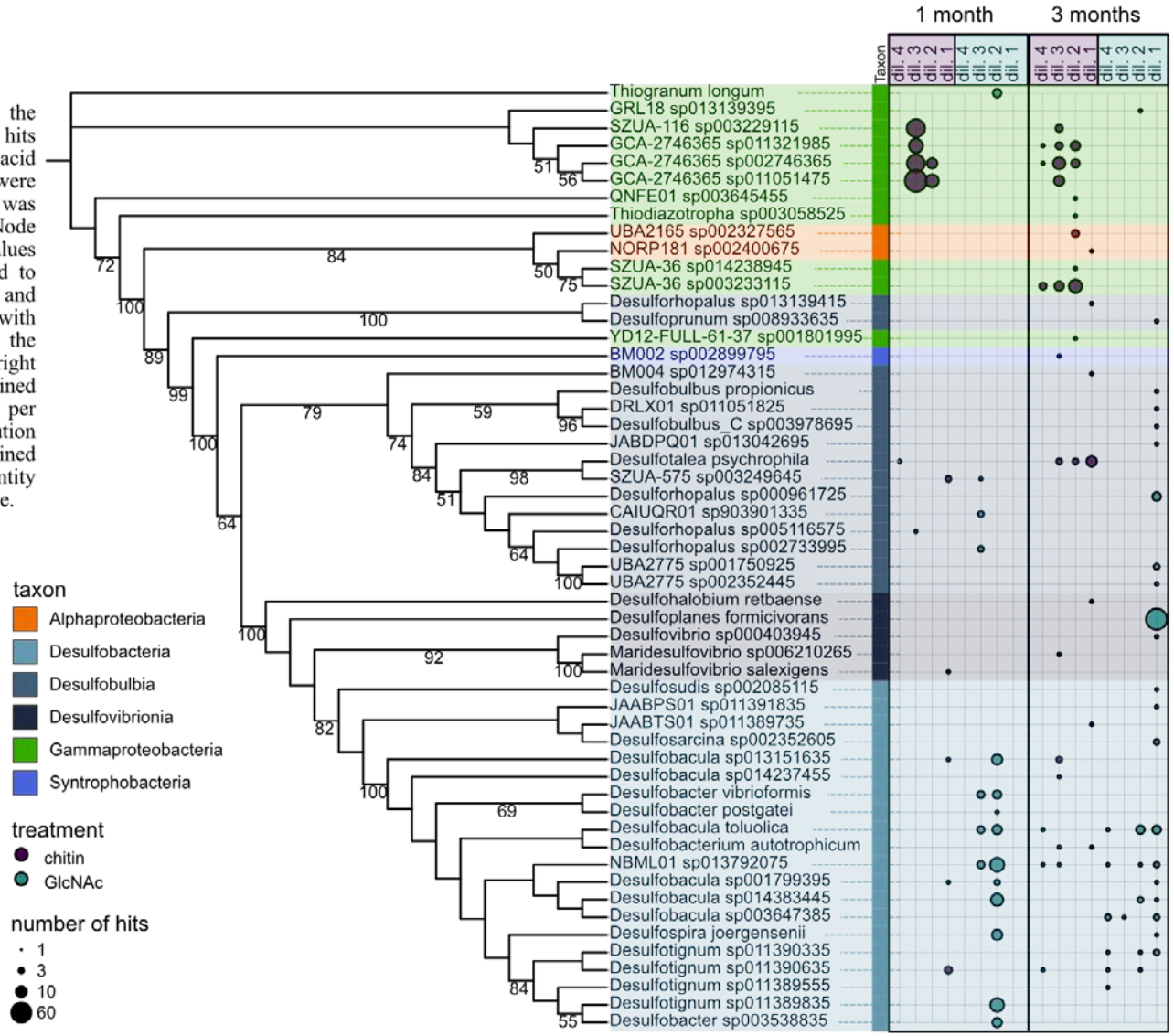

Figure 7. Phylogenetic tree showing the distribution of metagenome sequence hits mined from a GTDB DsrA amino acid database. GTDB DsrA sequences were aligned with MUSCLE and the tree was generated with IQTREE model LG+R6. Node labels correspond to bootstrap support values greater than 50%. Tip labels correspond to species hits from GTDB while tips and horizontal shading are colored by taxon, with higher taxonomic resolution in the Desulfobacterota. The faceted plot to the right contains a summary of the mined metagenomic sequence distribution per treatment (point color) separated by dilution and time. Point size indicates number of mined reads corresponding to at least a 95% identity match with the GTDB amino acid database.

normalized by read number in chitin amendments than in GlcNAc amendments (Supp. Fig. 8), with three of the four chitin incubations exhibiting an increase in *dsrA* diversity, with an average 82% increase in unique *dsrA*s, between the one-month and three-month incubation period. In contrast, *dsrA* diversity in GlcNAc incubations increased in two of four incubations and averaged less than half the increase observed in the chitin incubations, at 38%.

3.2 Methanogen proliferation in chitin treatments after sulfate depletion

Methanogenic clade abundance differences between treatments and time points were additionally supported by functional gene data. We mined methyl coenzyme reductase gene *mcrA*, found in all methanogenic and methanotrophic archaea, from the metagenomic data and found that, consistent with the 16S rRNA gene amplicon data, the taxonomic assignment of *mcrA* varied by carbon treatment. *Methanogenium* was more abundant in chitin treatments than GlcNAc in both 16S amplicon and metagenome sequence data; however, the detection of *Methanogenium mcrA* occurred earlier than in the iTag data (three months versus seven months; Fig. 8). Cultured *Methanogenium* are all hydrogenotrophic methanogens and not known to be associated with noncompetitive substrate use (Akinyemi et al., 2019; Oremland & Polcin, 1982); we therefore predicted the occurrence of *Methanogenium* to be associated with sulfate depletion. Indeed, at the final time point, *Methanogenium* 16S abundance was strongly negatively correlated with sulfate concentration ($p<0.05$, Spearman's rho = -0.719) when aggregating all dilutions and replicates in the chitin treatment.

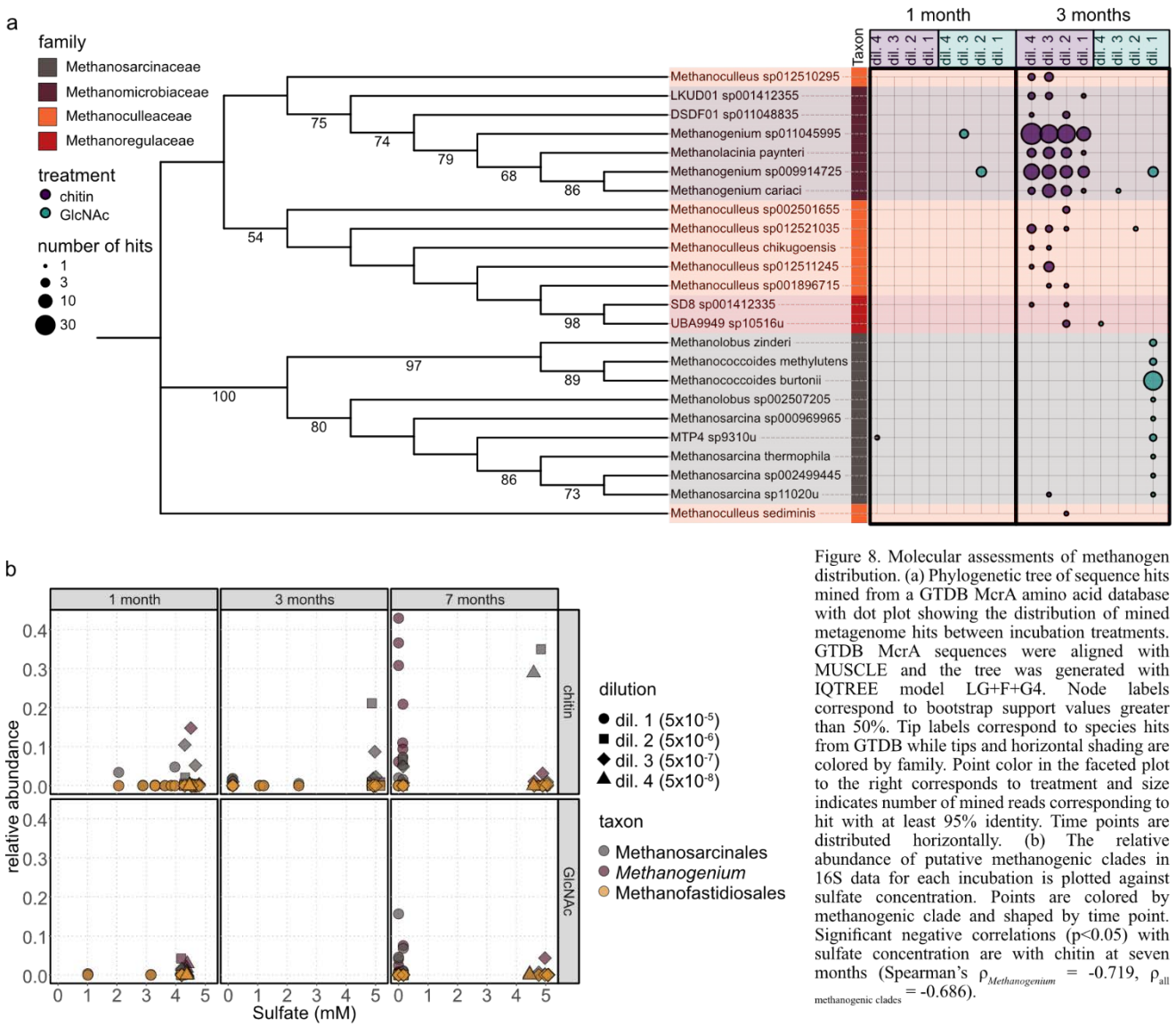

Figure 8. Molecular assessments of methanogen distribution. (a) Phylogenetic tree of sequence hits mined from a GTDB McrA amino acid database with dot plot showing the distribution of mined metagenome hits between incubation treatments. GTDB McrA sequences were aligned with MUSCLE and the tree was generated with IQTREE model LG+F+G4. Node labels correspond to bootstrap support values greater than 50%. Tip labels correspond to species hits from GTDB while tips and horizontal shading are colored by family. Point color in the faceted plot to the right corresponds to treatment and size indicates number of mined reads corresponding to hit with at least 95% identity. Time points are distributed horizontally. (b) The relative abundance of putative methanogenic clades in 16S data for each incubation is plotted against sulfate concentration. Points are colored by methanogenic clade and shaped by time point. Significant negative correlations ($p<0.05$) with sulfate concentration are with chitin at seven months (Spearman's $\rho_{\textit{Methanogenium}} = -0.719$, $\rho_{\text{all methanogenic clades}} = -0.686$).

Methanogenium 16S abundance did not correlate with sulfate utilization in any other treatment or time point, consistent with the indicator taxon analysis (Fig. 8b). Although *Methanogenium* was not detected in the specific sediment depth horizon used as the inoculum for this experiment, it was present at roughly 6% relative abundance in 16S rRNA gene surveys of a deeper horizon in the same sediment core.

DISCUSSION

Little is known about the anaerobic breakdown of complex polymers like chitin by microorganisms in deep sea sediments. This study aimed to answer outstanding questions in microbial ecology within this context through assessing the community response to the anaerobic respiration of complex carbon. Using this highly replicated and structured system, where we tracked geochemical output and community metrics in tandem over time, we received insights into the dynamics of anaerobic marine sediment communities. We determined the impact of carbon complexity on microbial community structure through assessing the compositional and metabolic changes over time, the role of functional redundancy of metabolic guilds in maintaining community performance, and the relationship between community structure and activity. Despite the expected influence of stochastic processes on community heterogeneity (Le Moigne et al., 2023), there was nonetheless a consistent relationship between complex carbon amendment and the maintenance of community diversity (e.g., Fig. 4a, 5, 6). Contributions to this signal may include potential underlying microbial interactions and interdependencies including syntrophy as well as

physical drivers of heterogeneity such as the insolubility of the input substrate and the spatially heterogeneous nature of the sediment inoculum (Probandt et al., 2018).

Anaerobic chitin degradation in other systems has been shown to proceed through the hydrolysis of chitin to oligomers (e.g., chitobiose and GlcNAc) followed by fermentation to small fatty acids or primary alcohols coupled to the reduction of available electron acceptors, including sulfate (Beier & Bertilsson, 2013; Wörner & Pester, 2019). We demonstrated that these two processes — substrate degradation and electron acceptor respiration — do not necessarily occur in lockstep. Chitin-amended microcosms exhibited a high level of acetate and ammonium accumulation that was initially decoupled from sulfate reduction with a 1:1 acetate:ammonium ratio (Fig. 2a). This metabolite accumulation ratio was in contrast to incubations with the chitin monomer GlcNAc, where acetate levels were three times that of ammonium. The ammonium concentration in relation to sulfate drawdown differs strongly between the two treatments even accounting for a potential time lag. Specifically, while chitin incubations exhibit a dramatic decrease in absolute ammonium concentration coupled to sulfate drawdown between the first two time points, GlcNAc incubations overall had a higher ammonium concentration of ammonium even as sulfate was used (Fig 2a). This response is therefore not likely to be solely a result of rapid early succession in metabolizing a simpler product. Because the idealized degradation of GlcNAc results in a stoichiometric acetate:ammonium ratio of 3:1, these results then suggested that chitin-amended communities either had high levels of acetate consumption at the first time point, or that the chitin-respiring community included fermenter groups producing alternative metabolic

products such as primary alcohols instead of acetate. Our ion chromatography method was unable to measure non-ionizable metabolites; however, we could exclude production of other small fatty acids such as propionate or lactate. In the absence of sufficient sulfate reduction to account for the oxidation of the predicted acetate (over 10 mM, Fig. 2b), metabolic pathways capable of acetate drawdown under these conditions include acetoclastic methanogenesis or syntrophic acetate oxidation. At the low temperatures of this experiment, syntrophic acetate oxidation is expected to be outcompeted by acetoclastic methanogenesis and therefore not expected to be present unless the methanogens are inhibited e.g., by high ammonium concentrations (>90 mM, Schnürer et al., 1999). The significant sulfate-coupled drawdown of ammonium in chitin-amended incubations between the first two time points is also notable, suggesting more complex interactions between the terminal process of sulfate reduction and upstream members that could be stimulated by chitin such as sulfate-coupled ammonium oxidation (Fdz-Polanco et al., 2001).

While prior work at hydrothermal vents have shown a lack of methanogenic enrichment in complex carbon amended thermophilic and mesophilic microcosms (Pérez Castro et al., 2021), our incubations maintained a modest methanogen signal in both marker genes and the 16S rRNA gene diversity surveys, suggesting a further influence of temperature (Fig. 8). Chitin-amended microcosms also accumulated high ammonium concentrations (Fig. 2a), so it is possible that acetoclastic methanogens are present but inhibited. The relative lack of sulfate coupled-acetate utilization is in contrast to prior reports from marine sediments demonstrating a preference of sulfate-reducing bacteria for small organic acids (Christensen,

1984; Glombitza et al., 2016). Additionally, the low abundance of methanogenic clades does not preclude their activity within these microcosms; not only are relative abundance and activity known to be decoupled (Pester et al., 2010), it is possible that some of these groups were below the detection limits of our analysis. Indeed, many of these microcosms showed heightened evidence of methanogenic taxa at later time points.

The presence of taxa known to utilize organosulfur substrates suggests the contribution of other sulfur-mediated pathways spanning a range of oxidation states from sulfate esters to methylated thiols. Some examples include the sulfated polysaccharide utilizing genus *Pontiella*, which is an indicator of activity in chitin-amended microcosms, as well as members of the family Methanofastidiosales which have the ability to reduce methylated thiols (Nobu et al., 2016; Van Vliet et al., 2020). The production and utilization of these sulfur compounds can allow for further niche partitioning and may contribute to diverse community composition and interactions, especially in the case of *Pontiella* which is additionally able to produce sulfated polysaccharides.

Chitin-amended incubations were able to retain both compositional and functional diversity over time and with increasing dilution, albeit with increasing variation at higher dilution microcosms (Fig. 4a). This indicates that the essential members required for insoluble polymer degradation were maintained at high inoculum dilution (up to dilution 3). Notably, community richness was largely invariant despite this extreme dilution of the starting sediment inoculum, implying diversity was distributed among sediment particles in a manner consistent with other particle-associated communities. Specifically, previous work has

shown that individual sand particles can retain a significant subset of overall community diversity (Probandt et al., 2018), potentially providing a seedbank allowing community success even in highly dynamic environments.

The stable alpha-diversity in chitin-amended incubations over the seven month course of the experiment, however, was underpinned by dynamic gains and losses of genera over time (Fig. 4b). The shuffling of genera across time was seen at even the highest dilutions and was dependent on chitin; GlcNAc-amended incubations exhibited a much more asymmetric response reflecting the alpha diversity shifts with more genera lost than gained at the three-month time point. This dynamic response appears to be an irreducible characteristic of the complex carbon impact on these communities and, in the absence of dispersal to drive the proliferation of diversity, has implications on the ability of chitin to support active community turnover. Further contributions to community structure during the anaerobic degradation of insoluble polymers may additionally include trophic interactions, nutrient auxotrophies, and niche partitioning (Embree et al., 2015; Fierer & Lennon, 2011; Marsland et al., 2019).

Although microbial community richness was enhanced and maintained down dilution in chitin-amended microcosms, our experiments did not support a strong correlation between alpha diversity and the terminal respiratory process (sulfate reduction). This is in agreement with other works which have demonstrated an unclear relationship between alpha diversity and ecosystem function or activity (Bell et al., 2005; Le Moigne et al., 2023; Shade, 2017). Individual core metabolic processes such as substrate degradation and respiration (as

determined through carbon dioxide accumulation in aerobic incubations) have been shown to be affected by changing community richness (Bell et al., 2005; Peter et al., 2011; C. Zhang et al., 2019). However, previous reports in amended freshwater microcosms have also demonstrated that diversity is not directly correlated with overall ecosystem performance; rather, taxonomic diversity is a descriptive metric whose power lies in comparison between treatments or conditions but not a priori connected with function (Le Moigne et al., 2023; Shade, 2017). In concordance with these observations, we observed a maintenance of functional and compositional diversity down dilution including putative sulfate reducing taxa and marker genes despite the depletion of sulfate reduction activity at the highest dilutions (dilution 3, dilution 4) of our chitin-amended microcosms (Fig. 7).

Since GlcNAc is a monomer of chitin, we hypothesized that the pathways and microbial communities responsible for the degradation of GlcNAc would be a subset of chitin-degrading assemblages. However, our analysis showed that while the dissimilarity of the two populations decreased over time, the overall communities were not nested, either by composition or by presumed function (Fig. 2, Fig. 5). Prior work has shown that complex carbon input to environmental communities resulted in “selfish” uptake rather than allow secondary degrader competition for degradation products (Brown et al., 2024). We infer from this observation that while microorganisms degrading oligomers or monomers will compete for the same niche, when in a mixed polysaccharide-degrading community they may be outcompeted by primary degraders. This suggests that more complex community

interactions during polymer degradation beyond simple addition of function may be involved and is in agreement with other work in freshwater sediments (Wörner & Pester, 2019).

Investigation on potential interacting microorganisms through community correlation analysis (Watts et al., 2019) provided a further method to probe the community dynamics of these polymer-amended microcosms. In our experiment, communities were composed of co-occurring units ("modules") containing terminal respirers - here, sulfate reducers or methanogens - and other species, such as putative fermenters or other heterotrophs. These groups were connected through positive co-occurrence patterns suggestive of likely interactions. Notably, taxa affiliated with sulfate reduction or methanogenesis were maintained within these modules up to dilution 3 in active microcosms containing chitin and GlcNAc, with a greater number of diverse interactions corresponding with the complex polymer treatment (Fig. 6). The complex carbon substrate supported both diversity of functions (through the proliferation and functional redundancy of metabolic genes) and diversity of interactions (through the maintenance of multiple unique co-occurrence modules). The underlying processes by which these modules assemble or are maintained are still unknown; however, their maintenance appears to be an intrinsic property of these microbial systems. In the specific case examining the contribution of the terminal respirer (sulfate reducer or methanogen) to community assembly, prior work has established the critical nature of the primary degradation process and by proxy the complexity of the primary substrate. Primary degradation is the rate-limiting step around which downstream metabolic

reactions must assemble (Arnosti et al., 1998). In the specific case examining the contribution of the terminal respirer (sulfate reducer or methanogen) to community assembly, sulfate-reducing microorganisms have been reported to support the upstream process of exoenzyme production through, for example, the crossfeeding of secondary metabolites (Pel & Gottschal, 1989).

Many of the terminal respirers that proliferated over the course of the experiment, especially in connection with carbon degradation activity, were notably below detection or exceedingly rare in the starting inoculum (Supp. Fig. 7). We observed that rare biosphere members responded more dynamically in chitin treatments compared with the GlcNAc monomer in our experiment. The gain and loss of rare taxa, defined here as below 0.1% relative abundance, occurred even at the highest dilutions of starting inoculum in contrast to the metabolic readout which showed significantly less activity at high dilution (Fig. 2b; Fig. 4b). Moreover, the proliferation of rare taxa was a major contributor to the dynamic response to complex carbon supplementation (Fig. 4b). In natural ecosystems, changes in community structure over time can be attributed to any one of several ecological factors - for example, dispersal, drift, or selection (Vellend, 2010). Some of these factors can be ruled out with our experimental setup, where each replicated microcosm represented a closed system with no emigration or immigration over the seven-month experiment. Rare biosphere members may contribute to the adaptability of ecosystems by enhancing their resistance to perturbations (Jousset et al., 2017; Lynch & Neufeld, 2015; Wisnoski & Lennon, 2021), and their contribution to the stability of diversity in our experiment supports this (Fig. 4b). Chitin-

amended replicates exhibited strong outgrowth in rare biosphere members, with highly dynamic change in taxa between time points while the overall diversity over time stayed stable. While sulfate-reducing bacteria and methanogenic archaea can be at high abundance in marine sediments (Goffredi et al., 2008; Leloup et al., 2009), our source sediment had not seen a large influx of organic matter for nearly two decades. During sampling, there was no sulfate drawdown within the sediment core (Supp. Fig. 1). It was not sulfidic and likely fully oxic due to the decades since the whale fall site was active. Despite this, the sediment community was still able to maintain a reservoir of methanogens and sulfate reducing bacteria that were taxonomically similar to previous observations in the same submarine canyon post carbon loading (Goffredi et al., 2008; Goffredi & Orphan, 2010). This suggested a conserved "seedbank" response to complex carbon amendment; the maintenance of the rare microbiome in these systems may contribute to community success and stability (Wisnoski & Lennon, 2021; Xun et al., 2021) and additionally suggest that critical processes such as sulfate reduction may be present even if these taxa are below detection. Despite the fact that methanogens were below detection in our inoculum, 16S data showed a major increase in relative abundance of *Methanogenium* in chitin treatments in the later time points. The presence of these hydrogenotrophic methanogens when sulfate is depleted supports the idea that a respiratory cascade occurs in sediment, with potential electron acceptors being utilized progressively according to their redox potential.

Whether through particle association, or by maintenance of functional complexity when degrading complex substrates, this work has highlighted mechanisms through which

biodiversity and functional redundancy might be maintained in cold, anoxic systems. The maintenance of diverse, viable methanogenic community members at low abundance that proliferate in response to organic matter loading has implications on methane emissions in marine environments that undergo regular pulses of complex carbon loading events. These environments may vary from nearshore ecosystems to the deep sea, providing a potential link between the sediment microbiome and climate processes (Borges et al., 2016; St. Pierre et al., 2022). Future work, unearthing the complex interactions between members of functional guilds, will additionally provide insight into the factors that drive the maintenance of microbial communities.

METHODS

Sample collection, incubation conditions, and media design

The sediment core was collected in 2018 on research cruise WF12-18 on the R/V *Western Flyer* with ROV *Doc Ricketts* at GPS coordinates 36.769873 N, 122.0829 W. The collection site was at a former whale fall site (emplacement October 2004) in the Monterey Bay at 1018 m depth. Depth horizons were sectioned from the sediment core and the 6-9 cm horizon was used for inoculum after anaerobic storage at 4 °C in an argon-gassed Mylar bag.

Colloidal chitin was prepared by dissolving 25 g chitin (Alfa Aesar catalog number J61206-36) in 150 mL 12N HCl; the resulting slurry was strained through a cheesecloth and precipitated in 1 L ice cold milli-Q water. After an overnight incubation at 4 °C, the mixture was neutralized to pH 7 with sodium hydroxide and washed three times with milli-Q water

using a 4 °C centrifugation step (10,000 x *g*, 20 minutes). The washed colloidal chitin was then freeze-dried before use in incubations. The sulfate-free artificial seawater medium consisted of 410.7 mM NaCl, 52.5 mM $MgCl_2$, 8.9 mM $CaCl_2$, 8.9 mM KCl, 0.84 mM KBr, 0.44 mM H_3BO_3, 0.1 mM $SrCl_2$, 0.07 mM NaF, 0.055 mM K_2HPO_4, 0.022 mM KH_2PO_4, 25 mM HEPES, and 1x SL-11 trace elements at pH 6 (15.467 μM Na_2-EDTA pH 7, 7.545 μM $FeCl_2$, 0.514 μM $ZnCl_2$, 0.505 μM $MnCl_2$, 0.097 μM H_3BO_3, 1.463 μM $CoCl_2$, 0.012 μM $CuCl_2$, 0.185 μM $NiCl_2$, 0.149 μM Na_2MoO_4). The medium was pH-adjusted to 7.5.

The sulfate-free artificial seawater medium was supplemented with 5 mM sodium sulfate and, depending on treatment, colloidal chitin (5.7 mg/mL), N-acetylglucosamine (5 mM), or no electron donor. Tenfold serial dilutions of a 1:1 sediment slurry in 1.75 mL total volume were anaerobically prepared in 2 mL deep well 96-well plates (VWR part number 89237-526) with plate rows corresponding to dilution and plate columns corresponding to biological replicates. These deep well plates were capped with silicone mats (VWR part number 89237-538) and sealed in separate Mylar bags with an anoxic headspace for each treatment. After incubation at 10 °C for one, three, and seven months, each well was sampled for microscopy, metagenome sequencing, 16S rRNA gene amplicon sequencing, and geochemistry. At each time point, 200 μL sample was filtered through a 0.2-micron filter plate (Pall product number 8019) into a polystyrene storage plate, which was sealed with an adhesive film (Biorad Microseal B) for ion chromatography. The filtrate was saved at -80 °C for DNA extraction. 100 μL of sample at each time point was fixed with a final concentration of 1% paraformaldehyde and stored at 4 °C for microscopy.

Geochemistry: quantification of major ions and metabolites

Samples for ion chromatography were stored at -20 °C until analysis, when they were diluted 1:50 and run on Dionex ICS-2000 or Thermo Integrion HPIC as previously described (Speth et al., 2022) on an AS19 anions and CS16 cations column. Analysis was focused on all twelve replicates from dilutions $5x10^{-5}$ to $5x10^{-7}$, with four replicates from the highest dilution ($5x10^{-8}$) for a total of 40 samples analyzed at each time point with some exceptions. Six samples were removed from GlcNAc treatments at the first and second time points (first time point: two samples at $5x10^{-7}$; second time point: three samples at $5x10^{-6}$ and one sample at $5x10^{-7}$) due to lack of sample; at the first time point, all twelve replicates from this treatment at the highest dilution ($5x10^{-8}$) were analyzed. Samples were run at the Water and Environment Laboratory (Caltech).

DNA extraction and sequencing

Samples were extracted using the Beckman DNAdvance kit (Beckman product number A48705) using the following protocol (adapted from Szabo et al., 2022). Samples were lysed with 20 µL of a 1,000U/µL lysozyme solution at 37 °C for 1.5 hours, 140 µL of a Proteinase K lysis mixture (132.25 µL LBH lysis buffer, 5.25 µL 0.8 U/µL Proteinase K, 2.5 µL freshly prepared 1M dithiothreitol) at 55 °C for 16-20 hours, and 40 µL of a 10% SDS solution at 65 °C for 2 hours. Lysate was gently mixed with 50 µL PBBA pre-bind buffer, avoiding bubbles, followed by addition of 85 µL BBE bind buffer. After room temperature incubation for 1

minute, beads were separated with a 7-minute incubation on a magnetic plate stand. Supernatant was removed and beads were washed three times with 170 μL of a freshly made 70% ethanol solution. Each wash involved thorough resuspension of pellet and subsequent incubation on a magnetic plate stand until solution cleared. After the final wash, remaining supernatant was removed using a 10 μL multichannel pipette and beads were incubated at room temperature for 5 minutes to allow drying of residual ethanol. The plate was then removed from magnet and DNA was eluted with a resuspension of beads in 30 μL EBA elution buffer, then magnetic separation and transfer of eluted DNA 10 μL at a time into a storage plate.

Extracted DNA was quantified with Picogreen (Invitrogen product number P7589), according to manufacturer's protocol.

Samples were submitted for 16S rRNA gene sequencing of the V4 hypervariable region to Argonne National Laboratories (Earth Microbiome Project barcoded primer set 515F 5'-GTGYCAGCMGCCGCGGTAA/806R 5'-GGACTACNVGGGTWTCTAAT) or Laragen (515F 5'-GTGYCAGCMGCCGCGGTAA/926R 5'-CCGYCAATTYMTTTRAG TTT). Both primer sets had Illumina adapters appended to the 5' end as described previously (Caporaso et al., 2012; Speth et al., 2022).

Samples were submitted for metagenome sequencing to the MIT core sequencing facility (Cambridge, MA, USA) after library preparation using the Nextera XT library preparation kit and quality control with a TapeStation 4200 (Agilent) using the HSDNA D1000 screen tape, both according to manufacturer's protocol.

16S rRNA amplicon sequence analysis

Demultiplexed 16S amplicon reads were put through the QIIME2 pipeline with denoised ASV abundances generated using DADA2 (Bolyen et al., 2019; Callahan et al., 2016). Taxonomy classification was done using a classifier trained on the SILVA SSU database release 138 (Quast et al., 2013; Yilmaz et al., 2014). Samples with fewer than 20 reads were removed from the analysis. All R analyses were done using R Statistical Software (version 4.0.3). Decontamination and abundance visualization of 16S data was done using the R phyloseq and decontam packages (Davis et al., 2018; McMurdie & Holmes, 2013). Diversity, dissimilarity, and species accumulation analyses were done using the vegan package (Oksanen et al., 2020), with NMDS analysis done on fourth-root transformed genus-agglomerated relative abundance data. Indicator species analysis was done using the indicspecies package (De Cáceres & Legendre, 2009) with the point biserial correlation coefficient corrected for site number. Correlation analysis was done using fastspar (Watts et al., 2019). Visualization of networks was done using the igraph R package (Csardi & Nepusz, 2005) and Cytoscape (Shannon et al., 2003). Correlation networks were then clustered with MCODE (Bader & Hogue, 2003). Nestedness was demonstrated through Euler plots of presence-absence transformed 16S rRNA sequence data with all dilutions and replicates combined for each treatment at each time point. Sulfate reducing and methanogenic taxa were defined generally as members of the phylum Desulfobacterota or orders Methanosarcinales, Methanofastidiosales (formerly the WSA2 group; Nobu et al., 2016), and Methanomicrobiales, respectively (Supp. Files**).**

Metagenomic analysis of metabolic marker genes

Metabolic marker genes for sulfate reduction (*dsrA*) and methanogenesis (*mcrA*) were mined from metagenomic sequence reads using a previously described protocol (Speth & Orphan, 2018) and manually curated databases derived from GTDB release 202 (Supp. Files).To prepare a reliable Hidden Markov Model (Eddy, 1998) for searching GTDB, taxonomically diverse DsrA and McrA amino acid sequences were identified from a non-redundant set of bacterial and archaeal genomes in the IMG database (I.-M. A. Chen et al., 2021) using the BLASTP (Altschul et al., 1990) function on their website. These sequences were filtered using UCLUST (Edgar, 2010) to extract sequences that were at least 50% dissimilar in sequence identity. The remaining highly dissimilar sequences were used to construct an HMM using the HMMbuild function of HMMer (Eddy, 2011). These HMMs were then used to query the genomes from GTDB r202 by using the hmmsearch function of HMMer. The resultant databases are made available as part of the supplement. Briefly, metagenome reads were searched against the database using DIAMOND (Buchfink et al., 2015). These reads were then searched against an outgroup consisting of the NCBI-nr protein reference database, and the BLAST score ratio (BSR) calculated between the two searches; a BSR threshold of 0.75 was applied. Reference DsrA phylogenetic trees were built using a MUSCLE alignment (Edgar, 2004) of the database sequences corresponding to mined metagenome sequences matching at least 95% identity with IQTREE (Minh et al., 2020) model LG+R6, bootstrapped 100 times. Reference McrA phylogenetic trees were generated similarly, with IQTREE model LG+F+G4. Visualization of trees was done with iTOL (Letunic & Bork, 2021).

ACKNOWLEDGMENTS

We thank S. Connon (Caltech) and the Argonne National Laboratory Environmental Sample Preparation and Sequencing Facility for their assistance with 16S rRNA gene amplicon sequencing. We also thank L. Lu (MIT) for DNA extraction assistance. This work was supported by the Simons Foundation – Principles in Microbial Ecology (PriME) collaboration.

SUPPLEMENTAL FIGURES AND TABLES

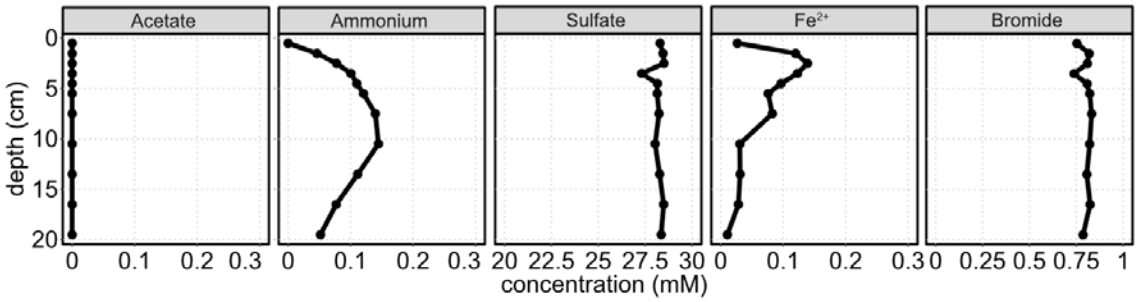

Supplemental Figure 1. Porewater geochemistry from a paired sediment push core at the whale fall site used in this experiment.

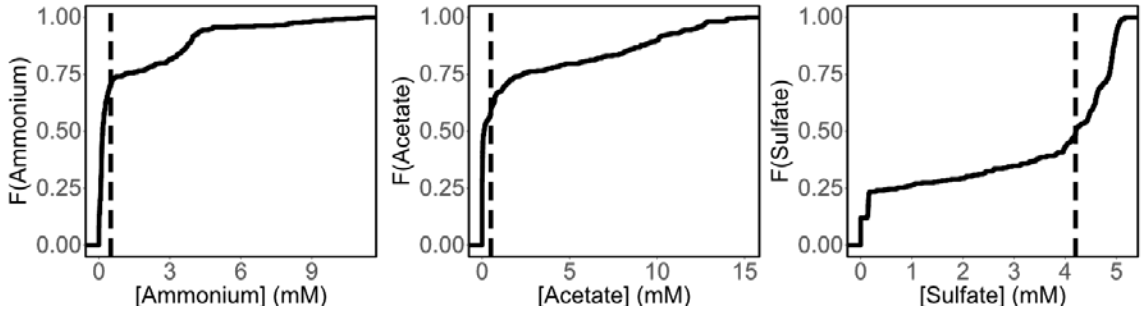

Treatment	Time point	n $[NH_4^+]$ > 0.5 mM	n $[Ac^-]$ > 0.5 mM	n $[SO_4^{2-}]$<4.2 mM	n active
None (n.m.)	1 month	n.m.	n.m.	n.m.	n.m.
None (n=40)	3 months	2	7	17	19
None (n=40)	7 months	3	13	22	22
GlcNAc (n=48)	1 month	13	15	33	23
GlcNAc (n=36)	3 months	20	19	18	21
GlcNAc (n=40)	7 months	29	28	26	29
Chitin (n=40)	1 month	20	25	15	29
Chitin (n=40)	3 months	4	12	13	14
Chitin (n=40)	7 months	5	14	14	15

Supplemental Figure 2. Empirical cumulative density functions describing the distribution of metabolite concentration. Activity thresholds are shown with vertical lines: ammonium and acetate thresholds are set at 0.5 mM; and sulfate is thresholded at 4.2 mM. Table below lists incubation counts meeting each threshold. n.m., not measured.

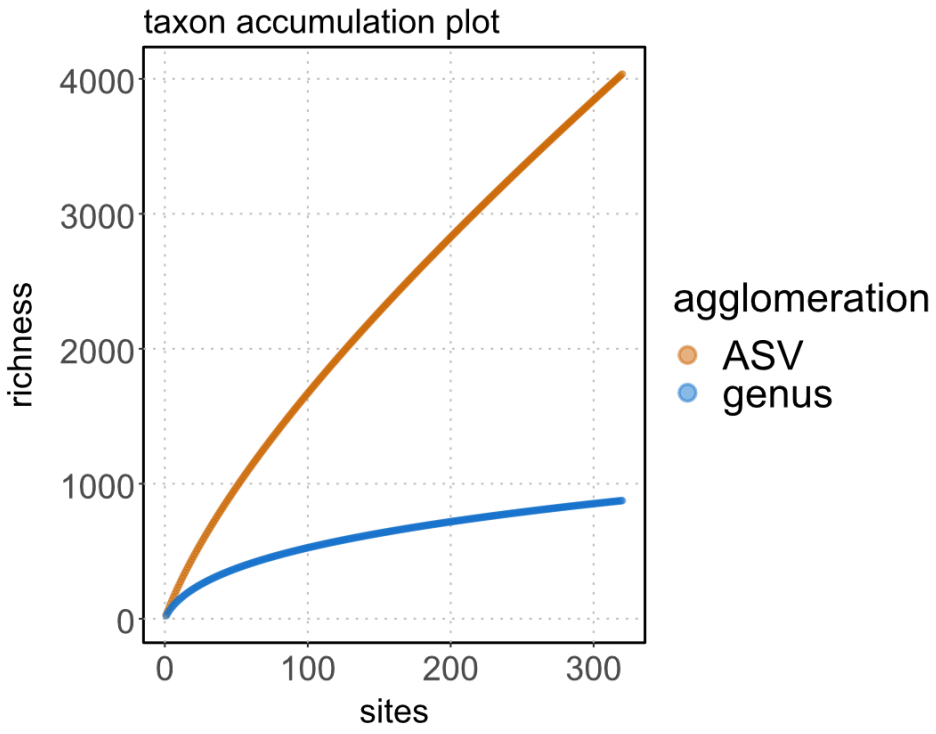

Supplemental Figure 3. Taxon accumulation plot for 16S sequencing data at the ASV level (orange) and agglomerated by genus (blue).

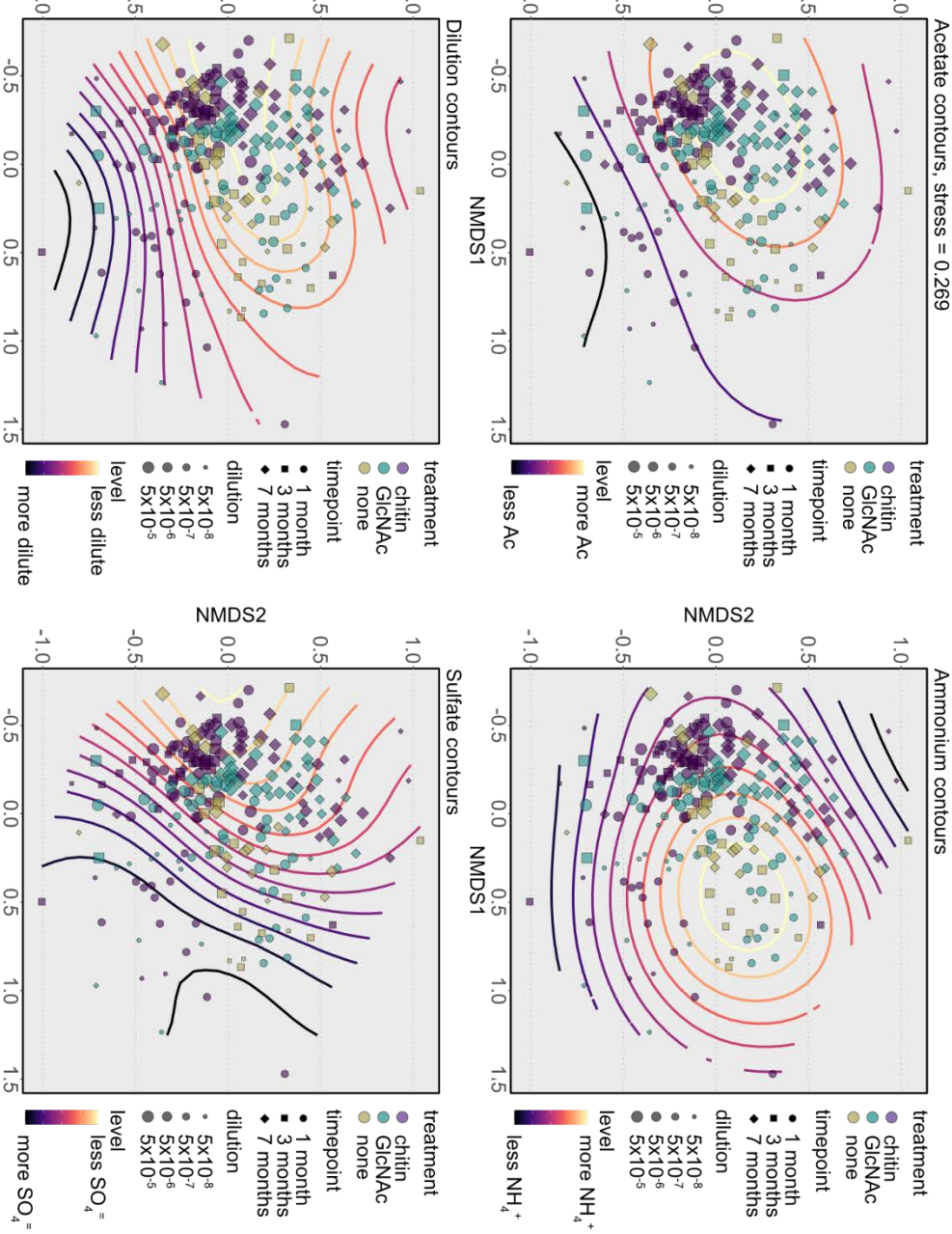

Supplemental Figure 4. NMDS plot with all samples containing geochemistry data plotted in the same pane. Contours correspond to metabolite concentration (acetate, ammonium, or sulfate) or dilution.

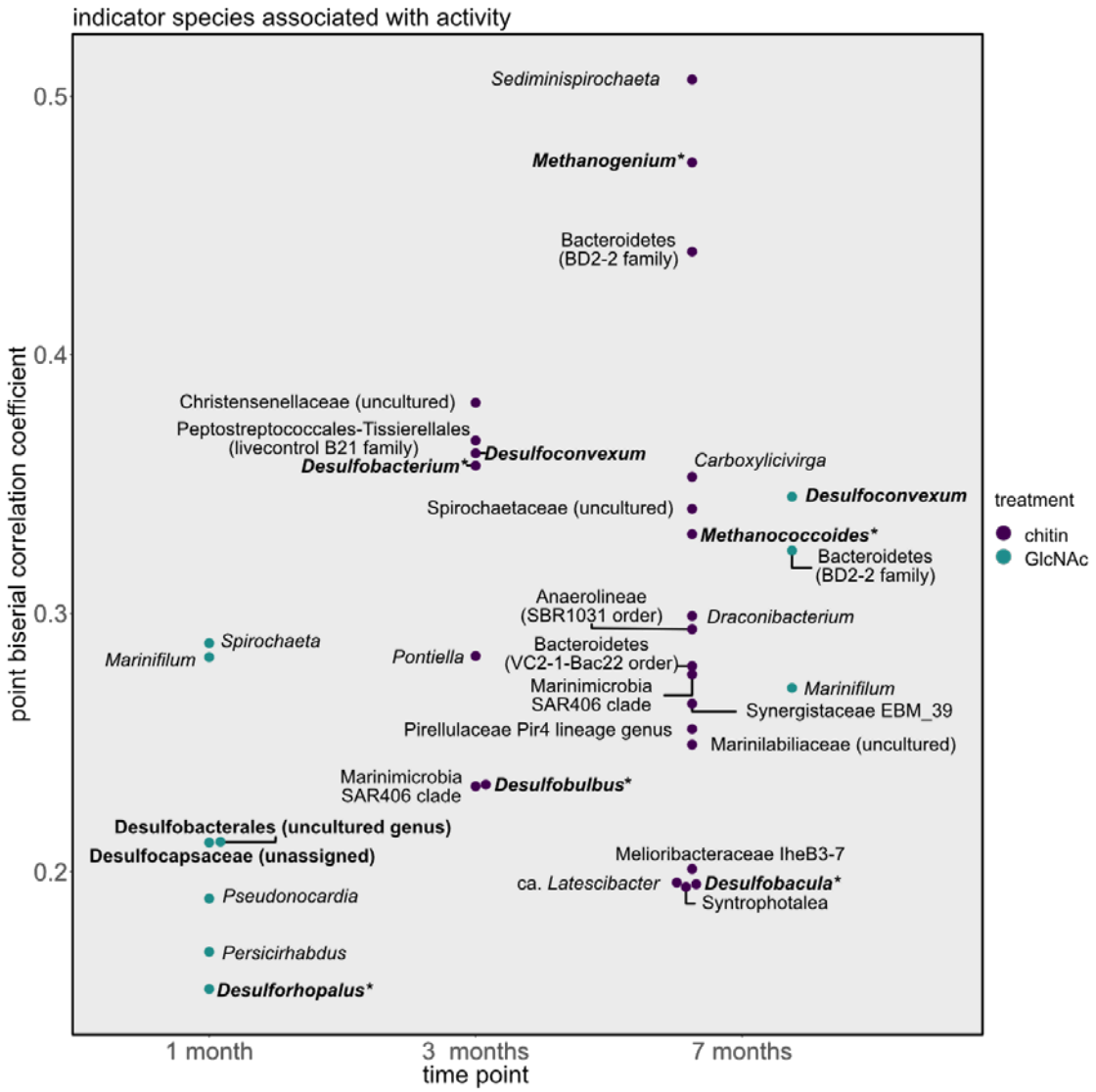

Supplemental Figure 5. Indicator taxon analysis demonstrates an enhanced number of differentially abundant genera associated with metabolic activity in chitin treatments (purple points) vs GlcNAc treatments (green points). Labels correspond to the lowest taxonomic level description available. Bolded labels indicate putative methanogens or sulfate-reducing bacteria, and asterisks denote genera supported with metabolic gene data (DsrA or McrA).

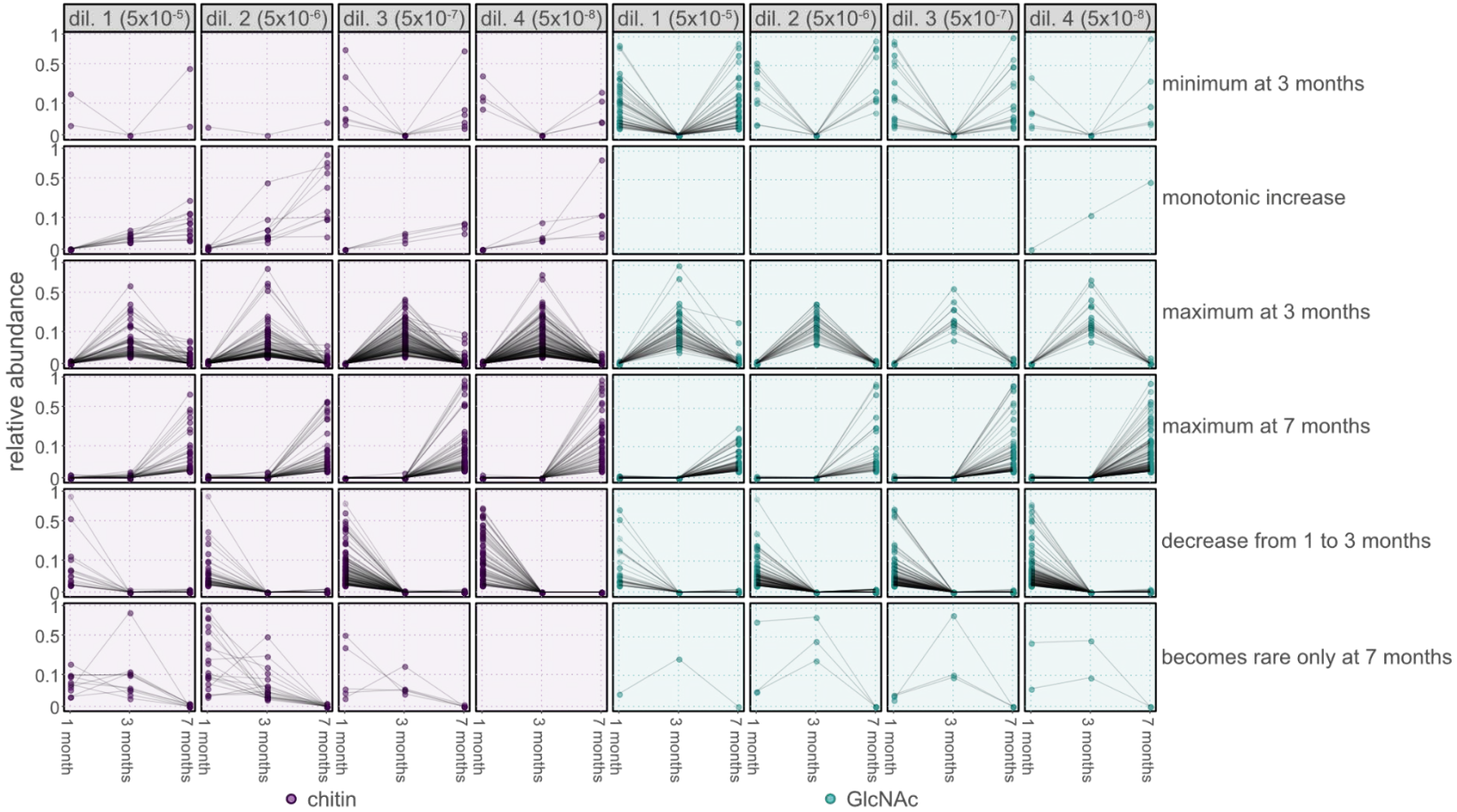

Supplemental Figure 6. Shifts in rare genus relative abundance over time, separated by general temporal trends (rows). Rare genera here are defined by any genus that was at less than 0.1% relative abundance at any time point.

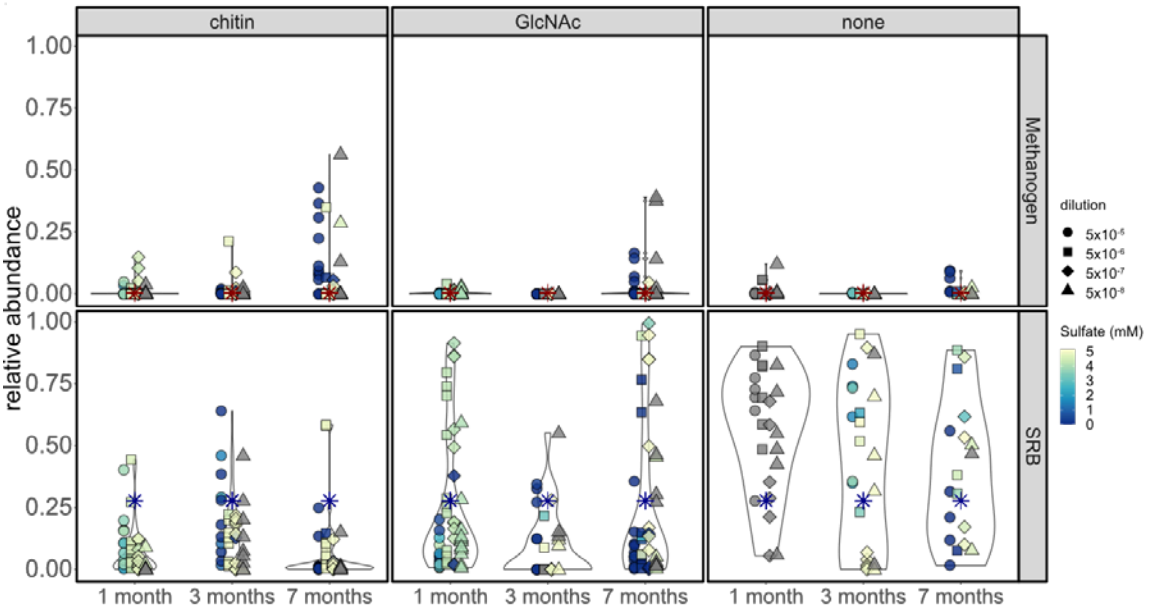

Supplemental Figure 7. Relative abundance of inferred methanogenic (top) and sulfate-reducing (bottom) taxa with 16S sequencing data. Point fill corresponds to sulfate concentration within each replicate and shape corresponds to dilution. Asterisks correspond to total relative abundance of these taxa in the source sediment.

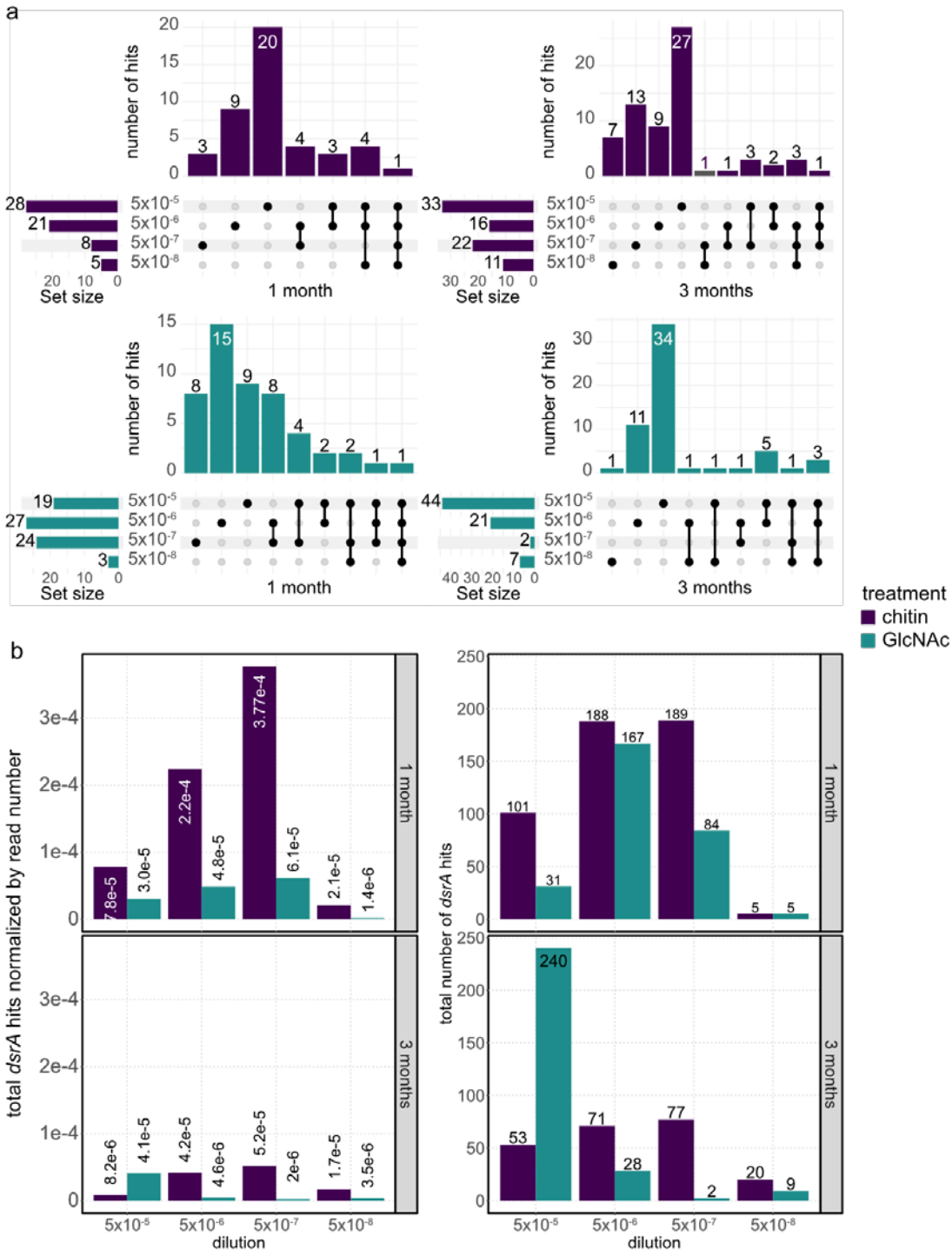

Supplemental Figure 8. (a) Mined sulfite reductase genes (*dsrA*) predominantly correspond to taxonomically unique hits within each dilution. Rows and bar color indicate supplied electron donor; columns indicate incubation time. Dot plots indicate combinations of dilutions with shared hits. Set sizes correspond to the number of unique hits per dilution. (b) Total number of *dsrA* hits mined from metagenomic sequences (right) and normalized by read number (left). With the exception of the lowest dilution at the second time point, chitin treatments contain more *dsrA* gene hits per read number than GlcNAc.

Supplemental Table 1. Per-treatment dissimilarity metric (ANOSIM R statistic) shows a maximum dissimilarity between chitin and GlcNAc treatments at three months in active incubations. Significant values are marked (** p<0.001; italics are not statistically significant).

	1 month	**3 months**	**7 months**
All incubations	0.241**	0.276**	0.167**
Active incubations	0.1875**	0.611**	*-0.035*

Supplemental Table 2. Means and standard deviations of per-dilution richness (Chao1) calculated from 16S rRNA gene amplicon sequence data. Samples with low read abundance were excluded from all analyses as described in Methods.

Chitin

DILUTION	TIME POINT	μ_{CHAO1}	σ_{CHAO1}	n
DIL 1 5x10^{-5}	1 month	40.25	15.65	12
DIL 2 5x10^{-6}	1 month	36.50	12.83	12
DIL 3 5x10^{-7}	1 month	22.33	11.39	12
DIL 4 5x10^{-8}	1 month	12.83	6.71	12
DIL 1 5x10^{-5}	3 months	57.36	22.44	11
DIL 2 5x10^{-6}	3 months	33.40	10.82	10
DIL 3 5x10^{-7}	3 months	23.36	19.06	11
DIL 4 5x10^{-8}	3 months	22.64	31.78	11
DIL 1 5x10^{-5}	7 months	46.00	16.69	11
DIL 2 5x10^{-6}	7 months	23.64	6.41	11
DIL 3 5x10^{-7}	7 months	23.82	9.60	11
DIL 4 5x10^{-8}	7 months	12.73	3.47	11

GlcNAc

DILUTION	TIME POINT	μ_{CHAO1}	σ_{CHAO1}	n
DIL 1 5x10^{-5}	1 month	29.00	11.39	12
DIL 2 5x10^{-6}	1 month	25.36	8.54	11
DIL 3 5x10^{-7}	1 month	26.58	11.74	12
DIL 4 5x10^{-8}	1 month	27.17	9.31	12
DIL 1 5x10^{-5}	3 months	6.44	4.00	9
DIL 2 5x10^{-6}	3 months	5.00	2.00	8
DIL 3 5x10^{-7}	3 months	3.80	1.10	5
DIL 4 5x10^{-8}	3 months	4.33	2.07	6
DIL 1 5x10^{-5}	7 months	52.18	11.10	11
DIL 2 5x10^{-6}	7 months	54.27	7.02	11
DIL 3 5x10^{-7}	7 months	30.00	12.16	11
DIL 4 5x10^{-8}	7 months	35.33	18.64	12

Supplemental Table 3. Sulfate concentration does not correlate strongly with diversity (richness). The table lists multiple linear regression analysis with R^2 and p values reported for each treatment/time point pair using model Chao1~[Sulfate].

TREATMENT	TIME POINT	R^2	p
GlcNAc	1 month	0.017	0.389
GlcNAc	3 months	0.092	0.182
GlcNAc	7 months	0.041	0.228
Chitin	1 month	0.205	3.36E-03
Chitin	3 months	0.452	9.8E-03
Chitin	7 months	0.510	1E-06

LIST AND DESCRIPTION OF SUPPLEMENTAL FILES

ch1_sulf_supplement_simper_active_bytreatment.xlsx: Similarity Percentage (SIMPER) analysis on significant ANOSIM analyses listing contribution of different genera to dissimilarity between chitin and GlcNAc treatments at each time point. Non-statistically significant rows ($p>0.05$) are italicized.

ch1_sulf_supplement_tab_functionalgroups.xlsx: a tabulation of the taxonomy data assigned to the "methanogen" or "SRB" functional groups.

ch1_gen_by_dil_by_t_act_module_colors.cys: A Cytoscape 3 session file for co-occurrence networks of 16S rRNA gene sequence data agglomerated by genus for active incubations. A network for each dilution, treatment, and time point was constructed.

ch1_sulf_supplement_active_fs_mcode_srbch4.xlsx: a tabulation of the data found in Figure 6, including the total number of MCODE-generated clusters, the total number of clusters containing nodes with methanogenic taxa, and the total number of clusters containing nodes in the Desulfobacterota for each treatment, time point, and dilution.

DsrA_gtdb_r202_sequences_clean.txt: GTDB release 202 amino acid sequences of DsrA pulled using a constructed DsrA HMM.

McrA_gtdb_r202_sequences_clean.txt: GTDB release 202 amino acid sequences of McrA pulled using a constructed McrA HMM.

Chapter 2

THE IN SITU RESPONSE OF DEEP SEA SEDIMENT COMMUNITIES TO COMPLEX CARBON LOADING

Sujung Lim[1], Ranjani Murali[2], Alexandra Z. Worden[3], Victoria J. Orphan[1,2]

[1] Division of Geological and Planetary Sciences, Caltech, Pasadena, CA 91125
[2] Division of Biology and Biological Engineering, Caltech, Pasadena, CA 91125
[3] Monterey Bay Aquarium Research Institute, Moss Landing, CA 95039

ABSTRACT

Seafloor communities are critically important to global carbon turnover and sequestration. Most of the carbon available for marine sediment communities is sourced from surface organic material sinking through the water column. With depth, this organic matter becomes less abundant and progressively more recalcitrant as labile elements are mineralized. Whale falls, in contrast, represent large episodic delivery of organics directly to the seafloor. These events result in a disturbance of the local sediment microbiome as the redox potential and geochemistry changes dramatically. Here, we assess how the seafloor sediment community at a 1000 m deep former whale fall site in Monterey Submarine Canyon responds to influxes of complex carbon. We used novel in situ seafloor injector core incubations and ex situ microcosm bottle experiments amended with the insoluble aminopolysaccharide chitin as our model carbon source. We demonstrated a consistent depth-dependent response by the sediment microbial community to chitin supplementation with a local maximum in single-cell translational activity (assessed by bio-orthogonal noncanonical amino acid tagging,

"BONCAT"). Moreover, the microbial community structure of these in situ injector core incubations at depth exhibited a consistent increase in richness over time (determined by 16S rRNA gene sequencing analysis). Finally, despite large early differences in the geochemical response between the ex situ laboratory microcosms and in situ seafloor incubations, over time the ex situ and in situ incubations had convergent patterns in their activity and community structure, suggesting that microcosms in the laboratory are in some ways good models for tracking the deep sea sediment microbial response to complex carbon loading.

INTRODUCTION

Marine sediments are a major contributor to the carbon and nutrient budget of the planet. While far removed from the sunlit, productive surface ocean, it is an enormous carbon reservoir, storing twice as much carbon as terrestrial soils at an estimated 2322 versus 1325 Pg C (Atwood et al., 2020; Köchy et al., 2015). Moreover, despite the extreme conditions of high pressure, low temperature, and slow rates of microbial metabolism, deep sea sediments are a major contributor to global carbon cycling through particulate organic matter remineralization or burial, CO_2 sequestration, and microbial metabolic activity.

Much of the organic matter input to the deep sea is in the form of marine snow; however, events such as whale falls transiently input massive amounts of organic matter in localized seafloor environments, equivalent to as much as 2000 years of marine snow deposition (C. R. Smith & Baco, 2003). This large carbon input alters the microbial and animal communities for months to years, representing a hotspot in biomass and activity relative to the surrounding

deep sea environment (Goffredi & Orphan, 2010; Lundsten et al., 2010; C. R. Smith & Baco, 2003). Previous work has documented the temporal community dynamics of phytodetrital supplementation of the marine sediment surface. Here, stimulation of deep marine sediments through organic loading manifested differentially over time. Uptake of isotopically-labeled input and other activity responses were observed on the order of days to weeks while other signals such as increased microbial biomass were only observed over longer periods of time of up to a year (Belley & Snelgrove, 2017; Kanzog et al., 2008; Kanzog & Ramette, 2009; Witte et al., 2003). Interestingly, the rapid activity response may be attributed to eukaryotes such as Foraminifera or benthic meiofauna while the bacterial or archaeal community utilized more degraded material on longer time scales (Belley & Snelgrove, 2017; Moodley et al., 2002; Witte et al., 2003). However, the extent to which specific organic material input affects existing anaerobic subsurface sediment microbial communities in situ especially in comparison to ex situ incubations is less well studied (e.g., Wirsen & Jannasch, 1986).

The sensitivity of the seafloor sediment community to disturbances such as a large influx of carbon is an outstanding and relevant question. In soil communities, the response of the local community to perturbations is thought to be a reflection of the both the taxonomic microbial diversity and their distribution of functions (Chaer et al., 2009; Girvan et al., 2005; Griffiths & Philippot, 2013). Specifically, a wider range of functional or taxonomic diversity present is hypothesized to mitigate the effects of a disturbance on the community. These perturbations can range from wildfire events (S.-H. Lee et al., 2017) to organic

supplementation (e.g., Kurm et al., 2019). Previous work (Shade, Peter, et al., 2012) has shown that the microbial community response to perturbation cannot be generalized to different environments and may depend on a variety of factors. For example, while environmental perturbations appear to have an outsized effect on soil microbial communities Allison & Martiny, 2008, freshwater and marine microbial communities are either less sensitive to ('resistant') or recover more quickly from ('resilient') disturbances (Baho et al., 2012; Jones et al., 2008; Shade, Read, et al., 2012). Additionally, the timescale of the perturbation (e.g., short-term "pulse" versus sustained "press" events) may contribute to a differential response as communities either oscillate around the original state or re-equilibrate to the new condition (DeAngelis et al., 2010; S.-H. Lee et al., 2017; Shade, Read, et al., 2012).

Most deep sea microbial experiments are conducted ex situ with shipboard or laboratory incubations (e.g., Hoffmann et al., 2017). Only a few have been conducted directly on the seafloor (e.g., Case et al., 2017; Edwards et al., 2003; Kanzog & Ramette, 2009; Witte et al., 2003) or have directly assessed the differences between in situ incubations and ex situ microcosm incubations. It is currently not well understood how relevant ex situ microcosms are to the community response in situ. To address this knowledge gap, we compared the response of in situ seafloor incubations and laboratory microcosm experiments to a complex carbon pulse in the form of chitin, an insoluble aminopolysaccharide that is among the most abundant biopolymers in the marine regime (Souza et al., 2011). The in situ experiments were conducted at a former whale fall site over a period of seven months, while the ex situ

experiments utilized sediment from the same site in laboratory bottle incubations. Changes in microbial community composition and activity were then tracked in response to the initial disturbance for three different periods of incubation (one, four, and seven months) at different sediment depths.

RESULTS

To determine the effect of chitin amendment on the in situ deep sea sediment microbial community at a former whale fall site, we use a remotely operated vehicle (ROV)-deployed novel injector sediment core system which delivered chitin directly to the seabed sediments (average depth of injection approximately 7 cm). Injector core experiments were collected after a period of one, four, and seven months (Fig. 1a, 1b). In addition to chitin, each injector core was amended with a combination of activity and chemical tracers including 0.5 mM L-homopropargylglycine (HPG), an alkyne-functionalized methionine analog acting as a tracer for single cell translational activity by bio-orthogonal noncanonical amino acid tagging ("BONCAT"; Hatzenpichler & Orphan, 2015), and 20 mM sodium bromide as an inert tracer to assess the amount and distribution of the injected fluid. The injected fluid was osmotically balanced with seawater using sodium chloride, and an estimated 9 mL was delivered into the sediment. Triplicate cores were deployed for each treatment (chitin and a no-carbon control) and incubation time period with an additional triplicate set of injector cores amended with monomer GlcNAc for the one-month incubation for a total of 21 injector cores at the site (Fig. 1b).

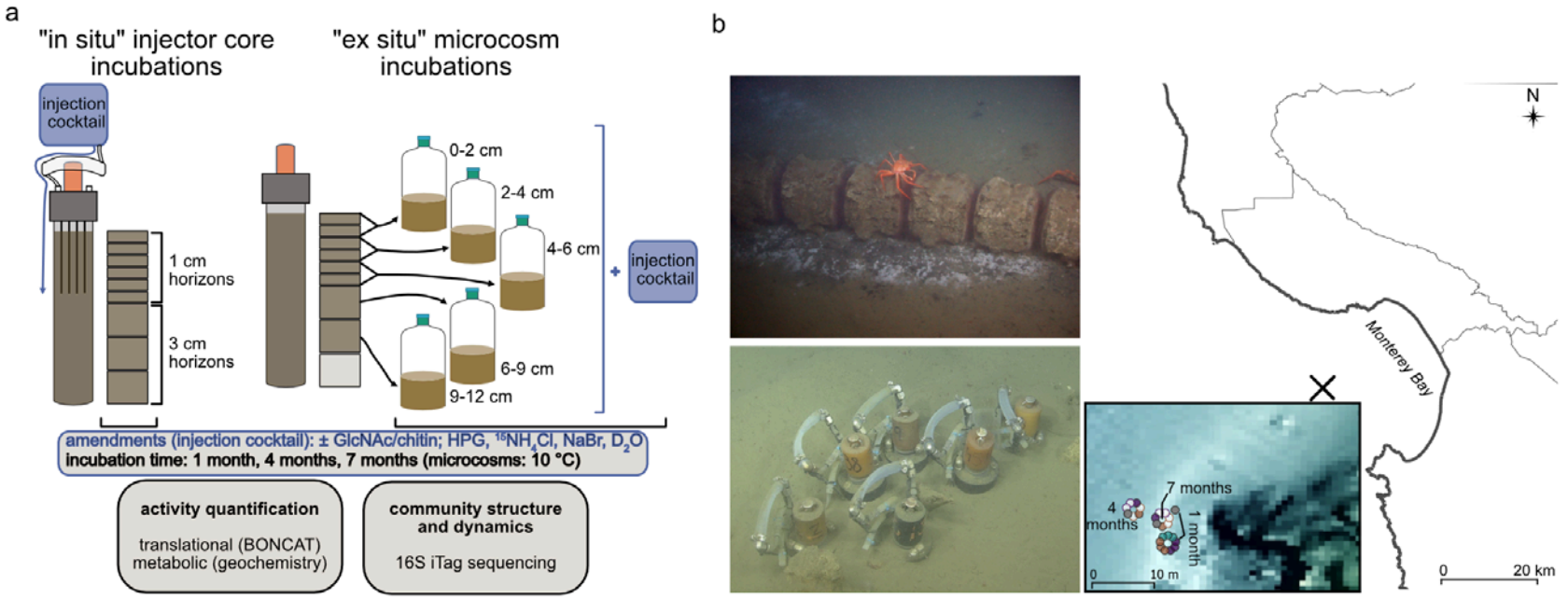

Figure 1. (a) Experimental setup of in situ injector core incubations and ex situ microcosm incubations. (b) Upper left: whale fall site showing vertebrae and sulfide-oxidizing mats thirteen months after emplacement (November 2005). Lower left: whale fall site with injector cores (December 2018); a degraded whale vertebra are visible in foreground of photo. Right: map of sample site (location denoted by "x") with inset showing core sampling schema on bathymetric data; filled circles are the subset of cores processed for 16S rRNA gene sequencing.

A separate sediment push core was collected adjacent to the injector cores during each of the in situ incubation experiment deployments and used for parallel ex situ microcosm experiments established in the laboratory 8-35 days after collection with the same carbon amendments as the injector cores. These incubations were partitioned into discrete depth horizons (from two to three cm thick) and incubated under anoxic conditions in 10 mL serum bottles at 10 °C with 6 mL of headspace over the same timeframe as the in situ experiments. Sampling for all experiments was destructive with each time point representing an independent incubation. Subsampling for both sets of incubations included geochemical analysis of major ions, frozen sediment for DNA extraction, and paraformaldehyde (PFA) fixed sediments for BONCAT (Hatzenpichler & Orphan, 2015). Due to sample processing constraints, we initially analyzed three replicates at the one-month time point but then focused on a single replicate for each subsequent time point and treatment, with each in situ injector core subsampled into eight to ten discrete depth horizons. This translated into 136 total samples for the in situ data set and 75 samples for the parallel ex situ microcosm experiments.

Geochemical analysis of the major anions and cations allowed determination of the chitin supplementation response as well as the extent to which the activity tracer and injection cocktail was distributed within the sediment column during the in situ incubation. Sodium bromide was used as a conservative tracer to calculate the concentration and distribution of the amendment cocktail within each core. The peak bromide concentration (1.7 mM) in the porefluids across all cores was seen at the 5-6 cm depth horizon of the injector core without

added carbon at one month; the majority of injector cores showed elevated bromide concentrations relative to the background (Fig. 2; Supp. Fig. 1). Accounting for in situ porewater bromide concentrations, the maximum extent of bromide enrichment was approximately 4.5% of the total concentration within the cocktail, corresponding to a maximum dilution factor of 22 with background porefluids. Sediment community composition was assessed in the injector cores using 16S rRNA gene iTag sequencing (Caporaso et al., 2012). Corresponding microbial anabolic activity was assessed using BONCAT, fluorescently counting the percent of cells that had actively assimilated the methionine analog HPG (Hatzenpichler & Orphan, 2015).

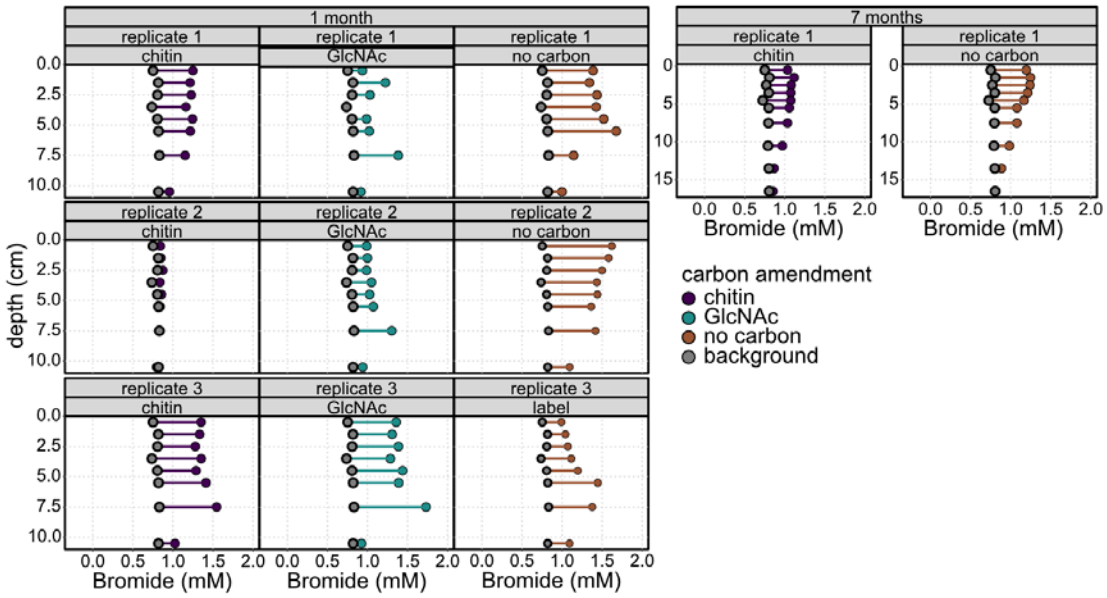

Figure 2. Concentrations of the passive tracer bromide document the amount and distribution of injection cocktail in the in situ injection core experiments at the one-month (left) and seven-month (right) incubations. Horizontal lines describe the extent of the bromide spike relative to an unamended background core (grey).

Ex situ incubations have a stronger chitin-driven metabolic and community response compared to in situ incubations

Because changes in the concentration of insoluble chitin are difficult to quantify directly in sediment incubations, we instead tracked the chitin degradation process through quantification of its expected degradation products, acetate and ammonium (see Chapter 1). The analysis of major ions from the in situ and ex situ incubations after one and seven months allowed us to determine the extent of substrate utilization through the accumulation of these products. We observed tenfold greater acetate and ammonium accumulation in the ex situ microcosms versus in situ (Fig. 3), with the highest amount of both acetate and ammonium (26.6 mM and 24.6 mM respectively) measured in the chitin-amended treatments. The maximum values of acetate and ammonium in the chitin treatments were not contemporaneous, with the high accumulation of acetate (26.6 mM) present only at the one-month incubation. In contrast, the ammonium concentration increased by as much as 15 mM in all measured ex situ incubations between one and seven months. These results are distinct from those seen in the diluted sediment incubations in Chapter 1, where chitin-amended incubations at the $5x10^{-5}$ dilution of sediment accumulated the maximum concentration of acetate and ammonium at the one-month time point. Chitin-amended ex situ incubations additionally demonstrated nearly complete sulfate drawdown at all but the lowest depth horizons by one month of incubation with full sulfate utilization by seven months of incubation (Fig. 3). The asynchronicity in the ammonium and acetate peaks in these ex situ incubations was also indicative of greater utilization of acetate coupled to sulfate reduction

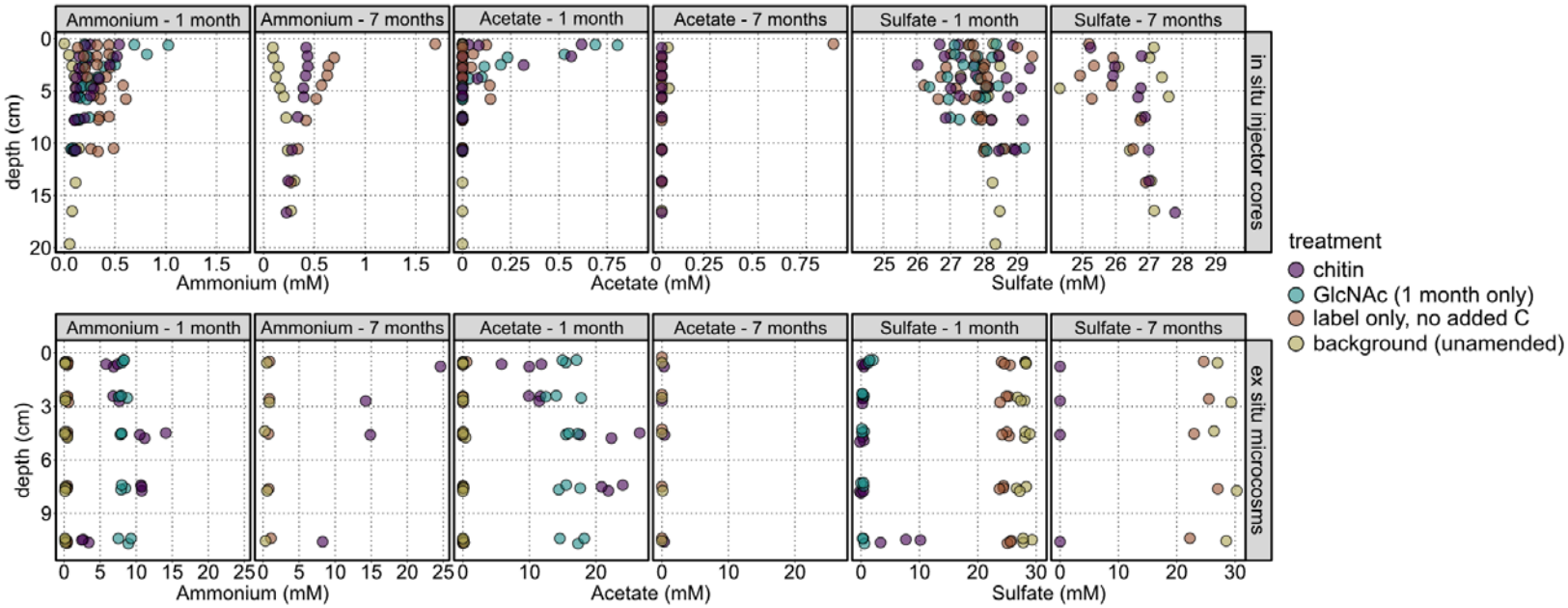

Figure 3. Ammonium, acetate, and sulfate data from both the one and seven month incubations demonstrated tenfold higher chitin and GlcNAc metabolism in ex situ laboratory microcosms (bottom) versus in situ injector core incubations (top). Moreover, there wasa complete to nearly complete sulfate drawdown in carbon-amended microcosms (rightmost two columns of plots).

early on, followed by continued substrate breakdown and subsequent acetate drawdown from terminal end members such as methanogens upon sulfate depletion. The 6-9 cm ex situ incubation was excluded from the dataset due to technical issues.

In contrast, carbon-amended in situ incubations had a more modest response, with little change in sulfate concentration over seven months of incubation and accumulation of low-millimolar concentrations of acetate and ammonium at less than 1/10 of what was observed ex situ. The ammonium profile in all amended in situ incubations was distinctly enriched relative to the background push core at shallower depths (Fig. 3, Supp. Fig. 2). The maximum concentration of acetate and ammonium (0.89 mM and 1.7 mM, respectively) was seen at seven months of incubation, surprisingly in the injector core with no added carbon (Fig. 3). Although ^{15}N-labeled ammonium was added to the amendment cocktail, we expected the impact of this addition to be minimal given the dilution of the amendment mixture into the greater volume of the injector core (<0.2 mM). The high amount of both metabolites seen in these non-chitin-amended injector cores at seven months relative to the background push core suggest a slow degradation response of endogenous organic matter stimulated by the injection cocktail.

Consistent with the geochemical evidence of active microbial degradation of chitin in the microcosm experiments, the addition of chitin was also found to contribute to the dissimilarity in community composition at both four and seven months of incubation. Moreover, while both in situ and ex situ chitin incubations were highly dissimilar from each other early on, this difference decreased by seven months, with neither the experiment type

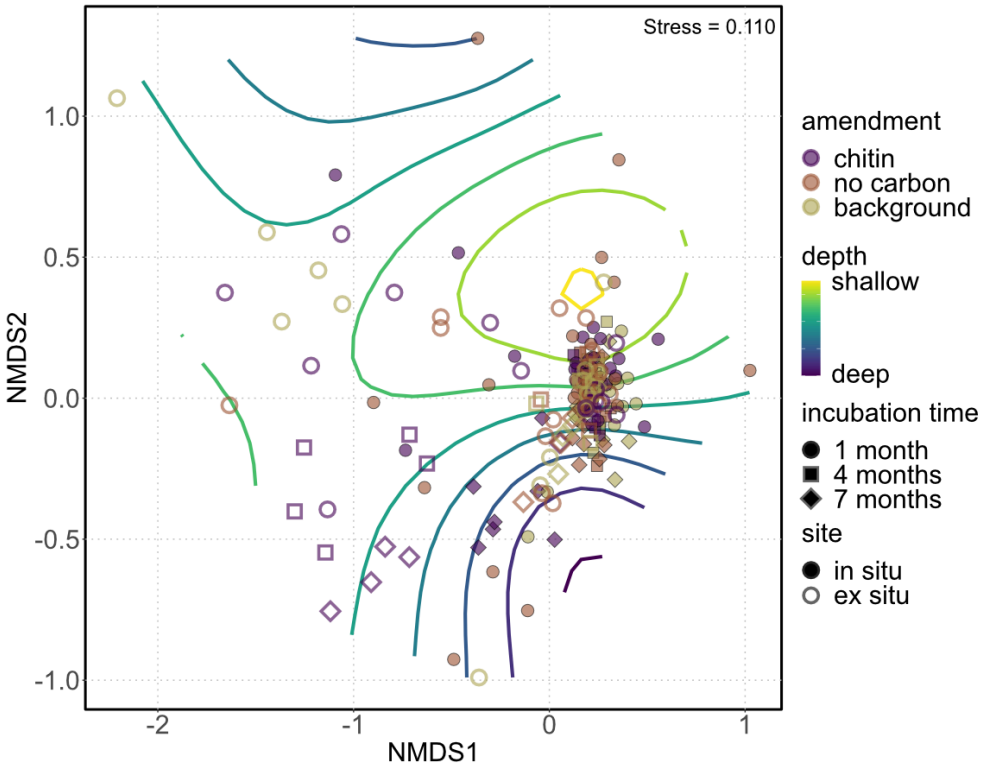

Figure 4. NMDS plot on square-root-transformed relative abundance data demonstrated 16S community dissimilarity driven by amendment in ex situ microcosm incubations early on. Chitin amendment resulted in a convergence of dissimilarity between in situ seafloor incubations and microcosms. Depth contours showed a depth-dependent contribution to dissimilarity with the greatest effect at the earliest (one month) incubation. Statistically significant contributions ($p<0.05$) of locale, depth, or amendment to dissimilarity at each time point are tabulated below; there were no statistically significant contributions of either factor to dissimilarity between chitin-amended treatments at the seven-month incubation.

Contributors to dissimilarity over both chitin and no-carbon samples ($p<0.05$)

Incubation time	site	depth	amendment	site:amendment
1 month	1.94	2.92	–	–
4 months	–	–	2.14	–
7 months	2.52	–	–	1.85

Contributors to dissimilarity in chitin-amended treatments only ($p<0.05$)

Incubation time	site	depth	site:depth
1 month	1.99	–	–
4 months	3.85	–	–
7 months	–	–	–

(in situ versus ex situ) nor depth contributing significantly to the dissimilarity between groups. Remarkably, at this final time point, microbial community composition of the in situ incubations converged toward the ex situ incubations (Fig. 4). This convergence of chitin-amended incubations was in contrast to the no-carbon control incubations and the unamended incubations, which all exhibited similar patterns of dissimilarity over time (Supp. Fig. 3). The perturbation of the sediment microbial community with chitin therefore appears to provide a consistent driving force shaping community composition both in bottle incubations and in situ on longer time scales.

Response of in situ single cell BONCAT activity to carbon amendment varies with sediment core depth

Translationally active cells within the injector cores were determined using BONCAT, enabling quantification of the percentage of microbial cells that had assimilated the methionine analog HPG during the in situ incubation. One replicate core was run at a subset of depths at each time point (Fig. 5). We observed the highest percentage of BONCAT positive cells at one month in chitin-amended incubations, with a maximum of over 20% of the total $7x10^8$ cells/mL displaying anabolic activity in the 3-4 cm depth horizon (Fig. 5). Although the cell counts were 6x lower in the chitin-amended incubation in the next adjacent depth horizon, they had a similarly high activity percentage. The BONCAT activity peak with depth at one month was not observed in the control injector cores without carbon, averaging 5.2% of $2.9x10^8$ cells active (Fig. 5). BONCAT activity in chitin-amended injector

cores at the other two time points was much lower, suggesting a transient early spike in cellular activity potentially in response to the initial chitin pulse. Control incubations without carbon amendment at the 5-6 cm depth horizon additionally appeared to be stimulated by the injection cocktail over time and had more active cells than the chitin amendments at four and seven months of incubation.

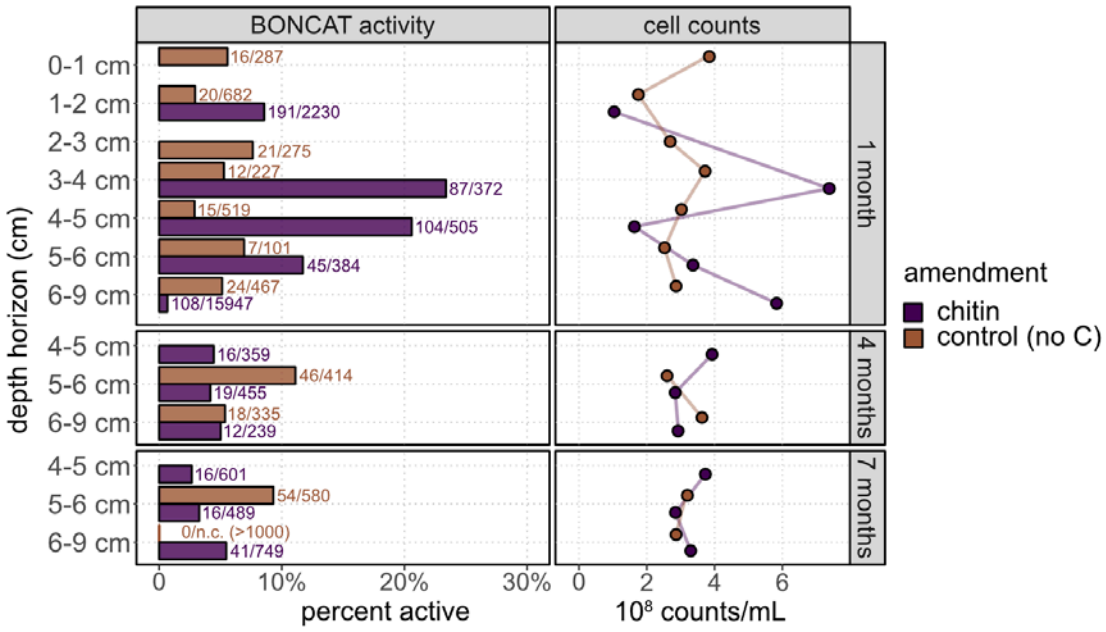

Figure 5. BONCAT counts show a depth- and amendment-dependent difference in single-cell translational activity that is not solely dependent on cell density (right plot). Barchart (left) shows percent of BONCAT-active cells in injector cores (in situ) cells at each depth horizon counted. The proportion of active cells counted per total number of cells counted in the BONCAT experiment is labeled next to the bars. The line plot (right) displays the cell count data for Percoll-separated sediment incubations. The highest extent of activity was in chitin-amended incubations at 3-5 cm depths, coincident with high bromide concentrations, suggesting an active community response to the carbon load.

Shifts in community structure and composition follow a depth-dependent trend in situ

By comparing chitin-amended to the control injector core incubations, we were able to assess the effect of chitin amendment on community structure independent of the addition of the injector core cocktail. In agreement with the activity patterns seen with depth, there was a strong depth-dependent trend in alpha diversity. Chitin-amended depth horizons ≥5 cm below surface exhibited a dynamic change in richness between the one, four and seven month incubations. While shallower sediment horizons (0-4 cm) largely became more rich over time, the deeper horizons dynamically increased and then decreased in diversity compared to the averaged control incubations (Fig. 6).

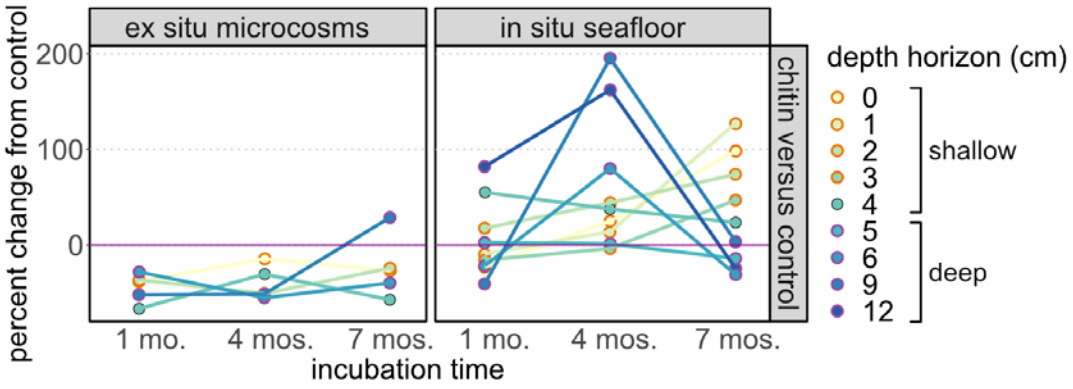

Figure 6. Shifts in community structure between treatment and control incubations exhibit a depth-dependent response in seafloor incubations. Lines show the change in Chao1 richness from the averaged control (after Chaer et al., 2009) in replicate one, with colors corresponding to the depth of the sediment horizon in the incubation. The temporal pattern shifts in the in situ injector cores at the 4-5 cm depth horizon, with shallower horizons (orange outlines) generally increasing in diversity relative to the control and deeper horizons (purple outlines) having an inflection point at the four month incubation. The purple horizontal line denotes no change in richness between the control (no carbon) and chitin-amended incubations.

We conducted an indicator taxon analysis (De Cáceres et al., 2010) in order to determine what genera, if any, were a statistically significant indicator of the response to carbon amendment. Following the differential diversity patterns by depth, the analysis grouped depths from incubations below 4 cm ("deep") and from 4 cm and above ("shallow"). The majority of these "indicator genera" were seen in in situ seafloor incubations in "deep" sediment horizons (Fig. 7, left). The strength of the association between the indicator taxon and carbon amendment was quantified at each time point using a point biserial correlation coefficient (De Cáceres et al., 2010). Only statistically significant indicator taxa are shown; therefore, the higher number of indicator taxa highlighted in the deeper sediment horizons

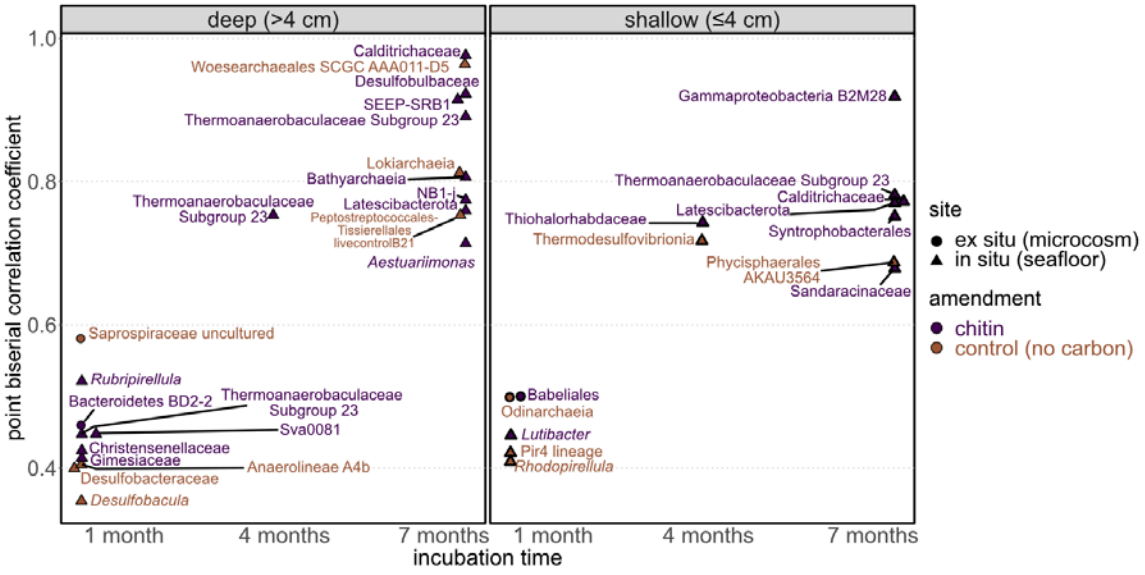

Figure 7. Genera contributing to differences in the amendment-specific community signal divided into deep (>4 cm) and shallow sediment horizons as determined through indicator taxon analysis (de Cáceres et al., 2010). Genera (or next highest taxonomic level) were statistically significant ($p<0.05$) indicators of the differential microbial response between chitin amendment and the no-carbon control. The point biserial correlation coefficient describes the strength of the correlation between the the taxon and the amendment at each time point with larger values corresponding to a higher correlation strength. Colors correspond to which treatment taxon presence is indicative of; shapes correspond to in situ injector core (triangles; n=32) or ex situ (circles; n=4) microcosm incubations.

indicated that these microbial communities exhibited a taxonomically robust response to chitin enrichment (Fig. 7).

The samples with the greatest range of diversity differences between in situ treatments — the four-month incubation — only had one statistically significant indicator taxon correlated to chitin amendment at each range of depths (Fig. 7). In incubations below 4 cm depth, this was a putative chemoheterotroph belonging to the Thermoanaerobaculaceae (Subgroup 23), an indicator genus also identified in the one- and seven-month chitin incubations. In the shallower incubations, this was a member of the Thiohalorhabdaceae. The paucity of indicator taxa despite a high variance in richness at the four-month time point suggested that the majority of the contribution to differences in community structure between the chitin-amended and control incubations is not taxonomically constrained to individual genera. Instead, it was likely a product of the combination of many distinct taxa at different depths.

In the ex situ microcosm incubations, the same strong dynamic signal between sediment depths was not present (Fig. 6, left). Ex situ chitin incubations were comparatively less rich than the no-carbon control treatment over time with the exception of the deepest sediment horizon incubation — 6 cm — which increased in richness at the final time point (Fig. 6, left). Notably, this diversity increase was also concurrent with a decrease in sulfate reduction and lower acetate and ammonium accumulation compared to microcosm incubations from shallower depths, suggestive of lower chitin degrading activity in the 6-9 cm ex situ incubation (Fig. 2).

Community differences between carbon amendments and incubation sites

Following the changes in metabolic product and community structure, we analyzed the 16S rRNA gene sequences to determine taxa that were conserved and differentiated between amendments. To capture an overview of community members associated with a specific carbon amendment, we combined all time points for each amendment as well as the in situ/ex situ combination and summarized the common genera between each incubation set. All abundance data were presence-absence transformed, including rare taxa (below 0.1% relative abundance). Many genera appeared to be shared between all treatments and between in situ versus ex situ experiments (323 genera; Fig. 8). Of these genera, close to half (159) were additionally shared with an independent sediment dilution series experiment amended with chitin and sulfate that was inoculated with the same source sediment (see Chapter 1; Fig. 8). That so many genera were shared between these incubations irrespective of amendment could be due to a variety of factors. The factors contributing to the maintenance of diversity across changing conditions could be due to the presence of metabolic microniches or spatial effects resulting from the heterogeneity of sediment particles. The fact that over half the genera present at any treatment (site and amendment) were shared with the rest, suggesting a large “core microbiome”. This continuity of composition suggested that the differential geochemical response seen between, for example, chitin-amended in situ and ex situ incubations may have been caused by a small subset of unique community members.

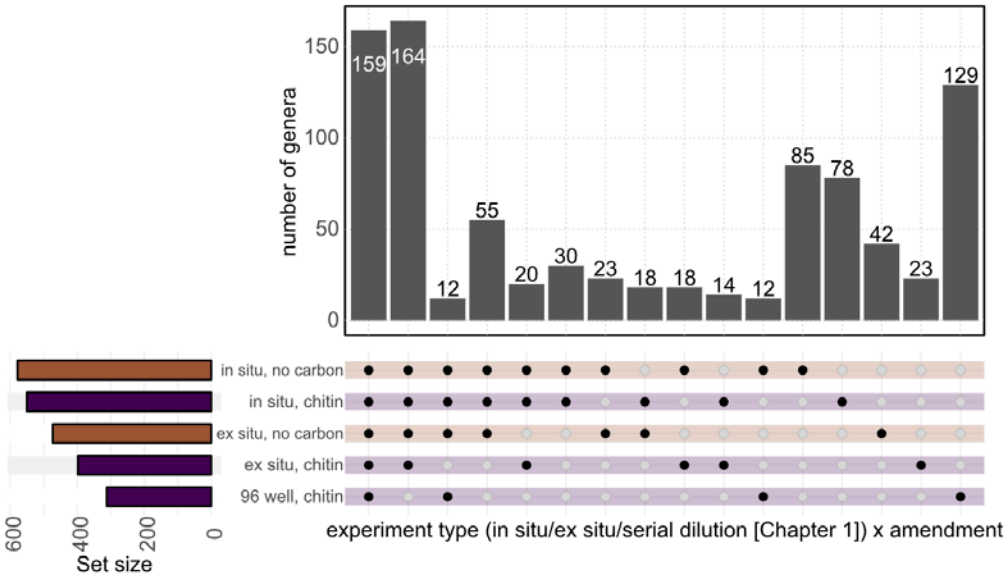

Figure 8. Upset plot demonstrating number of shared genera between site/treatment pairs, calculated from presence-absence transformed abundance tables. 164 genera are shared between all treatments and all sites (in situ seafloor incubation vs ex situ microcosm) within this experiment, with an equivalent magnitude of genera additionally shared with a separate chitin-amended serial dilution experiment with a common inoculum as the microcosm experiments (see Chapter 1).

Indicator taxon analysis (De Cáceres et al., 2010) allowed us to further determine whether the community members that did contribute to the differences between amendments had a consistent taxonomic signal. Indeed, we observed a greater indicator taxon signal in chitin versus the control incubations with 24 of the 36 total genera being statistically significant indicators of chitin amendment overall (Fig. 6). Moreover, the in situ injector cores contained the most indicator taxa (32/36), the majority of which were uncultured. In both depth categories, these included putative heterotrophic lineages that may be representative of the community response to organic loading. We based this tentative physiological characterization from sequence-based similarities with cultured heterotrophic representatives and occurrence of these lineages in other organic-rich environments such as tidal flats and

estuaries. Candidate heterotrophic taxa included Thermoanaerobaculaceae Subgroup 23, Calditrichaceae, *Rubripirellula*, *Aestuariimonas*, *Lutibacter*, Gammaproteobacteria B2M28 group, and Latescibacterota (Albert et al., 2021; Bonch-Osmolovskaya & Kublanov, 2021; Howe et al., 2023; Kallscheuer et al., 2020; S.-Y. Lee et al., 2012; Losey et al., 2013; Park et al., 2018). Some taxa were known to be cosmopolitan in marine sediments such as the Bathyarchaeia (Kubo et al., 2012). Other indicator taxa in the chitin-amended in situ incubations included members which may contribute to other key metabolic processes during anaerobic polymer degradation including sulfate reduction, small fatty acid oxidation, and syntrophic interactions. These included members from the uncultured Desulfobacterota group Sva0081, Desulfobulbaceae, and Syntrophobacterales. The uncultured Desulfobulbaceae representative had 94.7% sequence identity with a 16S rRNA gene sequence within the deep marine sediment-associated incomplete acetate oxidizer genus *Desulfogranum*. The type species of this genus is, uncharacteristically, able to utilize disaccharides in conjunction with sulfate reduction, suggesting a direct linkage between polymer degradation and terminal respiratory processes in the seafloor (Galushko & Kuever, 2020; Sass et al., 2002). Some taxa were related to organisms capable of sulfur oxidation, such as Gammaproteobacteria B2M28 and Thiohalorhabdaceae (Cifuentes et al., 2000; Sorokin et al., 2017).

Genera that were associated with the no-carbon control incubations — both injector core and ex situ microcosms — included ubiquitous marine microbes such as uncultured Woesearchaeales, Lokiarchaeia, and Pirellulaceae Pir4 lineage genera. We predicted a

distinct microbial community response to chitin amendment for the in situ incubations including polymer degraders and sulfate reducers. However, we were surprised to also detect indicator taxa in the no-carbon control incubations. Genera that were associated with in situ control injector cores included putative complex carbon-utilizing heterotrophic families Saprospiraceae and Anaerolineae A4b (Kondrotaite et al., 2022; Petriglieri et al., 2023) as well as potential sulfate reducing taxa *Desulfobacula*, Desulfobacteraceae, and Thermodesulfovibrionia. This suggested that the injection cocktail itself, independent of the chitin amendment, may have had a stimulatory effect on the sediment microbial community. Near the end of the experiment in the seven-month incubation, the majority of indicator taxa were associated with chitin amendment within the in situ injector cores. Here, 8 of 11 indicator taxa were within the deep sediment horizons and 6 of 7 attributed to the shallow horizons. Carbon amendment was more strongly correlated with the indicator taxa in these longer-term incubations than in the one-month incubation, as seen with a higher calculated point biserial correlation coefficient for these indicator taxa (Fig. 7). The number and strength of associations observed points to the influence of chitin shifting microbial community composition over time, enriching for taxa that can utilize the provided substrate in seabed sediments.

To corroborate the results from the indicator taxon analysis, we also employed an independent ANOSIM and SIMPER analyses to identify taxa that were driving the differences between our incubations. These results were in broad agreement with the indicator taxon analysis. Additionally, these analyses supported the observation of

convergent community dissimilarities at the final seven-month time point, with a value of 0.40 ($p<0.005$) for the ANOSIM R statistic of dissimilarity between in situ chitin and no-carbon control treatments at seven months. The top 17% of the dissimilarity at the final time point was contributed by the following SIMPER-determined taxa: Desulfobulbaceae, Thermoanaerobaculaceae subgroup 23, the phylum NB1-j, Latescibacterota, Gammaproteobacteria order BD7-8, Syntrophobacterales, Peptostreptococcales-Tissierellales genus livecontrolB21, Desulfosarcinaceae genus SEEP-SRB1, and the archaeal phylum Bathyarchaeia. These taxa all were statistically significant within the analysis ($p<0.05$) and were more abundant in chitin treatments with the exception of the Peptostreptococcales-Tissierellales taxon, which was more abundant in label-only treatments (Supp. Table 1).

DISCUSSION

An observation and outstanding methodological challenge in environmental microbiology is the plate count anomaly — past research has shown that only a fraction of environmental microbes are culturable (Staley & Konopka, 1985). Whether the culturable fraction is representative of the total local microbial community is a matter of great interest, as these laboratory-amenable species are often used to proxy ecological functions and interactions (Friedman et al., 2017; Harcombe et al., 2014; Kerr et al., 2002). Deep sea sediment microcosms necessarily result in multiple perturbations ranging from pressure and temperature shifts during sediment core recovery to the disturbance of the sediment matrix

through sediment collection and slurrying. The effects of these perturbations on the sediment microbial community is unclear, with some prior work suggesting contradictory responses to e.g., physical homogenization (Findlay et al., 1990; Kurtz et al., 1998). Using novel methodology involving injector cores that allowed for the direct perturbation of the subseafloor environment, our study consolidated in situ and microcosm incubations to determine whether in-situ microbial communities and the laboratory-amenable subset of these communities are comparable in functional behavior and composition.

We observed significant microbial activity with the addition of chitin in both in situ injector cores — as translational activity — and ex situ microcosm incubations — as metabolic activity — within one month of incubation. Notably, the maximum extent of activity at the one-month incubation was observed at adjacent depth horizons in the ex situ microcosms (4 cm) and in situ injector cores (3 cm) suggesting that there is a hotspot of primable microbes at this depth range. With in situ incubations, the highest activity was coincident with a maximum in cell counts from cells removed from the host sediment (Fig. 5). In situ incubations had an injection front that was localized near these depths (Fig. 2); however, the same concentration of label was added to all microcosm incubations during preparation. Therefore, the metabolic activity peak seen in the ex situ microcosms, and potentially also the in situ injector cores, was not solely due to the addition of the injection cocktail. Instead, there may be a depth-dependent structuring of the microbial community that is more responsive to our perturbation. We were able to determine taxa associated with chitin supplementation through our indicator taxon and SIMPER analyses (Clarke, 1993; De

Cáceres et al., 2010); although there was a strong metabolic response ex situ, the community signal was not statistically significant. In the closed system of the ex situ microcosm, metabolic products can accumulate rapidly while in situ injector cores are a more open system with a higher volume and free vertical diffusion of accumulated metabolites. The lack of consistent community response could then be due to stochastic factors shaping the microbial community in laboratory microcosms and the metabolic response uncoupled to community composition changes. For example, copiotrophic hetrerotrophs that are fast-growing may readily colonize and degrade chitin particles, resulting in the high accumulation of acetate and ammonium. However, if there is a large pool of potential competitive copiotrophs, stochastic effects would determine which member colonizes first, resulting in a selective sweep of the primary degrader and further downstream colonization effects culminating in distinct community trajectories between individual bottles. Particle heterogeneity in sediments or the structural complexity of substrates such as chitin may further support the separation of these communities.

In this chapter, we showed that the maintenance of microbial community diversity that we demonstrated across numerous replicates in ex situ incubations (in Chapter 1) is also relevant for in situ incubations. The demonstration that these communities remain robust to perturbation is of significant impact on our understanding of the “resilience” of marine microbial communities in the face of changing conditions. These results are consistent with earlier work on artificially implanted whale fall sites demonstrating a strong community

response to disturbance that slowly dissipates over time (Lundsten et al., 2010; C. Smith et al., 2014).

Although community composition did not have a unified relationship with metabolic activity either in situ or ex situ, there were consistent microorganisms that were stimulated in response to chitin addition. These community members were capable of relevant functions such as chitin degradation and sulfate reduction. In the in situ incubations, common taxa stimulated by chitin amendment included a few sulfate reducing genera such as *Desulfobacula* and some diverse genera associated with heterotrophy that may use the degradation products of chitin breakdown. Geochemistry data from the ex situ incubations also indicated the presence of an acetate sink after complete sulfate utilization that could be attributed to methanogenesis (Fig. 3). However, there was no evidence of methanogenic clades in our ex situ incubations despite prior studies from this whale fall site demonstrating the stimulation of methanogenesis near the seabed at the site of carbon loading (Goffredi et al., 2008). Acetate utilization in these sulfate-exhausted incubations could then be attributed to members below the detection limit of our analyses, or linked to cryptic oxidants through syntrophic processes (McDaniel et al., 2023; Szeinbaum et al., 2017).

Microcosm experiments are common in deep sea microbiological studies (Boetius & Lochte, 1994; Glombitza et al., 2016) and provide a laboratory-amenable method to probe the microbial ecology of these ecosystems. Our experiment showed that many genera were shared overall between in situ and ex situ incubations, indicating that a large percentage of deep sea taxa were retained under laboratory conditions (Fig. 8). However, the overall

community composition of the two experiment sets was very dissimilar and had differing alpha diversity patterns at the initial time points (Fig. 4, Fig. 6), suggesting that there are major differences in community assembly. Despite these differences, the activity patterns determined through single cell BONCAT activity in situ and changes in geochemistry ex situ at the one-month time point showed a consistent depth-dependent pattern. The highest number of BONCAT-active cells and most metabolite accumulation following chitin degradation in the ex situ incubations were at the same depth, indicating a consistency of community activity patterns despite laboratory incubation. Although chitin-amended in situ and ex situ communities had high early variability of activity and composition, by the final time point they converged (Fig. 4). These results suggest that while the microbial community in laboratory-maintained deep sea microcosms may differ from those in seafloor incubations, the larger trends of activity over depth are conserved. Prior reports studying the effect of disturbances ranging from sediment homogenization to surface organic loading on marine sediments have showed significant impacts on metabolic activity (Findlay et al., 1990; Hoffmann et al., 2017). We demonstrated that the microbial activity response to organic loading persisted below the seafloor surface and indeed is enhanced at depth (Fig. 5).

Future work will determine whether translational activity as well as metabolic activity has a depth-dependent response in ex situ microcosms. This would further support comparison of the two approaches — while ex situ incubations are more easily replicable and logistically less challenging, further work is needed to establish that they are a good proxy for environmental microbial interactions. Additionally, determining whether the community

composition-independent functional response in marine sediment to complex substrate loading was specific to chitin or is generalizable to atypical substrates and conditions would provide insight to the sediment community response to other pulse or press events. This is relevant to understanding the sediment community response to anthropogenic disturbances such as deep sea mining or oil spills on these critical environments (Haffert et al., 2020; Mason et al., 2014; Nogales et al., 2011).

METHODS

Sample collection and deployment of in situ incubations

Sediment cores were collected by ROV *Doc Ricketts* on R/V *Western Flyer* (owned and operated by Monterey Bay Aquarium Research Institute) on a series of cruises in Monterey Submarine Canyon, CA at a former blue whale carcass implanted in October 2004 at 1018 m depth (36.769873 N, 122.0829 W). The carcass, nearly fifteen years after emplacement, still contained intact, if degraded, vertebrae despite predictions of total degradation within a decade at this site (Fig. 1b; Lundsten et al., 2010) and the sediments were not sulfidic. See Supplemental Table 2 for a description of push core collection and injector core amendments. In situ incubations were deployed by introducing a cocktail of chemical and isotopic tracers (0.5 mM homopropargylglycine, 20 mM NaBr, 3.5% NaCl, 4 mM 10 at% $^{15}NH_4Cl$, and 1% D_2O) via a push core injector top directly to sediment adjacent to the vertebrae using ROV *Doc Ricketts*. A subset of cores at each time point was further amended with chitin (0.2 g added to 40 mL injection cocktail volume) or 10 mM N-acetylglucosamine. The injector core

assembly was developed by A. Worden's group at MBARI and consisted of a BioProcess container (Thermo Fisher) containing the amendment cocktail that is ultimately attached to stainless steel needles with perforated ends allowing injection into the sediment column. The injection is conducted through the ROV manipulator arm providing peristalsis of the amendment cocktail through 5.5" lengths of 1/2" x 1/8" ClearFlex 60 PVC tubing (Curbell Plastics). Check valves prevent backflow of the amendment cocktail. After injection, the assembly was left on the seafloor to incubate for one, four, or seven months before retrieval and processing.

All sediment cores were extruded shipboard from push core liners at 1 cm sediment horizons sampled down to 6 cm, after which 3 cm horizons were collected using polycarbonate spacer rings. The injector cores and a subset of standard push cores was then subsampled for DNA extraction, imaging, and geochemistry at each depth horizon. DNA sampling was done through transferring sediment with a sterile 1 cc cut off syringe to a 2 mLcryovial and stored at -80°C. Sediment was fixed for imaging by an overnight 4°C incubation of 0.75 mL sediment with 1 mL 1:1 4% paraformaldehyde:3x phosphate buffered saline (PBS) solution followed by two 3x PBS washes and resuspension in 1:1 3x PBS:100% ethanol. Fixed and washed sediment was then stored at -20°C. Sediment porewater for geochemistry was immediately extracted after core extrusion through centrifugation of 4 mL sediment at 16,100 x g for five minutes and subsequent supernatant filtration through a 0.2 µm 13 mm polyethersulfone syringe filter. During injector core sampling, the volume of the remaining

amount of amendment cocktail in the BioProcess containers and tubing was measured, allowing estimation of the quantity of amendment cocktail added in each injection.

A separate standard push core was extruded and the same depth horizons collected for ex situ incubations. These horizons were individually stored in Whirl-Pak bags (Nasco) and all bags sealed in Mylar under a purged argon atmosphere at 4°C. During core retrieval, seawater from immediately above push cores was also collected, filtered with a 0.2 µm Sterivex, and stored at 4°C for use with ex situ incubations.

Media design, conditions, and sampling of ex situ incubations

Collected sediment horizons were anoxically pooled in equivalent amounts in 2 cm increments down to 6 cmbsf. These 2 cm horizons as well as the 6-9 and 9-12 cm horizons were slurried 1:1 anoxically with N_2-sparged bottom water from the site where the sediment inoculum was collected. 4 mL of sediment slurry was added to each 10 mL serum vial and 0.4 mL of the injector core cocktail was added to each labeled incubation. 0.04 g chitin was added to each chitin-amended incubation and each GlcNAc-amended incubation contained 15 mM GlcNAc. Serum vials were incubated for one, four, and seven months at 10 °C before collection for DNA extraction, fixation for imaging, and geochemical analysis. 1 mL of slurry was stored in 2 mL cryovials at -80 °C for DNA extraction. 750 µL of slurry was fixed with 1 mL 1:1 4% paraformaldehyde:3x PBS overnight at 4 °C before two 3x PBS washes and resuspension with 1 mL 1:1 3x PBS:100% ethanol. Fixed and washed samples were

stored at -20°C. The remaining slurry was filtered through a 0.2 µm 13 mm polyethersulfone syringe filter for geochemical analysis.

DNA extraction and 16S rRNA amplicon sequencing analysis

DNA extractions were done with approximately 0.1 g wet weight sediment collected as described above using the PowerSoil kit (Qiagen). 16S rRNA gene iTag sequencing and downstream analysis was conducted as described previously using the 515F/926R primer set for the V4 hypervariable region (Chapter 1). Reads were processed through the QIIME2 pipeline with denoising done with DADA2 and singletons removed before taxonomy classification with the Silva 139 release. Dissimilarity analyses were done with the vegan package in R.

Geochemical analyses

Major anions and cations were quantified as described previously on the dual-channel ICS-2000 ion chromatography system (Dionex) using the AS19 and CS16 analytical columns (Speth 2022). Briefly, 0.2 µm-filtered samples were diluted 1:25 and run through the AS19 anions column with an isocratic method and the CS16 cations column through a gradient to optimize separation of the sodium and ammonium peaks (Green-Saxena et al., 2014). Samples were run at the Water and Environment Laboratory (Caltech).

Activity quantification, microscopy, and fluorescence in situ hybridization

PFA-fixed cells were separated from sediment using a Percoll density gradient (Orphan 2002). Briefly, 200 µL fixed sediment was added to 600 µL 1M TE (1M Tris HCl, 0.1 M EDTA pH 8) and 100 µL 100 µM sodium pyrophosphate and incubated at 60°C for 3 minutes. After cooling on ice, the sample was sonicated three times for 10 seconds at 4-6 W (power setting 3, Branson Sonifier 150 with C4333 style probe, Branson Ultrasonics, Dansbury, CT, USA) with a 10 second pause between each step. 1 mL of filter-sterilized (0.2 µm) Percoll was pipetted under the sample. After centrifugation at 16,000 x g for 20 minutes at 4°C, the upper aqueous layer, including the discolored layer with cells, is moved to a clean 2 mL microfuge tube (Eppendorf) then centrifuged again at 16,000 x g for 3 minutes at 4 °C. The supernatant was removed and pelleted cells are washed with 3x PBS by centrifugation at 16,000 x g for 3 minutes at 4 °C. The pellet was then resuspended in 100 µL 1:1 3x PBS:100% ethanol and stored at -20 °C.

Anabolically active cells were quantified using bio-orthogonal noncanonical amino acid tagging (BONCAT, Hatzenpichler & Orphan, 2015). Here, 10 µL Percoll-separated cells assimilating L-homopropargylglycine (HPG), an alkyne-functionalized methionine analog, were spotted on a PTFE-printed slide and were fluorescently labeled using an azide -containing Oregon Green dye with copper-catalyzed click reaction, which allowed cells to be visualized on the basis of their HPG uptake and incorporation into proteins. Cells were then overlaid with a 4.5 ng/µL DAPI solution in Citifluor AF1 (Electron Microscopy Services). Percent activity was assessed by counting Oregon Green-fluorescent cells and

DAPI-fluorescent cells in at least 15 fields of view at 60X. For cell counts, 10 µL of Percoll-separated cells were filtered with a 25 mm 0.2 µm polycarbonate filter (Millipore) with a 5 µm Durapore backing filter (Millipore). Filtered cells were washed with 0.2 µm filter sterilized 1x PBS and stained with the DAPI-Citifluor solution as above. For all microscopy, cells were visualized using an Olympus epifluorescence microscope with a 350 nm and 480 nm filter set and a 60X Plan Apochromat oil immersion objective.

ACKNOWLEDGMENTS

We are grateful to the crew of the R/V *Western Flyer*, the pilots of the ROV *Doc Ricketts*, S. Sudek (MBARI), R. Harbeitner-Clark (MBARI), A. Worden (MBARI), and the MBARI engineering team who developed the injector push core system, without whose expertise the in situ seafloor incubations could not have been conducted. We additionally thank S. Connon (Caltech) for assistance with 16S rRNA gene amplicon sequencing and R. Horak (Caltech) for assistance with Percoll-based cell separation. This work was supported by the Simons Foundation – Principles in Microbial Ecology (PriME) collaboration, by the Center for Dark Energy Biosphere Investigations (C-DEBI), and with ship time and support from Monterey Bay Aquarium Research Institute (MBARI).

SUPPLEMENTAL FIGURES AND TABLES

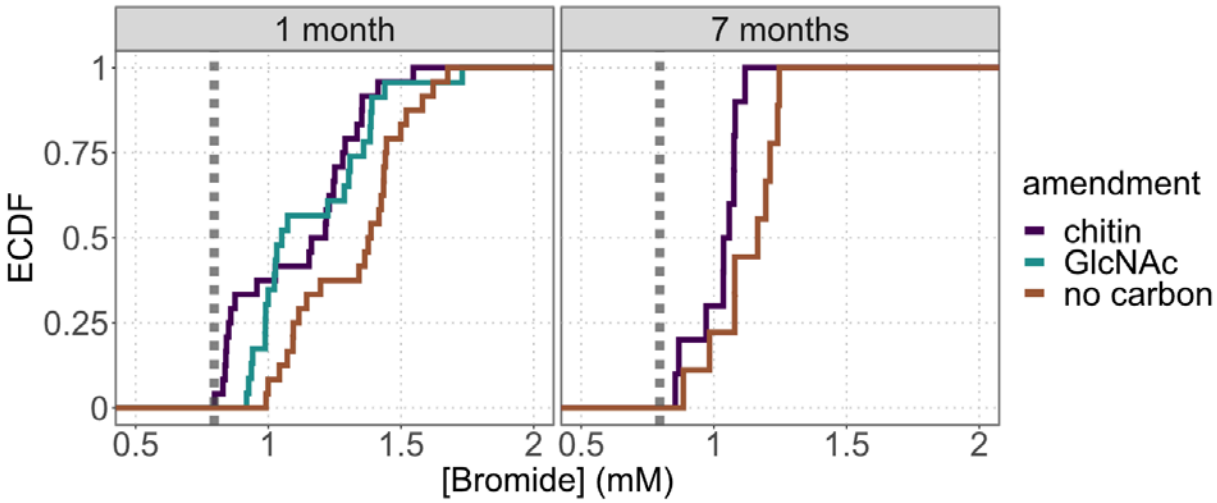

Supplemental Figure 1. Empirical cumulative density function (ECDF) showing distribution of porewater bromide concentration in injector cores over all depths for each treatment (colored lines). Nearly all injector cores exhibited bromide enrichment relative to the averaged background bromide concentration in a parallel unamended sediment core (dashed vertical line).

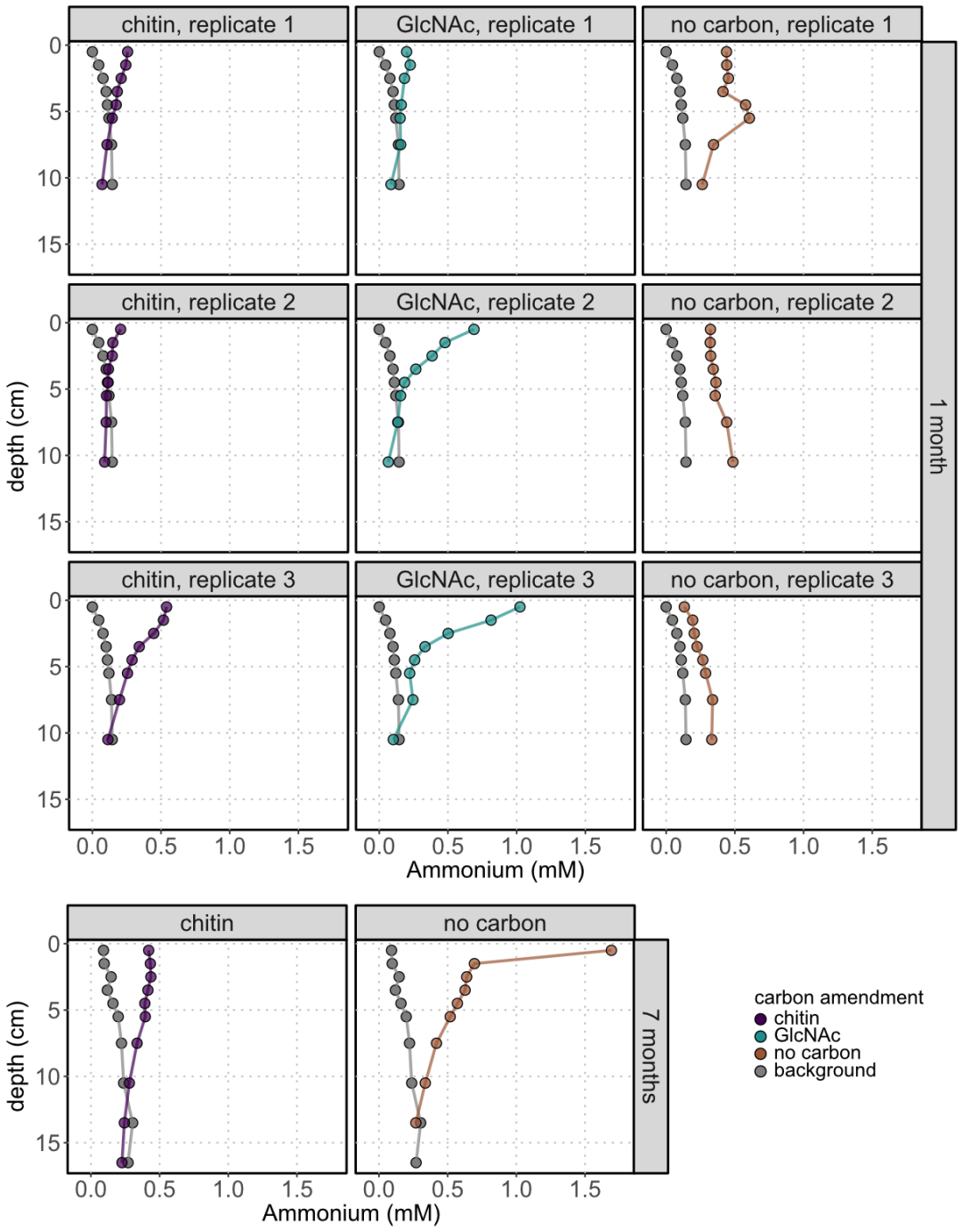

Supplemental Figure 2. Porewater ammonium concentrations measured in in situ seafloor incubations versus the background, unamended push core. There is a distinct ammonium response in the injector cores even without additional carbon supplementation in the longest (seven month) incubation.

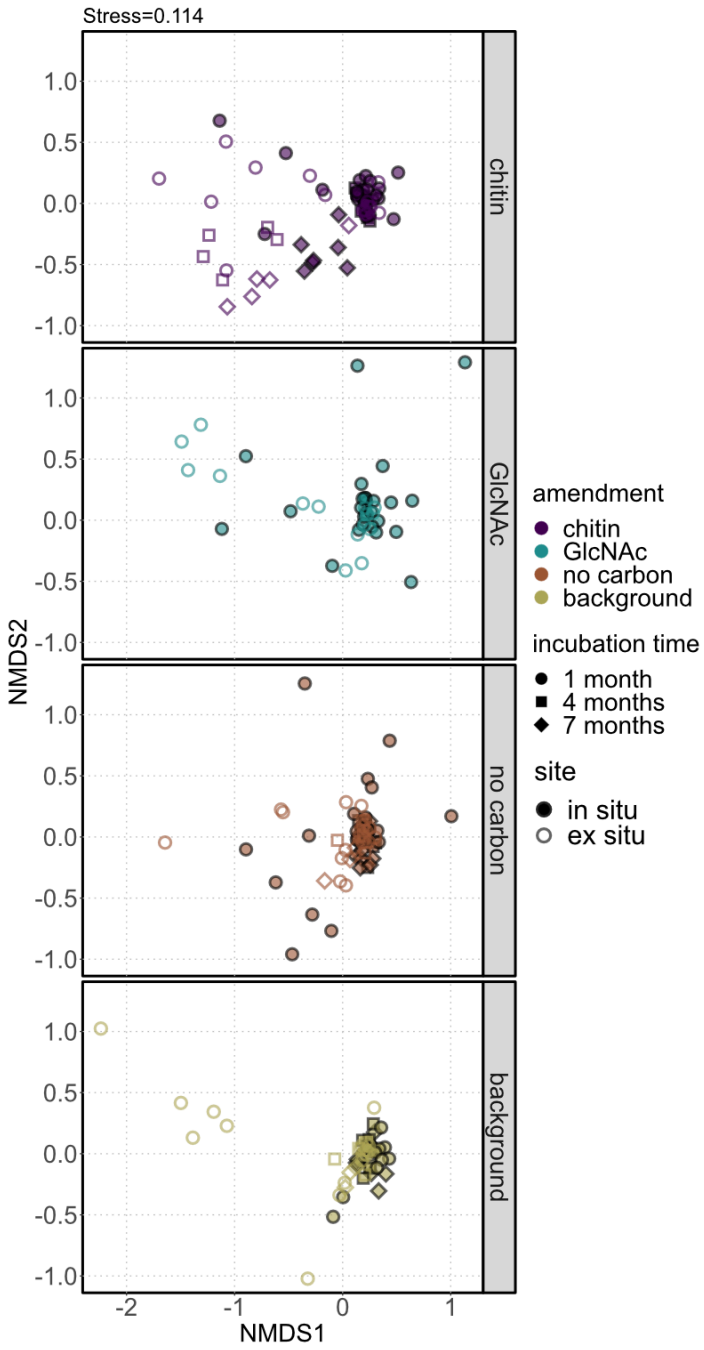

Supplemental Figure 3. NMDS plot on square-root-transformed relative abundance data faceted by amendment show a differential dissimilarity pattern between chitin-amended incubations and the other amendments over time. While GlcNAc-, no-carbon-, and unamended incubations exhibit similar dissimilarity patterns with the highest dissimilarity at one month of incubation with ex situ microcosm incubations (empty points), chitin-amended in situ incubations converge toward chitin-amended ex situ incubations.

Supplemental Table 1. SIMPER analysis of in situ incubations at the final timepoint; the ANOSIM R statistic between amendments for these incubations was 0.404 with p<0.005. Taxa contributing to the top 25% of dissimilarity between amendments are listed, with statistically significant taxa shown in bold (p<0.05)

Kingdom	Phylum	Class	Order	Family	Genus	larger	Cumulative sum	p
Bacteria	**Desulfobacterota**	**Desulfobulbia**	**Desulfobulbales**	**Desulfobulbaceae**	**uncultured**	**chitin**	**0.011**	**0.005**
Bacteria	**Acidobacteriota**	**Thermoanaerobaculia**	**Thermoanaerobaculales**	**Thermoanaerobaculaceae**	**Subgroup_23**	**chitin**	**0.022**	**0.001**
Bacteria	Bacteroidota	Bacteroidia	Bacteroidales	Bacteroidetes_BD2-2	Bacteroidetes_BD2-2	label	0.041	0.443
Bacteria	**NB1-j**	**NB1-j**	**NB1-j**	**NB1-j**	**NB1-j**	**chitin**	**0.050**	**0.007**
Bacteria	**Latescibacterota**	**Latescibacterota**	**Latescibacterota**	**Latescibacterota**	**Latescibacterota**	**chitin**	**0.059**	**0.004**
Bacteria	Desulfobacterota	Desulfuromonadia	Sva1033	Sva1033	Sva1033	label	0.068	0.834
Archaea	**Crenarchaeota**	**Bathyarchaeia**	**Bathyarchaeia**	**Bathyarchaeia**	**Bathyarchaeia**	**chitin**	**0.076**	**0.026**
Bacteria	Proteobacteria	Gammaproteobacteria	B2M28	B2M28	B2M28	chitin	0.085	0.063
Bacteria	**Proteobacteria**	**Gammaproteobacteria**	**BD7-8**	**BD7-8**	**BD7-8**	**chitin**	**0.101**	**0.049**
Bacteria	**Desulfobacterota**	**Syntrophobacteria**	**Syntrophobacterales**	**uncultured**	**uncultured**	**chitin**	**0.109**	**0.003**
Bacteria	Myxococcota	Polyangia	Polyangiales	Sandaracinaceae	uncultured	chitin	0.133	0.156
Bacteria	Desulfobacterota	Desulfobacteria	Desulfobacterales	Desulfobacteraceae	Desulfobacter	chitin	0.140	0.697
Bacteria	**Firmicutes**	**Clostridia**	**Peptostreptococcales-Tissierellales**	**Peptostreptococcales-Tissierellales**	**livecontrolB21**	**label**	**0.162**	**0.043**
Bacteria	**Desulfobacterota**	**Desulfobacteria**	**Desulfobacterales**	**Desulfosarcinaceae**	**SEEP-SRB1**	**chitin**	**0.169**	**0.008**
Bacteria	Proteobacteria	Gammaproteobacteria	AT-s2-59	AT-s2-59	AT-s2-59	chitin	0.175	0.553
Bacteria	Fusobacteriota	Fusobacteriia	Fusobacteriales	Fusobacteriaceae	Psychrilyobacter	label	0.195	0.422
Bacteria	Desulfobacterota	Desulfobacteria	Desulfobacterales	Desulfosarcinaceae	LCP-80	label	0.202	0.503
Bacteria	Desulfobacterota	Desulfobacteria	Desulfobacterales	Desulfolunaceae	uncultured	label	0.215	0.798
Archaea	Asgardarchaeota	Lokiarchaeia	Lokiarchaeia	Lokiarchaeia	Lokiarchaeia	label	0.221	0.021
Bacteria	DTB120	DTB120	DTB120	DTB120	DTB120	chitin	0.234	0.712

Supplemental Table 2. List of amendments and samples analyzed for ex situ microcosm incubations (top) and in situ injector core incubations (bottom). Highlighted cores were analyzed with BONCAT (Fig. 5). Information on sediment push cores used as inoculum is additionally included in ex situ microcosm sample data.

EX SITU MICROCOSMS

dive record	core name	amendment	depth horizons	time (months)	lat	long	n (16S)	n (geochem)
DR1105	PC44	none	0-2, 2-4, 4-6, 6-9, 9-12	1	36.77151	-122.082903	3	3
DR1105	PC44	chitin	0-2, 2-4, 4-6, 6-9, 9-12	1	36.77151	-122.082903	3	3
DR1105	PC44	GlcNAc	0-2, 2-4, 4-6, 6-9, 9-12	1	36.77151	-122.082903	3	3
DR1056	PC80	none	0-2, 2-4, 4-6, 6-9, 9-12	4	36.77153	-122.082955	1	0
DR1056	PC80	chitin	0-2, 2-4, 4-6, 6-9, 9-12	4	36.77153	-122.082955	1	0
DR1030	PC66	none	0-2, 2-4, 4-6, 6-9, 9-12	7	36.77147	-122.082893	1	1
DR1030	PC66	chitin	0-2, 2-4, 4-6, 6-9, 9-12	7	36.77147	-122.082893	1	1

IN SITU INJECTOR CORE INCUBATIONS

dive record	core name	amendment	replicate	time (months)	lat	long	16S	geochem
DR1107	IC1	none	1	7	36.77151	-122.082903	+	+
DR1107	IC4	none	2	7	36.77151	-122.082903	-	-
DR1107	IC6	none	3	7	36.77151	-122.082903	-	-
DR1107	IC14	chitin	2	7	36.77151	-122.082903	-	-
DR1107	IC15	chitin	3	7	36.77151	-122.082903	-	-
DR1107	IC12	chitin	1	7	36.77151	-122.082903	+	+
DR1105	IC10	none	2	4	36.77153	-122.082955	-	-
DR1105	IC17	none	1	4	36.77153	-122.082955	+	-
DR1105	IC19	none	3	4	36.77153	-122.082955	-	-
DR1105	IC23	chitin	1	4	36.77153	-122.082955	+	-
DR1105	IC24	chitin	2	4	36.77153	-122.082955	-	-
DR1105	IC25	chitin	3	4	36.77153	-122.082955	-	-
DR1112	IC21	chitin	2	1	36.77147	-122.082893	+	+
DR1112	IC22	chitin	3	1	36.77147	-122.082893	+	+
DR1112	IC26	chitin	1	1	36.77147	-122.082893	+	+
DR1112	IC42	GlcNAc	1	1	36.77147	-122.082893	+	+
DR1112	IC44	GlcNAc	2	1	36.77147	-122.082893	+	+
DR1112	IC46	GlcNAc	3	1	36.77147	-122.082893	+	+
DR1112	IC2	none	1	1	36.77152	-122.08288	+	+
DR1112	IC9	none	2	1	36.77152	-122.08288	+	+
DR1112	IC38	none	3	1	36.77152	-122.08288	+	+
DR1030	PC48	background	1	7	36.77151	-122.082903	+	+
DR1056	PC80	background	1	4	36.77153	-122.082955	+	+
DR1105	PC44	background, live mud	1	1	36.77147	-122.082893	+	-
DR1105	PC69	background, geochem	1	1	36.77147	-122.082893	-	+

Chapter 3

ENERGY AVAILABILITY CONSTRAINS ANAEROBIC MICROBIAL COMMUNITIES BY NICHE LIMITATION

Sujung Lim[1*], Ranjani Murali[2], Daan R. Speth[2§], Rachel E. Szabo[3], Otto X. Cordero[3], Victoria J. Orphan[1,2*]

[1] Division of Geological and Planetary Sciences, Caltech, Pasadena, CA 91125
[2] Division of Biology and Biological Engineering, Caltech, Pasadena, CA 91125
[3] Department of Civil and Environmental Engineering, Massachusetts Institute of Technology, Cambridge, MA 02139
[§] present address: Division of Microbial Ecology, Centre for Microbiology and Environmental Systems Science, University of Vienna, Vienna, Austria

ABSTRACT

Marine sediments experience dynamic shifts in energy availability through the input of oxidizable carbon that can promote transitions down redox gradients. Continental margin sediments receive a constant input of marine snow from the productive sunlit surface ocean and occasionally receive large inputs of more labile organic matter from sudden carbon loading events such as whale falls. Upon the input of oxidizable organic matter, the local seafloor can quickly become anoxic after exhausting the oxygen in the oxic sediment-water interface. Subsequently, the microbial communities are hypothesized to respire the available electron acceptors in order of potential, with high potential electron acceptors such as nitrate utilized first. The changing redox environment and energy availability is predicted to impact the structure of microbial ecosystems, especially those degrading complex carbon and reliant on tight trophic connections between upstream primary degraders and terminal electron

acceptor respirers. The influence of energy availability in the form of dominant electron accepting processes on the structure and function of organic carbon-degrading anaerobic microbial communities in deep sea ecosystems in poorly understood. Here, we conducted a highly replicated set of serially diluted anoxic marine sediment incubations supplied with varying electron acceptors including sulfate, ferric iron, and nitrate, and either the polymer chitin or its monomer GlcNAc as electron donors. The production of metabolites (acetate and ammonium), consumption of electron acceptor, and changes in community (16S rRNA iTAG and metagenomic sequencing) were tracked over the course of seven months in the 10 °C incubations. While the complexity of input carbon and its effect on sediment microbial communities was discussed in Chapter 1, we additionally demonstrate here that the free energy of the system had a significant impact on deep sea sediment microbial community structure and function. In these communities, we observed redox potential-dependent shifts in metabolic products with the highest potential electron acceptors (nitrate and ferric iron) accumulating the most ammonium and acetate. Lower taxonomic and functional gene diversity was seen in the ferric iron oxide-reducing chitin incubation set, potentially demonstrating restricted trophic interactions in communities challenged through transferring electrons between insoluble substrates. Finally, low-energy regimes such as those reducing sulfate or not provided with a terminal electron acceptor exhibited a proliferation of specialist terminal members such as methanogens.

INTRODUCTION

Despite a lack of easily oxidizable carbon, deep sea sediment is responsible for a significant amount of organic matter turnover, with an estimated 90% of input organic matter degraded (Hedges & Keil, 1995; LaRowe et al., 2020). This organic matter is in a wide variety of stages of degradation scaling on its age from relatively more labile to recalcitrant (Burdige, 2007; Canfield, 1994; Hedges et al., 2000). However, there are hotspots of productivity in the deep sea such as methane seeps and whale falls that result in the direct deposition of oxidizable organic matter (Boetius & Wenzhöfer, 2013; C. R. Smith & Baco, 2003). In these organic-rich areas as well as other sedimentary regimes such as nearshore coastal and estuarine environments, transitions occur through gradients of differing redox potential within the sediment (Froelich et al., 1979; Yücel, 2013). The environment quickly becomes anoxic as oxygen is exhausted from the upper layers. In these anaerobic zones, microbes preferentially utilize the highest potential electron acceptors available before moving to less thermodynamically favorable regimes such as methanogenesis (Bethke et al., 2011; Jørgensen, 1982).

Microbes such as sulfate-reducers and methanogens that utilize lower potential electron acceptors are not generally thought to be able to degrade complex carbon such as polysaccharides alone. However, much of the organic matter that reaches the seafloor is complex — usually polymeric and/or aromatic (Arndt et al., 2013; Arnosti et al., 2021). In the case of a polysaccharide electron donor, trophic interactions between primary degraders able to cleave the polymer and downstream terminal respirers are hypothesized to play an

important role in the mineralization of organic matter. Moreover, complex carbon is thought to promote functional and systematic microbial diversity and support community structure through the maintenance of functional redundancy (Q. Chen et al., 2022).

In marine regimes, which exhibit dynamic shifts in local energy availability due to turbidity and riverine input resulting in rapidly changing oxidizable organic matter loading (Reader et al., 2019; Talling et al., 2024), the relationship between the free energy in the system and the microbial community is especially interesting. The energetics of the environment is driven by the midpoint potential of both the electron donor — the organic matter input — and the electron acceptor present. Therefore, we expect that the available electron acceptors may impact microbial community structure in these seafloor systems. Low energy metabolic processes such as syntrophies found in methane seeps and at the terminal stages of anaerobic digestion encourage cooperation to keep limiting products at a low enough concentration to maintain the thermodynamic favorability of the net reaction. This requirement of cooperation is not expected to exist in higher energy regimes where instead members may compete for resources. Prior modeling work has addressed the community interactions in high energy systems, including competitive dynamics between denitrifiers and nitrate reducers that produce ammonia (Jia et al., 2020), and the transition between anaerobic and aerobic metabolism in the ocean (Zakem et al., 2020), primarily through applications of resource-ratio theory. However, less work has compared the impact of energy availability across a wide gradient on marine sediment-hosted communities. Much of the existing literature is focused on the interactions between community members with varying energetics in

freshwater systems, or on a more restricted scale (e.g., the ferric iron-to-sulfate transition) in deep marine sediments (Graw et al., 2018; Lovley & Phillips, 1987; Roden & Wetzel, 2003).

Chapter 1 of this thesis has highlighted the impact of complex carbon in supporting activity, taxonomic diversity, and functional redundancy in deep marine sediments; this chapter emphasizes the effect of terminal electron acceptor redox potential in these seafloor communities, especially with regard to the distribution of functions. We generated highly replicated incubations of serially diluted whale fall sediment and incubated them with a pairwise combination of electron acceptors nitrate, ferric iron, sulfate, and no electron acceptor (also described as 'methanogenic') and chitin or N-acetylglucosamine (GlcNAc) as electron donors. Control incubations were also done without added carbon. A subset of these incubations was then sampled at three time points to determine their metabolic response and community composition (using 16S rRNA gene amplicon and metagenomic sequencing).

RESULTS

Chitin degradation and metabolic product accumulation generally followed the midpoint potential of the provided electron acceptor

We tracked the utilization of chitin and GlcNAc through quantification of their predicted metabolic products — ammonium and acetate — in our incubations at the three time points (one, three, and seven months). While there was a consistent pattern of time-dependent shifts in the ratio between acetate and ammonium in the sulfate-reducing chitin incubations (see

Chapter 1), the other three electron acceptor treatments instead showed a strong relationship between the midpoint potential of the electron acceptor and amount of ammonium produced. Over the course of the entire experiment, incubations without an electron acceptor reached a maximum ammonium concentration of 2.16 mM, while sulfate-containing incubations reached 11.4 mM, ferric iron-containing incubations 15.8 mM, and nitrate-containing incubations accumulated up to 16 mM ammonium (Fig. 1, right). The same trend was seen in acetate concentrations with nitrate, sulfate, and no electron acceptor-containing microcosms (maximum concentrations 19.3 mM, 11.4, and 3 mM respectively). Iron-reducing incubations accumulated higher concentrations of acetate (28.7 mM), perhaps due to the potential difficulty in forming communities bridging between an insoluble electron acceptor and insoluble electron donor. Consistent with this, the soluble monomer GlcNAc did not show a large accumulation of acetate in the iron treatment. In fact, GlcNAc-amended incubations showed a similar relationship between metabolite accumulation (ammonium) and electron acceptor redox potential, with the exception of 'methanogenic' and sulfate-reducing conditions which accumulated similar amounts of ammonium (5.5 and 4.8 mM, respectively; Fig. 1, left). Here, nitrate-reducing incubations accumulated the most ammonium (a maximum of 13.8 mM) and iron-reducing incubations produced up to 10.4 mM.

The hypothesized degradation pathway from GlcNAc to acetate results in one mole of ammonium and three moles of acetate per mole of GlcNAc (see Chapter 1). Because we supplied the GlcNAc incubations with 5 mM GlcNAc, we expected an upper bound of 5 mM

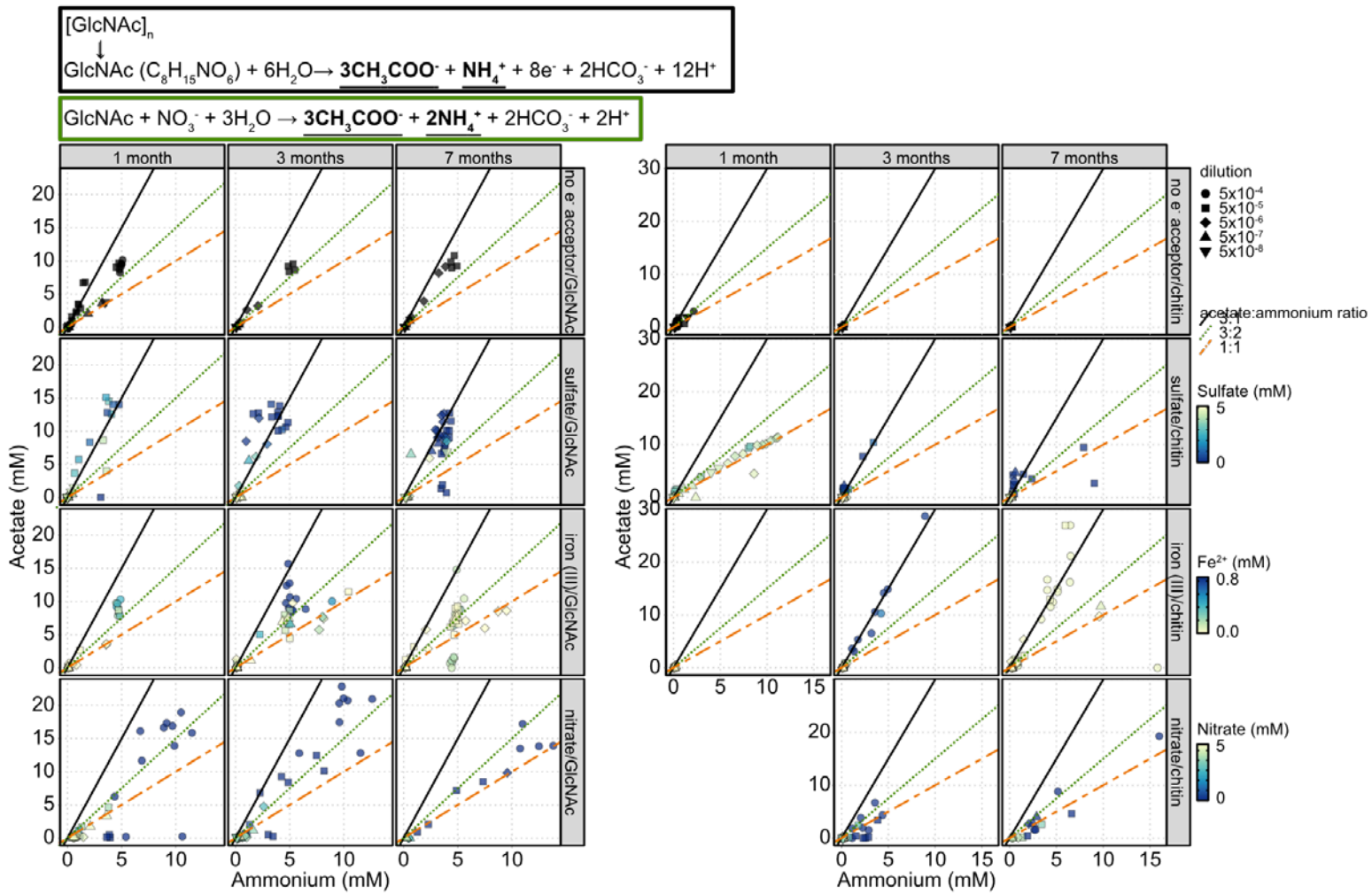

Figure 1. Geochemistry data demonstrate an electron acceptor-based shift in acetate and ammonium accumulation in GlcNAc- (left) and chitin-oxidizing (right) incubations. We expected a product ratio of 3:1:8 acetate:ammonium:electrons per equivalent of GlcNAc (and, by proxy, chitin) oxidized; deviations from this expected 3:1 stoichiometric ratio may indicate downstream product utilization or other changes in the carbon oxidation process. Notably, nitrate/GlcNAc (left, bottom row) incubations exhibited a high amount of ammonium production that was not coupled to the expected amount of acetate accumulation but instead approached a 3:2 acetate:ammonium trend, consistent with DNRA (dotted green line; overall formula is in green box). The maximum extent of ammonium accumulation in these treatments was generally correlated to the redox potential of the supplied electron acceptor, as well.

ammonium from these microcosms. Nitrate-reducing incubations produced several times this, likely due to dissimilatory reduction of nitrate to ammonium (DNRA; Fig. 1, left, bottom) rather than denitrification to N_2 or N_2O. Moreover, the ratio between acetate and ammonium produced averaged to 1.15:1 at one month (n=41), 1.62:1 at three months (n=42), and 1.15:1 at seven months (n=16) when weighted by ammonium concentration — values that are much lower than the expected ratio of 3:1 acetate:ammonium. We also observed elevated ammonium in the iron-reducing GlcNAc-amended incubations, albeit to a lesser extent than the nitrate-reducing incubations. The maximum ammonium concentration of iron-reducing GlcNAc incubations was 10.4 mM, double the amount expected from the concentration of GlcNAc provided.

The sediment incubations that were not amended with a terminal electron acceptor additionally accumulated less acetate than expected (Fig. 1, top row), with an ammonium-weighted average acetate:ammonium ratio at 1.95:1 at one month (n=54), 1.72:1 at three months (n=16), and 2.14:1 at the final time point (n=16) in GlcNAc-amended incubations (Fig. 1, left, top row) rather than the expected 3:1 acetate:ammonium ratio. While chitin-amended incubations accumulated considerably less acetate and ammonium than GlcNAc-amended incubations, these incubations also exhibited significant acetate utilization with an ammonium-weighted average ratio less than 3:2 at all time points. The decreased acetate accumulation despite the absence of a provided terminal electron acceptor is suggestive of acetate utilization either through methanogenic disproportionation or syntrophy.

Control sediment incubations unamended with exogenous carbon accumulated a maximum of nearly 3 mM ammonium during the experiment (Supp. Files). This observed elevated ammonium could be attributed to endogenous carbon, possibly carried over from the inoculum, and was mostly seen in the lower dilution incubations ($5x10^{-4}$, $5x10^{-5}$). Finally, the iron-reducing chitin-amended incubations had an ammonium-weighted average acetate:ammonium ratio of 2.58:1, exhibiting little to no relative acetate utilization from the expected stoichiometric product ratio of 3:1.

Effect of high electron acceptor midpoint potential or electron acceptor insolubility on communities

To test the effect of electron acceptor and donor amendments on microbial community structure, we analyzed the community dissimilarity from 16S rRNA gene sequencing data using NMDS. While the geochemical data showed a strong electron acceptor-mediated response, the corresponding community composition showed only a small (but statistically significant) contribution to the dissimilarity at each time point (Supp. Table 1). Trends are visible at the three-month time point, with nitrate-amended incubations clustering together (Fig. 2a) and greater dissimilarity among the iron-amended incubations (Fig. 2a, 2b). The three-month time point had high concentrations of acetate and ammonium for most treatments. Acetate and ammonium contours on community data at this time point showed that ammonium concentration could be a driver for the dissimilarity of the iron-reducing community (Fig. 2b).

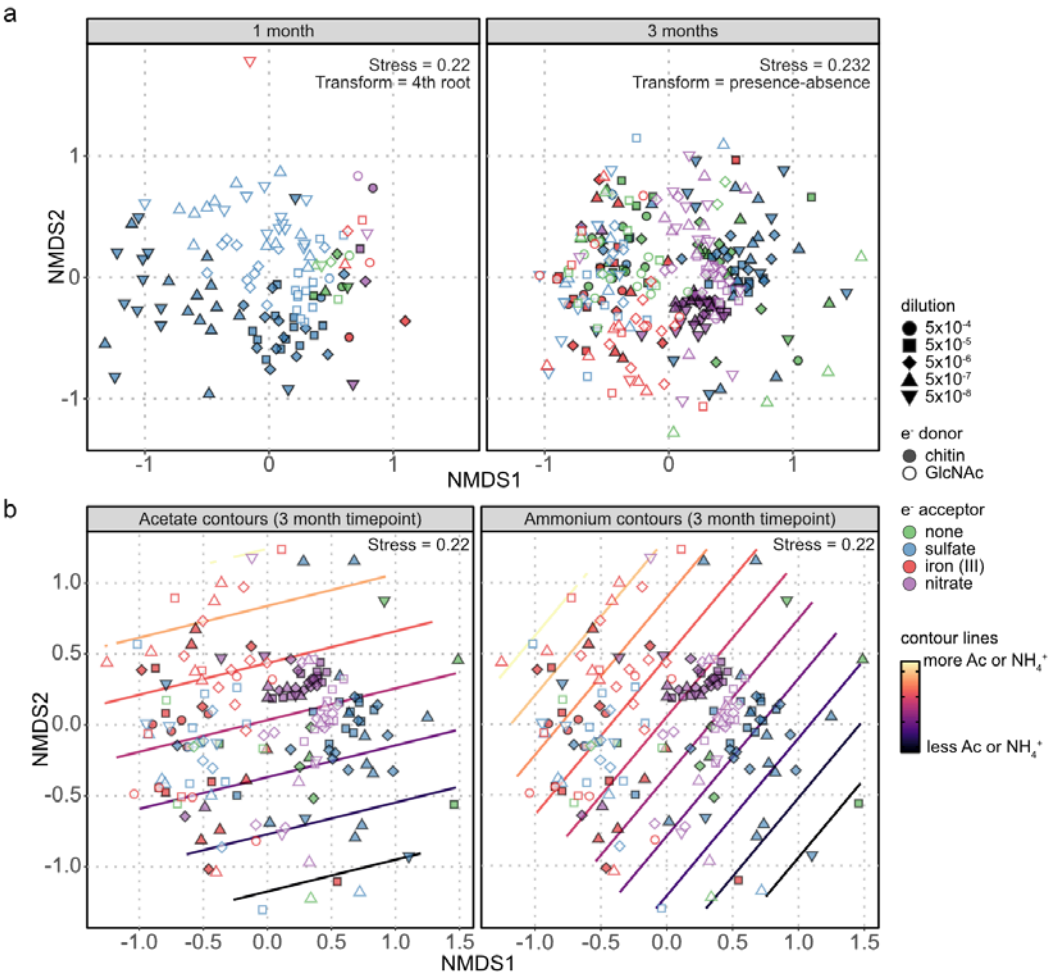

Figure 2. NMDS plots show dissimilarity of genus-agglomerated 16S sequences between supplied electron acceptors (point color). (a) Dissimilarity of all analyzed incubations calculated at one and three month time points; over time, the dissimilarity of nitrate-reducing communities (purple) was relatively low and iron-reducing communities (red) tended to be divergent. (b) Dissimilarity between presence-absence transformed communities with geochemistry data at the three month time point. Contours showing the contribution of metabolic product concentration (left, acetate contours; right, ammonium contours) indicate a potential contribution of ammonium to iron/GlcNAc (red, unfilled points) community dissimilarity.

Alpha diversity analysis of the community data at three months of incubation also showed an electron acceptor-dependent response which varied depending on the provided electron donor. In the three-month chitin incubations, iron-reducing incubations had significantly lower mean Chao1 richness than the other two electron acceptor treatments (iron: μ_{Chao1}=5.9, σ_{Chao1}=6.5, n=23; sulfate: μ_{Chao1}=32.9, σ_{Chao1}=26.2, n=45; nitrate: μ_{Chao1}=46.4, σ_{Chao1}=21,

n=43), further supporting the hypothesis that the microbial community was challenged through the combination of insoluble electron acceptor and donor (Fig. 3, top; Supp. Table 2). GlcNAc incubations did not exhibit the same decreased richness in iron-reducing incubations; however, nitrate-reducing incubations were significantly more diverse than either of the other electron acceptors and the no electron acceptor control (Fig. 3, bottom; Supp. Table 2). All incubations at three months with a similar magnitude of richness (iron/chitin, sulfate/GlcNAc, no electron acceptor/chitin, no electron acceptor/GlcNAc) also had a similar magnitude of Simpson's evenness (iron/chitin: $\mu_{Inv.Simpson}$=2.8, $\sigma_{Inv.Simpson}$=1.4, n=23; sulfate/GlcNAc: $\mu_{Inv.Simpson}$=3.3, $\sigma_{Inv.Simpson}$=1.9, n=33; none/chitin: $\mu_{Inv.Simpson}$=5.3, $\sigma_{Inv.Simpson}$=3.4, n=45; none/GlcNAc: $\mu_{Inv.Simpson}$=4.2, $\sigma_{Inv.Simpson}$=2.3, n=28).

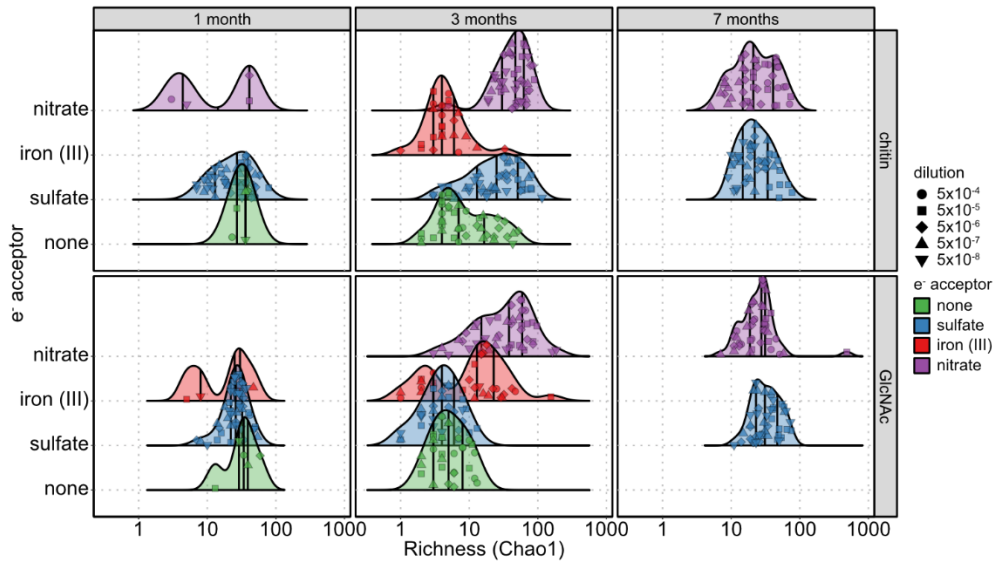

Figure 3. Chao1 diversity distributions of 16S rRNA gene sequence data demonstrate a transient differential effect with insoluble substrates. Iron-reducing chitin-amended incubations (center, top, red fill) exhibited reduced richness at three months, suggesting that substrate solubility contributes a selective effect. Moreover, at this time point, nitrate-reducing GlcNAc-oxidizing incubations (center, bottom, purple fill) had increased richness. This diversity increase was temporary, and by the final time point, sulfate and nitrate-reducing communities regardless of amendment had similar Chao1 richness (right).

Despite the greater diversity in the nitrate/GlcNAc incubations at the three-month time point, analysis of chitin metabolism genes from the metagenomic data showed lower gene diversity of chitin and GlcNAc metabolic genes relative to the parallel sulfate-reducing incubations (Fig. 4). Additionally, for chitinase, N-acetylglucosamine kinase, N-acetylglucosamine-6-phosphate deacetylase, and glucosamine-6-phosphate deaminase, the sulfate-reducing incubations with chitin had the highest gene diversity, suggesting a community response to natively present electron acceptors that is enhanced by complex carbon.

Electron acceptor redox potential restricts functional gene diversity

We assessed the functional diversity of methanogenesis, as the common hypothesized downstream function between all electron acceptors, by mining the methanogen marker gene methyl coenzyme reductase (*mcrA*). There were systematic shifts in *mcrA* genes present between treatments and time points. We assigned taxonomy to the *mcrA* genes mined through 95% identity with a reference amino acid sequence (see Methods). As reported previously, sulfate-containing incubations amended with chitin or GlcNAc were differentiable at three months on the basis of a family-level *mcrA* fingerprint with chitin-amended incubations being enriched in the Methanomicrobiales.

Although none of the other electron acceptors exhibited the same per-family signal between chitin and GlcNAc seen in sulfate-reducing incubations, we observed a consistent taxonomic signal within *mcrA* genes belonging to the Methanosarcinaceae in the iron-reducing

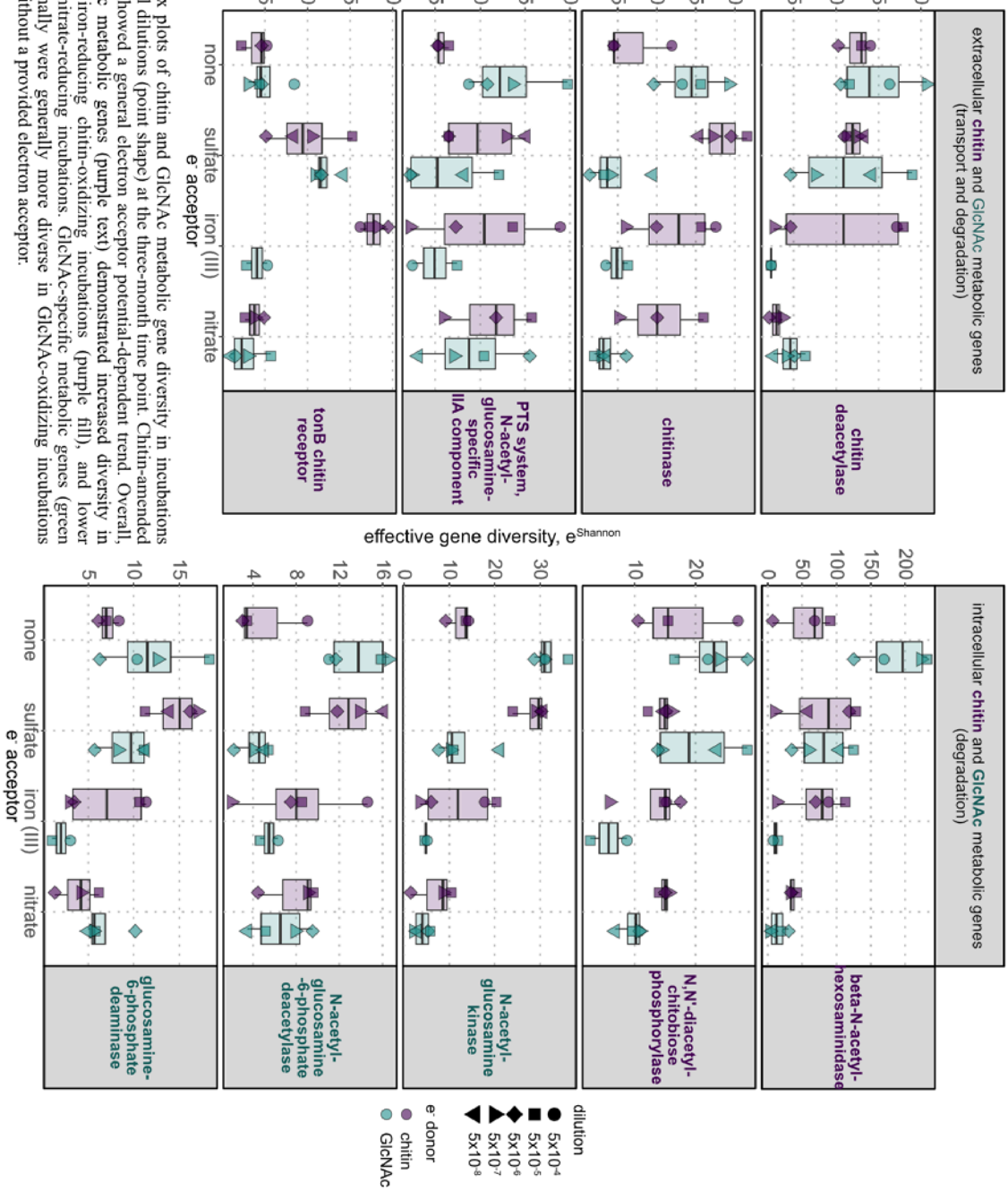

Figure 4. Box plots of chitin and GlcNAc metabolic gene diversity in incubations combining all dilutions (point shape) at the three-month time point. Chitin-amended incubations showed a general electron acceptor potential-dependent trend. Overall, chitin-specific metabolic genes (purple text) demonstrated increased diversity in sulfate and iron-reducing chitin-oxidizing incubations (purple fill), and lower diversity in nitrate-reducing incubations. GlcNAc-specific metabolic genes (green text) additionally were generally more diverse in GlcNAc-oxidizing incubations (green fill) without a provided electron acceptor.

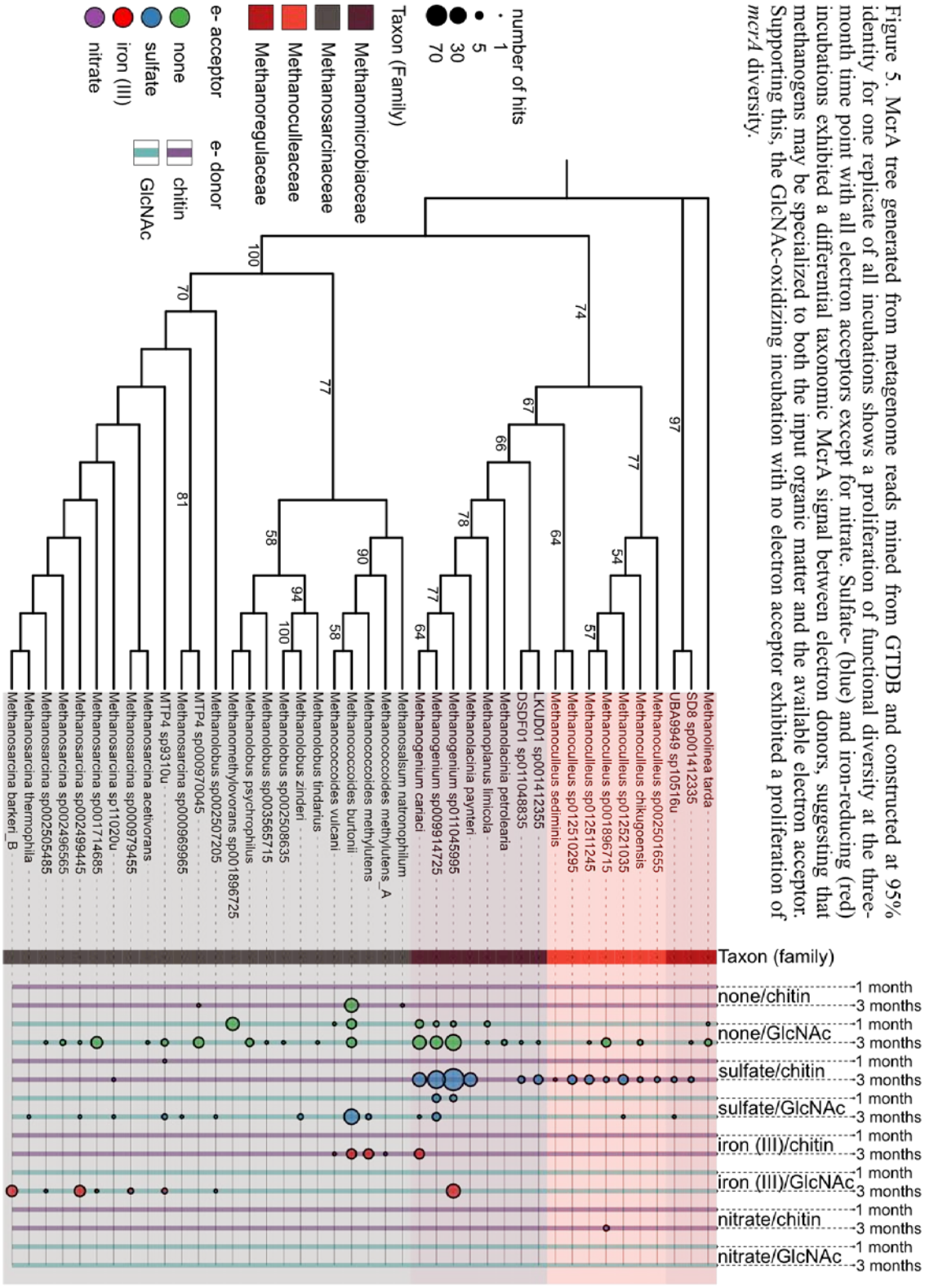

Figure 5. McrA tree generated from metagenome reads mined from GTDB and constructed at 95% identity for one replicate of all incubations shows a proliferation of functional diversity at the three-month time point with all electron acceptors except for nitrate. Sulfate- (blue) and iron-reducing (red) incubations exhibited a differential taxonomic McrA signal between electron donors, suggesting that methanogens may be specialized to both the input organic matter and the available electron acceptor. Supporting this, the GlcNAc-oxidizing incubation with no electron acceptor exhibited a proliferation of *mcrA* diversity.

incubations. GlcNAc-amended iron-reducing incubations were generally enriched in the metabolically diverse *Methanosarcina* genus and chitin-amended incubations were enriched in *Methanococcoides* while both incubation sets had members of the hydrogenotrophic genus *Methanogenium* (Fig. 5; Akinyemi et al., 2019).

We expected incubations with no provided terminal electron acceptor to be enriched in methanogens utilizing acetate given the geochemistry data showing lower acetate concentrations than expected from the GlcNAc or chitin provided (Fig. 1, top row). In agreement with the geochemistry data, GlcNAc-amended incubations without added electron acceptor maintained a high level of *mcrA* diversity. Interestingly, the chitin amendments harbored a lower diversity of this marker gene, suggesting that there are energetic limitations on the maintenance of diverse methanogenic clades, especially with complex carbon as the feedstock. Finally, nitrate-containing microcosms contained very few to no *mcrA* genes within the one- and three-month time points. These data were largely in agreement with the 16S rRNA sequence data (Fig. 6b), which showed a strong negative correlation between *Methanogenium* and ammonium concentration. Those methanogenic clades that were associated with high ammonium concentration in our incubation set, such as the amounts seen in ferric iron-reducing incubations, were members of the Methanosarcinales.

Iron- and nitrate-reducing microcosms additionally accumulated millimolar amounts of formate over the course of the experiment (Fig. 6a). The accumulation of formate, a substrate for methanogenesis that all hydrogenotrophic methanogens are capable of using, may be a signal of metabolic imbalance in these amendments and is coincident with a lack of a

methanogenic functional signal in nitrate-reducing microcosms as well as an additional signifier of an interruption of trophic flow in iron-reducing microcosms.

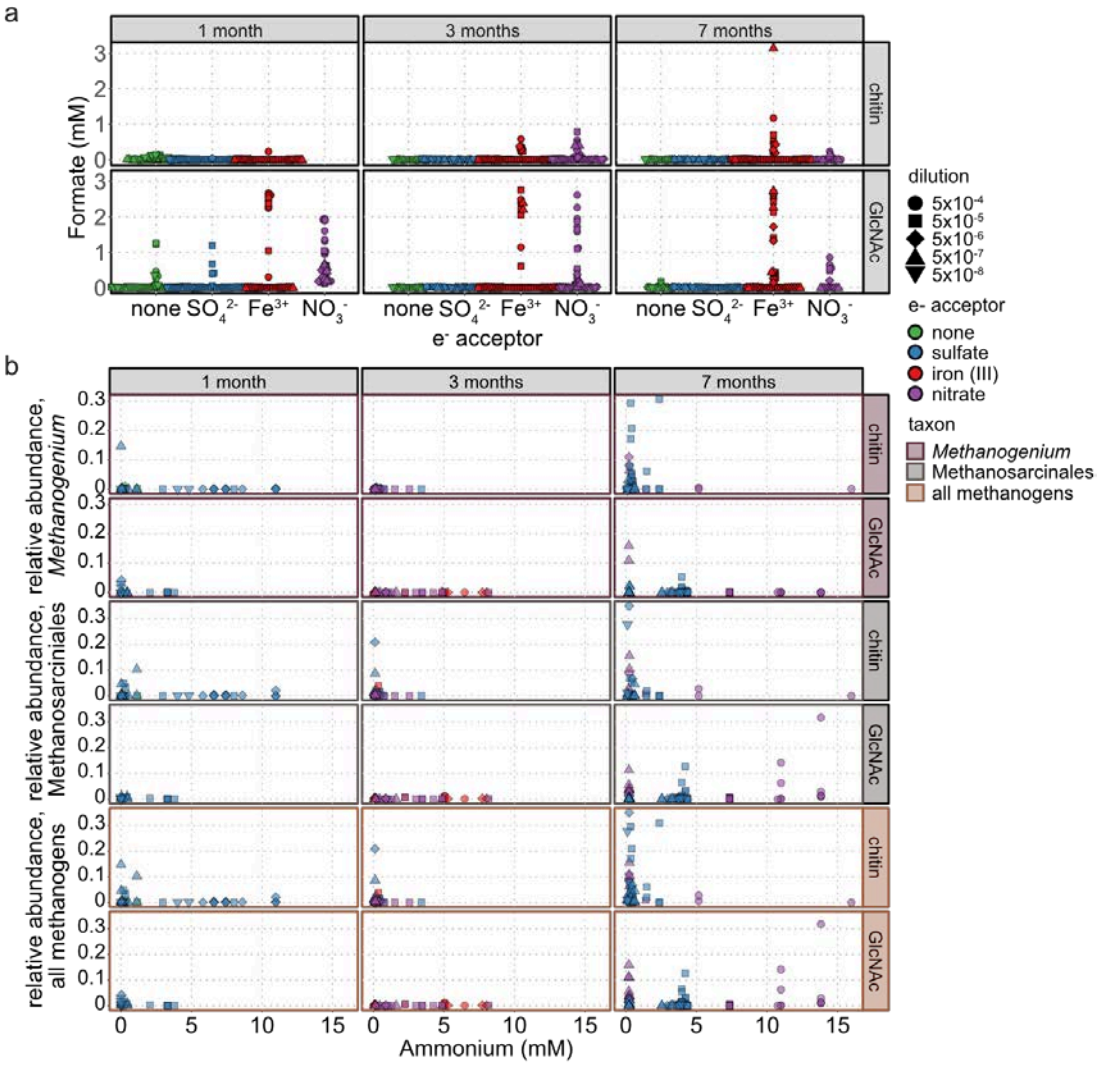

Figure 6. Geochemical and molecular signals allude to inhibition of methanogens. (a) Formate accumulated at three and seven month time points in nitrate (purple) and ferric iron (red) incubations. This trend was not seen with the no electron acceptor-containing and sulfate-reducing incubations, and in the case of nitrate was coincident with methanogen marker gene abundance (Fig. 5). Ferric iron incubations also accumulated formate in both electron donor conditions, possibly due to the difficulty of respiring an insoluble substrate. (b) 16S rRNA gene relative abundances of methanogenic taxa showed a strong negative correlation between ammonium concentration and *Methanogenium* relative abundance, while members of the Methanosarcinales were not as affected.

DISCUSSION

This study provided insight into the contribution of energy availability to sediment-hosted microbial communities. Through varying the available terminal electron acceptors provided to sediment microcosms, we observed trends in these communities' ability to oxidize the polymer chitin or its monomer GlcNAc. Specifically, we observed that the electron acceptor present had the greatest effect on and was able to significantly modify the dynamics of chitin degradation, a behavior that could potentially be generalized to other complex substrates in the marine regime.

Here, methanogens are supported by the presence of a terminal electron acceptor in chitin treatments; incubations lacking the terminal electron acceptor accumulated less ammonium and acetate and had lower methanogenic marker gene diversity (Fig. 1, 5). Moreover, when an electron acceptor was supplied, the lowest potential electron acceptors exhibited the highest gene diversity in chitin-oxidizing incubations both with methanogenic marker genes and in upstream processes; genes involved in chitin metabolism were more diverse in sulfate- and iron-reducing incubations versus nitrate-reducing incubations (Fig. 4). This may be because the sediment community members are specialized to the local electron acceptors present. While iron and sulfate are abundant in marine sediments, nitrate is uncommon in our sample site. We can infer that a greater number of microbes adapted to chitin degradation and sulfate reduction are present in the source sediment than those adapted to nitrate reduction, resulting in a correspondingly high diversity of taxonomy and function in chitin and sulfate incubation. Specialized sediment members could be outcompeted by generalists

such as copiotrophic facultative anaerobes in the high-energy nitrate-containing incubations. Interestingly, the meager methanogen response seen in our nitrate-reducing microcosms is only present in chitin-oxidizing incubations, suggesting that in spite of the stresses upon introducing a high-energy substrate into a low-energy system, complex carbon was still able to support greater methanogen diversity than a simpler substrate.

In the case of the simpler electron donor, GlcNAc, we observed, as expected, higher activity in the nitrate-reducing incubations. The maximum amount of ammonium produced was greater than the hypothesized maximum from the supplied GlcNAc, even accounting for carbon carryover from the initial inoculum. This, along with the ratio of acetate to ammonium approaching 3:2 rather than the expected stoichiometric product ratio of 3:1 (Fig. 1, left), suggested an alternative metabolism besides denitrification may be involved — namely, dissimilatory reduction of nitrate to ammonia (DNRA). Denitrifying and DNRA microbes are known to compete for nitrate, and previous reports suggest that acetate stimulates DNRA in favor of denitrification or in conditions of excess electron donor (van den Berg et al., 2016, 2017); the high amount of acetate produced in these incubations would meet both conditions and support the hypothesis that DNRA is the major nitrate sink in these incubations. Additionally, there were no methanogenic marker genes at high identity to known references present in the GlcNAc and nitrate incubations, and few in the chitin and nitrate incubations. Ammonium is known to have an inhibitory effect on some methanogenic archaea at high concentrations (100-300 mM; Koster & Lettinga, 1984; Sprott & Patel, 1986). Although the ammonium concentration in the nitrate-reducing incubations did not have such a high

concentration, we cannot discount that it was a contributing factor in the lack of methanogenic functional genes observed. Upstream metabolic genes corresponding to GlcNAc utilization, primarily the intracellular metabolic genes, tended to be less diverse in the nitrate-reducing incubations relative to the no electron acceptor incubations as well (Fig. 4). These incubations had the highest taxonomic diversity, despite the lack of functional diversity, suggesting that the pool of diversity is centered around neither the primary degradation process nor methanogenesis.

Insoluble substrates, whether in the form of the electron acceptor (ferric iron) or electron donor (chitin) may provide an additional challenge to communities that is amplified when both acceptor and donor are insoluble. This manifested in geochemical output, community dissimilarity, and methanogenic marker gene diversity (Fig. 1, 2a, 5), and likely was due to the difficulty of transferring electrons between two solid substrates. There was little acetate utilization in the ferric iron/chitin incubations, despite the presence of methanogen marker genes from the methylotrophic methanogen *Methanococcoides* and, unexpectedly, hydrogenotrophic methanogen *Methanogenium* (Akinyemi et al., 2019; L'Haridon et al., 2014). These abundance patterns were also seen, albeit at low relative abundance, in our 16S rRNA gene survey. The presence of a hydrogenotrophic methanogen taxon in conjunction with formate accumulation (Fig. 6a) and high acetate accumulation suggests a breakdown in the degradation process and the trophic handoff of electrons from the primary degraders to terminal respirers. Interestingly, the iron/chitin response with regard to formate accumulation, community dissimilarity, and methanogenic marker gene distribution is

distinct from the no electron acceptor/chitin response, suggesting that other factors such as the midpoint potential of the electron acceptor are involved in structuring these microcosms. This behavior is in contrast to prior reports which suggested that stratified environments allow the maintenance of diversity by restricting dispersal and "winner-take-all" events (Kerr et al., 2002), likely due to the necessity of interfacing two insoluble substrates exceeding the ability of the community to sustain diversity.

The methanogenic marker genes were taxonomically distributed in iron-reducing incubations between chitin and GlcNAc amendments, with GlcNAc-oxidizing incubations exhibiting a greater quantity of acetoclastic members of the Methanosarcinaceae (Fig. 5). In marine sediments, prior reports have shown that syntrophy rather than acetoclastic methanogenesis is primary driver of methanogenic acetate utilization (Beulig et al., 2018). Contrary to these reports, we observed an enrichment of acetoclastic methanogens at the three-month time point both in marker genes and in the 16S data in conjunction with active acetate utilization in the iron/GlcNAc treatments, suggesting that the iron-responding methanogenic acetate sink is mediated by acetoclastic methanogens in these sediment systems.

In this work, we demonstrate the impact of high- versus low-energy regimes on community structure and functional diversity. We are unable to unilaterally determine whether this effect was due to competitive dynamics in a high-energy system or community members specialized to a low-energy seafloor environment being incompatible with reduction of a high potential electron acceptor. We observed that the complexity, insolubility, and energy

availability of the substrate were able to drive community dynamics; these dynamics can then feedback on the ecophysiological response of individual members such as methanogens and the primary degraders. Future work will determine the role other terminal respiratory processes, including iron reduction, denitrification, and DNRA, have in contributing to community diversity and the geochemical dynamics observed.

METHODS

Sample collection, incubation conditions, and media design

The sediment inoculum was collected from a whale fall site in Monterey Bay at 1020 m depth, slurried 1:1 in artificial seawater, and diluted into deep well 96-well plates as described previously (Chapter 1). The medium used was 1575 µL artificial seawater medium supplemented with pairwise combinations of the electron acceptors sodium sulfate (5 mM), sodium nitrate (4 mM), poorly crystalline iron oxide (0.01 g/well), and no electron acceptor; and the electron donors colloidal chitin (0.01 g/well) or N-acetylglucosamine (5 mM). An incubation set containing the provided electron acceptors and no electron donor was included as a control. Colloidal chitin and the artificial seawater medium were prepared as described in Chapter 1. Poorly crystalline iron oxide was prepared by neutralizing dissolved $FeCl_2$ to pH 7 with NaOH, subsequent washing in dH_2O, and freeze-drying. Sampling at one, three, and seven-month time points included filtration of 200 µL of sample on a 0.2 micron 96-well plate filter (Pall product number 8019) with the filtrate retained at -80 °C for DNA extraction (see Chapter 1 for further detail).

Geochemistry analyses and quantification of major ions

A portion of the filtered samples were diluted 1:50 and run on a Dionex ICS-2000 or Thermo Integrion HPIC as previously described on an AS19 anions and CS16 cations column (Speth et al., 2022). Due to analytical constraints and lack of sample in some cases, ion chromatography was done on a subset of the replicates. Sulfate-reducing incubations were analyzed as described in Chapter 1. Incubations were analyzed according to the schema in the supplement (Supp. Table 3). Ferrous iron was quantified in iron-reducing incubations with the Ferrozine assay (Stookey, 1970) using the following protocol. 2 mM Ferrozine reagent (Sigma) was prepared in 6.5 M acidified ammonium acetate dissolved in 1N HCl. The reagent was added to the filtered samples in a dilution-dependent manner: 10 μL of the $5x10^{-2}$ dilution, 50 μL of the $5x10^{-3}$ dilution, and 100 μL of subsequent dilutions were added to 100 μL of Ferrozine reagent, after which ferrous iron was quantified colorimetrically at 562 nm.

16S rRNA gene amplicon sequence analysis

DNA was extracted from incubations using the Beckman DNAdvance kit, quantified with Picogreen, and 16S rRNA gene amplicons sequenced as described in Chapter 1 using primers for the V4 hypervariable region. Samples sequenced at Argonne National Laboratories used Earth Microbiome Project barcoded primer set 515F/806R and samples sequenced at Laragen used primer set 515F 5'-GTGYCAGCMGCCGCGGTAA/926R 5'-

CCGYCAATTYMTTTRAGTTT (Chapter 1). Due to sampling constraints, a subset of incubations was extracted and sequenced as described in the supplement (Supp. Table 4). Data was demultiplexed and put through a QIIME2 (v2019.7) pipeline with denoised ASV abundances generated using DADA2 (Bolyen et al., 2019; Callahan et al., 2016). Taxonomy classification was done using a classifier trained on the SILVA SSU database release 138 (Quast et al., 2013; Yilmaz et al., 2014). Samples with fewer than 15 reads were removed from the analysis. All R analyses were done using R Statistical Software (version 4.0.3). The decontam and phyloseq R packages were used for decontamination and handling of 16S data; the vegan package was used for alpha diversity (Chao1, Inverse Simpson) and dissimilarity analyses (Davis et al., 2018; McMurdie & Holmes, 2013; Oksanen et al., 2020). NMDS analyses were done using the lowest stress transformation; for the one-month time point this was a fourth-root transform, while for three- and seven-month time points this was a presence-absence transformation. All 16S rRNA gene sequencing analyses except for the Chao1 diversity analysis were done on genus-agglomerated data.

Metagenomic sequence analysis

Libraries for metagenomic sequencing were made using one replicate of the first two time points with the Nextera XT kit and quality control done with the TapeStation 4200 HSDNA D1000 screen tape as described in Chapter 1.

Methyl coenzyme reductase genes (*mcrA*) were mined from unassembled metagenomes using a previously described protocol (Speth & Orphan, 2018) and a manually curated

database derived from GTDB release 202 as described in Chapter 1. Mined *mcrA* reads were assigned a taxonomy based on a 95% identity to the reference amino acid sequence. A phylogenetic tree was then constructed using the reference McrA sequences with IQTREE model LG+I+G4, bootstrapped 100 times (Minh et al., 2020). Trees were visualized with iTOL (Letunic & Bork, 2021).

Metagenomic reads were then coassembled with Plass (Steinegger et al., 2019) and contigs greater than 100 amino acids in length kept. Coassemblies were made by combining dilutions at each time point and electron acceptor/donor pair. Assemblies were then clustered using MMseqs (Steinegger & Söding, 2017) and annotated using a custom HMM database for chitin and GlcNAc metabolic genes. Metagenome reads were then aligned to the annotated Plass assemblies with PALADIN (Westbrook et al., 2017) and gene relative abundances calculated normalized against read counts for housekeeping genes. Effective gene diversity was calculated from these gene relative abundances with the formula $e^{Shannon}$.

ACKNOWLEDGMENTS

We thank S. Connon (Caltech) and the Argonne National Laboratory Environmental Sample Preparation and Sequencing Facility for their assistance with 16S rRNA gene amplicon sequencing. We also thank L. Lu (MIT) and R. Szabo (MIT) in the O. Cordero group (MIT) for DNA extraction and metagenomic sequence analysis assistance. This work was supported by the Simons Foundation – Principles in Microbial Ecology (PriME) collaboration.

SUPPLEMENTAL TABLES

Supplemental Table 1. Adonis metric describing the contribution (R^2) show a small but significant contribution of each listed factor (electron acceptor or electron donor) to community dissimilarity. Formula: e^- acceptor * e^- donor. df, degrees of freedom. p, p-value. Statistically significant contribution ($p<0.05$) are in bold.

	1 month (fourth root)			**3 months (presence-absence)**			**7 months (presence-absence)**		
	df	**R^2**	p	df	**R^2**	p	df	R^2	p
e^- acceptor	3	**0.0426**	**0.001**	3	*0.0065*	*0.974*	1	**0.0364**	**0.001**
e^- donor	1	**0.0356**	**0.001**	1	**0.0358**	**0.001**	1	**0.0191**	**0.001**
e^- acceptor: e^- donor	3	**0.0322**	**0.017**	3	*0.0075*	*0.931*	1	**0.0203**	**0.001**
residuals	277			112			173		

Supplemental Table 2. Tukey's HSD comparison of mean Chao1 between electron acceptor/electron donor pairs at 3 months. diff, difference in mean Chao1. lwr and upr, lower and upper bounds of 95% confidence interval. p_{adj}, adjusted p-value. Statistically significant differences in Chao1 are in bold.

	diff	**lwr**	**upr**	**p_{adj}**
none:chitin-Fe:chitin	7.28043	-10.949	25.5098	0.92555
SO_4:chitin-Fe:chitin	**27.0193**	**9.16354**	**44.8751**	**0.00016**
NO_3:chitin-Fe:chitin	**40.549**	**22.5534**	**58.5447**	**0**
none:chitin-NO_3:chitin	**-33.269**	**-48.571**	**-17.966**	**0**
SO_4:chitin-none:chitin	**19.7389**	**4.60092**	**34.8769**	**0.0022**
SO_4:chitin-NO_3:chitin	-13.53	-28.385	1.32606	0.10388
NO_3:GlcNAc-Fe:GlcNAc	**24.3611**	**7.59352**	**41.1287**	**0.00035**
none:GlcNAc-Fe:GlcNAc	-13.821	-32.439	4.79646	0.31552
SO_4:GlcNAc-Fe:GlcNAc	-15.114	-33.012	2.78515	0.1681
none:GlcNAc-NO_3:GlcNAc	**-38.183**	**-54.95**	**-21.415**	**0**
SO_4:GlcNAc-none:GlcNAc	-1.2922	-19.191	16.6066	1
SO_4:GlcNAc-NO_3:GlcNAc	**-39.475**	**-55.44**	**-23.509**	**0**

Supplemental table 3. Sample table for major ions analysis; number of replicates run at each dilution, time point, and electron acceptor/donor pair

	no e- acceptor/chitin				**no e- acceptor/GlcNAc**				**no e- acceptor/no e- donor**		
dilution	1 month	3 months	7 months		1 month	3 months	7 months		1 month	3 months	7 months
$5x10^{-4}$	6	0	0		6	0	0		6	0	0
$5x10^{-5}$	12	4	4		12	4	4		6	4	4
$5x10^{-6}$	12	4	4		12	4	4		6	4	4
$5x10^{-7}$	12	4	4		12	4	4		6	4	4
$5x10^{-8}$	6	4	4		12	4	4		6	4	4
	sulfate/chitin				**sulfate/GlcNAc**				**sulfate/no e- donor**		
dilution	1 month	3 months	7 months		1 month	3 months	7 months		1 month	3 months	7 months
$5x10^{-4}$	0	0	0		0	0	0		0	0	0
$5x10^{-5}$	12	12	12		12	12	12		0	12	12
$5x10^{-6}$	12	12	12		12	9	12		0	12	12
$5x10^{-7}$	12	12	12		10	11	12		0	12	12
$5x10^{-8}$	4	4	4		12	4	4		0	4	4
	iron (III)/chitin				**iron (III)/GlcNAc**				**iron (III)/no e- donor**		
dilution	1 month	3 months	7 months		1 month	3 months	7 months		1 month	3 months	7 months
$5x10^{-4}$	8	12	12		8	12	12		8	12	12
$5x10^{-5}$	8	10	12		8	12	12		8	12	12
$5x10^{-6}$	8	12	12		8	12	12		8	12	12
$5x10^{-7}$	8	12	12		8	12	12		8	12	12
$5x10^{-8}$	0	0	0		0	0	0		0	0	0
	nitrate/chitin				**nitrate/GlcNAc**				**nitrate/no e- donor**		
dilution	1 month	3 months	7 months		1 month	3 months	7 months		1 month	3 months	7 months
$5x10^{-4}$	0	7	4		11	8	4		0	0	4
$5x10^{-5}$	0	12	4		12	12	4		0	4	4
$5x10^{-6}$	0	12	4		12	12	4		0	4	4
$5x10^{-7}$	0	6	4		6	6	4		0	4	4
$5x10^{-8}$	0	4	0		0	0	0		0	4	0

Supplemental Table 4. Sample table for 16S rRNA gene amplicon sequencing; number of replicates run at each dilution, time point, and electron acceptor/donor pair

	no e- acceptor/chitin				**no e- acceptor/GlcNAc**				**no e- acceptor/no e- donor**		
dilution	1 month	3 months	7 months		1 month	3 months	7 months		1 month	3 months	7 months
$5x10^{-4}$	1	10	0		1	11	0		1	0	0
$5x10^{-5}$	1	9	0		1	8	0		1	1	0
$5x10^{-6}$	1	10	0		1	3	0		1	1	0
$5x10^{-7}$	1	10	0		1	6	0		1	1	0
$5x10^{-8}$	1	1	0		1	0	0		1	0	0
	sulfate/chitin				**sulfate/GlcNAc**				**sulfate/no e- donor**		
dilution	1 month	3 months	7 months		1 month	3 months	7 months		1 month	3 months	7 months
$5x10^{-4}$	1	1	0		1	0	0		1	1	0
$5x10^{-5}$	12	11	11		12	9	11		6	6	5
$5x10^{-6}$	12	11	11		11	8	11		6	5	5
$5x10^{-7}$	12	11	11		12	7	11		6	6	5
$5x10^{-8}$	12	11	11		12	9	12		6	6	3
	iron (III)/chitin				**iron (III)/GlcNAc**				**iron (III)/no e- donor**		
dilution	1 month	3 months	7 months		1 month	3 months	7 months		1 month	3 months	7 months
$5x10^{-4}$	1	5	0		1	6	0		1	1	0
$5x10^{-5}$	0	8	0		1	5	0		1	1	0
$5x10^{-6}$	1	4	0		1	9	0		1	1	0
$5x10^{-7}$	0	6	0		1	7	0		1	1	0
$5x10^{-8}$	0	0	0		1	1	0		1	1	0
	nitrate/chitin				**nitrate/GlcNAc**				**nitrate/no e- donor**		
dilution	1 month	3 months	7 months		1 month	3 months	7 months		1 month	3 months	7 months
$5x10^{-4}$	1	0	11		1	1	11		1	1	0
$5x10^{-5}$	1	10	11		0	11	11		1	1	0
$5x10^{-6}$	1	11	11		0	11	11		0	1	0
$5x10^{-7}$	0	11	11		0	11	11		1	1	0

LIST AND DESCRIPTION OF SUPPLEMENTAL FILES

geochem_w_activity_alleacc.txt: All geochemistry data used in the 96-well experiment series with column including activity thresholding.

REFERENCES

Akinyemi, T. S., Shao, N., & Whitman, W. B. (2019). Methanogenium. In *Bergey's Manual of Systematics of Archaea and Bacteria* (pp. 1–9). John Wiley & Sons, Ltd. https://doi.org/10.1002/9781118960608.gbm00507.pub2

Albert, S., Hedberg, P., Motwani, N. H., Sjöling, S., Winder, M., & Nascimento, F. J. A. (2021). Phytoplankton settling quality has a subtle but significant effect on sediment microeukaryotic and bacterial communities. *Scientific Reports*, *11*(1), Article 1. https://doi.org/10.1038/s41598-021-03303-x

Allison, S. D., & Martiny, J. B. H. (2008). Resistance, resilience, and redundancy in microbial communities. *Proceedings of the National Academy of Sciences*, *105*(supplement_1), 11512–11519. https://doi.org/10.1073/pnas.0801925105

Altschul, S. F., Gish, W., Miller, W., Myers, E. W., & Lipman, D. J. (1990). Basic local alignment search tool. *Journal of Molecular Biology*, *215*(3), 403–410. https://doi.org/10.1016/S0022-2836(05)80360-2

Aluwihare, L. I., Repeta, D. J., Pantoja, S., & Johnson, C. G. (2005). Two Chemically Distinct Pools of Organic Nitrogen Accumulate in the Ocean. *Science*, *308*(5724), 1007–1010. https://doi.org/10.1126/science.1108925

Arndt, S., Jørgensen, B. B., LaRowe, D. E., Middelburg, J. J., Pancost, R. D., & Regnier, P. (2013). Quantifying the degradation of organic matter in marine sediments: A review and synthesis. *Earth-Science Reviews*, *123*, 53–86. https://doi.org/10.1016/j.earscirev.2013.02.008

Arnosti, C., Jørgensen, B., Sagemann, J., & Thamdrup, B. (1998). Temperature dependence of microbial degradation of organic matter in marine sediments:polysaccharide hydrolysis, oxygen consumption, and sulfate reduction. *Marine Ecology Progress Series*, *165*, 59–70. https://doi.org/10.3354/meps165059

Arnosti, C., Wietz, M., Brinkhoff, T., Hehemann, J.-H., Probandt, D., Zeugner, L., & Amann, R. (2021). The Biogeochemistry of Marine Polysaccharides: Sources, Inventories, and Bacterial Drivers of the Carbohydrate Cycle. *Annual Review of Marine Science*, *13*(1), 81–108. https://doi.org/10.1146/annurev-marine-032020-012810

Arzayus, K. M., & Canuel, E. A. (2005). Organic matter degradation in sediments of the York River estuary: Effects of biological vs. physical mixing. *Geochimica et Cosmochimica Acta*, *69*(2), 455–464. https://doi.org/10.1016/j.gca.2004.06.029

Atwood, T. B., Witt, A., Mayorga, J., Hammill, E., & Sala, E. (2020). Global Patterns in Marine Sediment Carbon Stocks. *Frontiers in Marine Science*, *7*. https://www.frontiersin.org/articles/10.3389/fmars.2020.00165

Bader, G. D., & Hogue, C. W. (2003). An automated method for finding molecular complexes in large protein interaction networks. *BMC Bioinformatics*, *4*(1), 2. https://doi.org/10.1186/1471-2105-4-2

Baho, D. L., Peter, H., & Tranvik, L. J. (2012). Resistance and resilience of microbial communities – temporal and spatial insurance against perturbations. *Environmental Microbiology*, *14*(9), 2283–2292. https://doi.org/10.1111/j.1462-2920.2012.02754.x

Bak, F., & Widdel, F. (1986). Anaerobic degradation of indolic compounds by sulfate-reducing enrichment cultures, and description of Desulfobacterium indolicum gen. nov., sp. Nov. *Archives of Microbiology*, *146*(2), 170–176. https://doi.org/10.1007/BF00402346

Beier, S., & Bertilsson, S. (2013). Bacterial chitin degradation—Mechanisms and ecophysiological strategies. *Frontiers in Microbiology*, *4*(149), 1–12. https://doi.org/doi: 10.3389/fmicb.2013.00149

Bell, T., Newman, J. A., Silverman, B. W., Turner, S. L., & Lilley, A. K. (2005). The contribution of species richness and composition to bacterial services. *Nature*, *436*(7054), Article 7054. https://doi.org/10.1038/nature03891

Belley, R., & Snelgrove, P. V. R. (2017). The role of infaunal functional and species diversity in short-term response of contrasting benthic communities to an experimental food pulse. *Journal of Experimental Marine Biology and Ecology*, *491*, 38–50. https://doi.org/10.1016/j.jembe.2017.03.005

Bethke, C. M., Sanford, R. A., Kirk, M. F., Jin, Q., & Flynn, T. M. (2011). The thermodynamic ladder in geomicrobiology. *American Journal of Science*, *311*(3), 183–210. https://doi.org/10.2475/03.2011.01

Beulig, F., Røy, H., Glombitza, C., & Jørgensen, B. B. (2018). Control on rate and pathway of anaerobic organic carbon degradation in the seabed. *Proceedings of the National Academy of Sciences*, *115*(2), 367–372. https://doi.org/10.1073/pnas.1715789115

Bienhold, C., Boetius, A., & Ramette, A. (2012). The energy–diversity relationship of complex bacterial communities in Arctic deep-sea sediments. *The ISME Journal*, *6*(4), Article 4. https://doi.org/10.1038/ismej.2011.140

Blodau, C., & Knorr, K.-H. (2006). Experimental inflow of groundwater induces a "biogeochemical regime shift" in iron-rich and acidic sediments. *Journal of Geophysical Research: Biogeosciences*, *111*(G2). https://doi.org/10.1029/2006JG000165

Bochdansky, A., & Herndl, G. (1992). Ecology of amorphous aggregations (marine snow) in the Northern Adriatic Sea. V. Role of fecal pellets in marine snow. *Marine Ecology Progress Series*, *89*, 297–303. https://doi.org/10.3354/meps089297

Boetius, A., & Lochte, K. (1994). Regulation of microbial enzymatic degradation of organic matter in deep-sea sediments. *Marine Ecology Progress Series*, *104*, 299–307. https://doi.org/10.3354/meps104299

Boetius, A., & Wenzhöfer, F. (2013). Seafloor oxygen consumption fuelled by methane from cold seeps. *Nature Geoscience*, *6*(9), 725–734. https://doi.org/10.1038/ngeo1926

Bolyen, E., Rideout, J. R., Dillon, M. R., Bokulich, N. A., Abnet, C. C., Al-Ghalith, G. A., Alexander, H., Alm, E. J., Arumugam, M., Asnicar, F., Bai, Y., Bisanz, J. E., Bittinger, K., Brejnrod, A., Brislawn, C. J., Brown, C. T., Callahan, B. J., Caraballo-Rodríguez, A. M., Chase, J., … Caporaso, J. G. (2019). Reproducible, interactive, scalable and extensible microbiome data science using QIIME 2. *Nature Biotechnology*, *37*(8), Article 8. https://doi.org/10.1038/s41587-019-0209-9

Bonch-Osmolovskaya, E. A., & Kublanov, I. V. (2021). *Calditrichaceae*. In W. B. Whitman (Ed.), *Bergey's Manual of Systematics of Archaea and Bacteria* (1st ed., pp. 1–3). Wiley. https://doi.org/10.1002/9781118960608.fbm00368

Borges, A. V., Champenois, W., Gypens, N., Delille, B., & Harlay, J. (2016). Massive marine methane emissions from near-shore shallow coastal areas. *Scientific Reports*, *6*(1), Article 1. https://doi.org/10.1038/srep27908

Bowles, M. W., Mogollón, J. M., Kasten, S., Zabel, M., & Hinrichs, K.-U. (2014). Global rates of marine sulfate reduction and implications for sub–sea-floor metabolic activities. *Science*, *344*(6186), 889–891. https://doi.org/10.1126/science.1249213

Braby, C. E., Rouse, G. W., Johnson, S. B., Jones, W. J., & Vrijenhoek, R. C. (2007). Bathymetric and temporal variation among Osedax boneworms and associated megafauna on whale-falls in Monterey Bay, California. *Deep Sea Research Part I: Oceanographic Research Papers*, *54*(10), 1773–1791. https://doi.org/10.1016/j.dsr.2007.05.014

Brown, S., Lloyd, C. C., Giljan, G., Ghobrial, S., Amann, R., & Arnosti, C. (2024). Pulsed inputs of high molecular weight organic matter shift the mechanisms of substrate utilisation in marine bacterial communities. *Environmental Microbiology*, e16580. https://doi.org/10.1111/1462-2920.16580

Bryant, M. P. (1979). Microbial Methane Production—Theoretical Aspects. *Journal of Animal Science*, *48*(1), 193–201. https://doi.org/10.2527/jas1979.481193x

Buchfink, B., Xie, C., & Huson, D. H. (2015). Fast and sensitive protein alignment using DIAMOND. *Nature Methods*, *12*(1), Article 1. https://doi.org/10.1038/nmeth.3176

Burdige, D. J. (2007). Preservation of Organic Matter in Marine Sediments: Controls, Mechanisms, and an Imbalance in Sediment Organic Carbon Budgets? *Chemical Reviews*, *107*(2), 467–485. https://doi.org/10.1021/cr050347q

Caffrey, J. M., Hollibaugh, J., Bano, N., & Haskins, J. (2010). Effects of upwelling on short-term variability in microbial and biogeochemical processes in estuarine sediments from Elkhorn Slough, California, USA. *Aquatic Microbial Ecology*, *58*, 261–271. https://doi.org/10.3354/ame01387

Callahan, B. J., McMurdie, P. J., Rosen, M. J., Han, A. W., Johnson, A. J. A., & Holmes, S. P. (2016). DADA2: High-resolution sample inference from Illumina amplicon data. *Nature Methods*, *13*(7), Article 7. https://doi.org/10.1038/nmeth.3869

Canfield, D. E. (1989). Sulfate reduction and oxic respiration in marine sediments: Implications for organic carbon preservation in euxinic environments. *Deep Sea Research Part A. Oceanographic Research Papers*, *36*(1), 121–138. https://doi.org/10.1016/0198-0149(89)90022-8

Canfield, D. E. (1994). Factors influencing organic carbon preservation in marine sediments. *Chemical Geology*, *114*(3), 315–329. https://doi.org/10.1016/0009-2541(94)90061-2

Caporaso, J. G., Lauber, C. L., Walters, W. A., Berg-Lyons, D., Huntley, J., Fierer, N., Owens, S. M., Betley, J., Fraser, L., Bauer, M., Gormley, N., Gilbert, J. A., Smith, G., & Knight, R. (2012). Ultra-high-throughput microbial community analysis on the

Illumina HiSeq and MiSeq platforms. *The ISME Journal*, *6*(8), 1621–1624. https://doi.org/10.1038/ismej.2012.8

Case, D. H., Ijiri, A., Morono, Y., Tavormina, P., Orphan, V. J., & Inagaki, F. (2017). Aerobic and Anaerobic Methanotrophic Communities Associated with Methane Hydrates Exposed on the Seafloor: A High-Pressure Sampling and Stable Isotope-Incubation Experiment. *Frontiers in Microbiology*, *8*. https://doi.org/10.3389/fmicb.2017.02569

Chaer, G., Fernandes, M., Myrold, D., & Bottomley, P. (2009). Comparative Resistance and Resilience of Soil Microbial Communities and Enzyme Activities in Adjacent Native Forest and Agricultural Soils. *Microbial Ecology*, *58*(2), 414–424. https://doi.org/10.1007/s00248-009-9508-x

Chassard, C., Delmas, E., Robert, C., & Bernalier-Donadille, A. (2010). The cellulose-degrading microbial community of the human gut varies according to the presence or absence of methanogens. *FEMS Microbiology Ecology*, *74*(1), 205–213. https://doi.org/10.1111/j.1574-6941.2010.00941.x

Chen, I.-M. A., Chu, K., Palaniappan, K., Ratner, A., Huang, J., Huntemann, M., Hajek, P., Ritter, S., Varghese, N., Seshadri, R., Roux, S., Woyke, T., Eloe-Fadrosh, E. A., Ivanova, N. N., & Kyrpides, N. C. (2021). The IMG/M data management and analysis system v.6.0: New tools and advanced capabilities. *Nucleic Acids Research*, *49*(D1), D751–D763. https://doi.org/10.1093/nar/gkaa939

Chen, Q., Lønborg, C., Chen, F., Gonsior, M., Li, Y., Cai, R., He, C., Chen, J., Wang, Y., Shi, Q., Jiao, N., & Zheng, Q. (2022). Increased microbial and substrate complexity result in higher molecular diversity of the dissolved organic matter pool. *Limnology and Oceanography*, *67*(11), 2360–2373. https://doi.org/10.1002/lno.12206

Christensen, D. (1984). Determination of substrates oxidized by sulfate reduction in intact cores of marine sediments1. *Limnology and Oceanography*, *29*(1), 189–191. https://doi.org/10.4319/lo.1984.29.1.0189

Cifuentes, A., Antón, J., Benlloch, S., Donnelly, A., Herbert, R. A., & Rodríguez-Valera, F. (2000). Prokaryotic Diversity in Zostera noltii-Colonized Marine Sediments. *Applied and Environmental Microbiology*, *66*(4), 1715–1719. https://doi.org/10.1128/AEM.66.4.1715-1719.2000

Clarke, K. R. (1993). Non-parametric multivariate analyses of changes in community structure. *Australian Journal of Ecology*, *18*(1), 117–143. https://doi.org/10.1111/j.1442-9993.1993.tb00438.x

Csardi, G., & Nepusz, T. (2005). The Igraph Software Package for Complex Network Research. *InterJournal*, *Complex Systems*, 1695.

Dagg, M., Benner, R., Lohrenz, S., & Lawrence, D. (2004). Transformation of dissolved and particulate materials on continental shelves influenced by large rivers: Plume processes. *Continental Shelf Research*, *24*(7), 833–858. https://doi.org/10.1016/j.csr.2004.02.003

Davis, N. M., Proctor, D. M., Holmes, S. P., Relman, D. A., & Callahan, B. J. (2018). Simple statistical identification and removal of contaminant sequences in marker-gene and

metagenomics data. *Microbiome*, *6*(1), 226. https://doi.org/10.1186/s40168-018-0605-2

De Cáceres, M., & Legendre, P. (2009). Associations between species and groups of sites: Indices and statistical inference. *Ecology*, *90*(12), 3566–3574. https://doi.org/10.1890/08-1823.1

De Cáceres, M., Legendre, P., & Moretti, M. (2010). Improving indicator species analysis by combining groups of sites. *Oikos*, *119*(10), 1674–1684. https://doi.org/10.1111/j.1600-0706.2010.18334.x

DeAngelis, K. M., Silver, W. L., Thompson, A. W., & Firestone, M. K. (2010). Microbial communities acclimate to recurring changes in soil redox potential status. *Environmental Microbiology*, *12*(12), 3137–3149. https://doi.org/10.1111/j.1462-2920.2010.02286.x

Dick, J. M., Yu, M., Tan, J., & Lu, A. (2019). Changes in Carbon Oxidation State of Metagenomes Along Geochemical Redox Gradients. *Frontiers in Microbiology*, *10*. https://doi.org/10.3389/fmicb.2019.00120

Durkin, C. A., Mock, T., & Armbrust, E. V. (2009). Chitin in Diatoms and Its Association with the Cell Wall. *Eukaryotic Cell*, *8*(7), 1038–1050. https://doi.org/10.1128/EC.00079-09

Eddy, S. R. (1998). Profile hidden Markov models. *Bioinformatics (Oxford, England)*, *14*(9), 755–763. https://doi.org/10.1093/bioinformatics/14.9.755

Eddy, S. R. (2011). Accelerated Profile HMM Searches. *PLOS Computational Biology*, *7*(10), e1002195. https://doi.org/10.1371/journal.pcbi.1002195

Edgar, R. C. (2004). MUSCLE: A multiple sequence alignment method with reduced time and space complexity. *BMC Bioinformatics*, *5*(1), 113. https://doi.org/10.1186/1471-2105-5-113

Edgar, R. C. (2010). Search and clustering orders of magnitude faster than BLAST. *Bioinformatics*, *26*(19), 2460–2461. https://doi.org/10.1093/bioinformatics/btq461

Edwards, K. J., McCollom, T. M., Konishi, H., & Buseck, P. R. (2003). Seafloor bioalteration of sulfide minerals: Results from in situ incubation studies. *Geochimica et Cosmochimica Acta*, *67*(15), 2843–2856. https://doi.org/10.1016/S0016-7037(03)00089-9

Embree, M., Liu, J. K., Al-Bassam, M. M., & Zengler, K. (2015). Networks of energetic and metabolic interactions define dynamics in microbial communities. *Proceedings of the National Academy of Sciences*, *112*(50), 15450–15455. https://doi.org/10.1073/pnas.1506034112

Enke, T. N., Datta, M. S., Schwartzman, J., Cermak, N., Schmitz, D., Barrere, J., Pascual-García, A., & Cordero, O. X. (2019). Modular Assembly of Polysaccharide-Degrading Marine Microbial Communities. *Current Biology*. https://doi.org/10.1016/j.cub.2019.03.047

Fdz-Polanco, F., Fdz-Polanco, M., Fernández, N., Urueña, M. A., García, P. A., & Villaverde, S. (2001). Combining the biological nitrogen and sulfur cycles in

anaerobic conditions. *Water Science and Technology*, *44*(8), 77–84. https://doi.org/10.2166/wst.2001.0469

Fierer, N., & Lennon, J. T. (2011). The generation and maintenance of diversity in microbial communities. *American Journal of Botany*, *98*(3), 439–448. https://doi.org/10.3732/ajb.1000498

Findlay, R., Trexler, M., Guckert, J., & White, D. (1990). Laboratory study of disturbance in marine sediments: Response of a microbial community. *Marine Ecology Progress Series*, *62*, 121–133. https://doi.org/10.3354/meps062121

Finke, D. L., & Snyder, W. E. (2008). Niche Partitioning Increases Resource Exploitation by Diverse Communities. *Science*, *321*(5895), 1488–1490. https://doi.org/10.1126/science.1160854

Friedman, J., Higgins, L. M., & Gore, J. (2017). Community structure follows simple assembly rules in microbial microcosms. *Nature Ecology & Evolution*, *1*(5). https://doi.org/10.1038/s41559-017-0109

Froelich, P. N., Klinkhammer, G. P., Bender, M. L., Luedtke, N. A., Heath, G. R., Cullen, D., Dauphin, P., Hammond, D., Hartman, B., & Maynard, V. (1979). Early oxidation of organic matter in pelagic sediments of the eastern equatorial Atlantic: Suboxic diagenesis. *Geochimica et Cosmochimica Acta*, *43*(7), 1075–1090. https://doi.org/10.1016/0016-7037(79)90095-4

Fuhrman, J. A. (2009). Microbial community structure and its functional implications. *Nature*, *459*(7244), Article 7244. https://doi.org/10.1038/nature08058

Galushko, A., & Kuever, J. (2020). Desulfogranum gen. nov. In *Bergey's Manual of Systematics of Archaea and Bacteria* (pp. 1–5). John Wiley & Sons, Ltd. https://doi.org/10.1002/9781118960608.gbm01873

Girvan, M. S., Campbell, C. D., Killham, K., Prosser, J. I., & Glover, L. A. (2005). Bacterial diversity promotes community stability and functional resilience after perturbation. *Environmental Microbiology*, *7*(3), 301–313. https://doi.org/10.1111/j.1462-2920.2005.00695.x

Glombitza, C., Adhikari, R. R., Riedinger, N., Gilhooly, W. P., Hinrichs, K.-U., & Inagaki, F. (2016). Microbial Sulfate Reduction Potential in Coal-Bearing Sediments Down to ~2.5 km below the Seafloor off Shimokita Peninsula, Japan. *Frontiers in Microbiology*, *7*. https://www.frontiersin.org/articles/10.3389/fmicb.2016.01576

Goffredi, S. K., & Orphan, V. J. (2010). Bacterial community shifts in taxa and diversity in response to localized organic loading in the deep sea. *Environmental Microbiology*, *12*(2), 344–363. https://doi.org/10.1111/j.1462-2920.2009.02072.x

Goffredi, S. K., Orphan, V. J., Rouse, G. W., Jahnke, L., Embaye, T., Turk, K., Lee, R., & Vrijenhoek, R. C. (2005). Evolutionary innovation: A bone-eating marine symbiosis. *Environmental Microbiology*, *7*(9), 1369–1378. https://doi.org/10.1111/j.1462-2920.2005.00824.x

Goffredi, S. K., Wilpiszeski, R., Lee, R., & Orphan, V. J. (2008). Temporal evolution of methane cycling and phylogenetic diversity of archaea in sediments from a deep-sea

whale-fall in Monterey Canyon, California. *The ISME Journal*, *2*(2), 204–220. https://doi.org/10.1038/ismej.2007.103

Goldford, J. E., Lu, N., Bajić, D., Estrela, S., Tikhonov, M., Sanchez-Gorostiaga, A., Segrè, D., Mehta, P., & Sanchez, A. (2018). Emergent simplicity in microbial community assembly. *Science (New York, N.Y.)*, *361*(6401), 469–474. https://doi.org/10.1126/science.aat1168

Gooday, G. W. (1990). The Ecology of Chitin Degradation. In K. C. Marshall (Ed.), *Advances in Microbial Ecology* (pp. 387–430). Springer US. https://doi.org/10.1007/978-1-4684-7612-5_10

Graw, M. F., D'Angelo, G., Borchers, M., Thurber, A. R., Johnson, J. E., Zhang, C., Liu, H., & Colwell, F. S. (2018). Energy Gradients Structure Microbial Communities Across Sediment Horizons in Deep Marine Sediments of the South China Sea. *Frontiers in Microbiology*, *9*. https://doi.org/10.3389/fmicb.2018.00729

Green-Saxena, A., Dekas, A. E., Dalleska, N. F., & Orphan, V. J. (2014). Nitrate-based niche differentiation by distinct sulfate-reducing bacteria involved in the anaerobic oxidation of methane. *The ISME Journal*, *8*(1), 150–163. https://doi.org/10.1038/ismej.2013.147

Griffiths, B. S., & Philippot, L. (2013). Insights into the resistance and resilience of the soil microbial community. *FEMS Microbiology Reviews*, *37*(2), 112–129. https://doi.org/10.1111/j.1574-6976.2012.00343.x

Haffert, L., Haeckel, M., de Stigter, H., & Janssen, F. (2020). Assessing the temporal scale of deep-sea mining impacts on sediment biogeochemistry. *Biogeosciences*, *17*(10), 2767–2789. https://doi.org/10.5194/bg-17-2767-2020

Harcombe, W. R., Riehl, W. J., Dukovski, I., Granger, B. R., Betts, A., Lang, A. H., Bonilla, G., Kar, A., Leiby, N., Mehta, P., Marx, C. J., & Segrè, D. (2014). Metabolic Resource Allocation in Individual Microbes Determines Ecosystem Interactions and Spatial Dynamics. *Cell Reports*, *7*(4), 1104–1115. https://doi.org/10.1016/j.celrep.2014.03.070

Harwood, C. S., & Canale-Parola, E. (1983). Spirochaeta isovalerica sp. Nov., a Marine Anaerobe That Forms Branched-Chain Fatty Acids as Fermentation Products. *International Journal of Systematic and Evolutionary Microbiology*, *33*(3), 573–579. https://doi.org/10.1099/00207713-33-3-573

Hatzenpichler, R., & Orphan, V. J. (2015). Detection of Protein-Synthesizing Microorganisms in the Environment via Bioorthogonal Noncanonical Amino Acid Tagging (BONCAT). In T. J. McGenity, K. N. Timmis, & B. Nogales (Eds.), *Hydrocarbon and Lipid Microbiology Protocols: Single-Cell and Single-Molecule Methods* (pp. 145–157). Springer. https://doi.org/10.1007/8623_2015_61

Hausmann, B., Knorr, K.-H., Schreck, K., Tringe, S. G., Glavina del Rio, T., Loy, A., & Pester, M. (2016). Consortia of low-abundance bacteria drive sulfate reduction-dependent degradation of fermentation products in peat soil microcosms. *The ISME Journal*, *10*(10), Article 10. https://doi.org/10.1038/ismej.2016.42

Hedges, J. I., Eglinton, G., Hatcher, P. G., Kirchman, D. L., Arnosti, C., Derenne, S., Evershed, R. P., Kögel-Knabner, I., de Leeuw, J. W., Littke, R., Michaelis, W., & Rullkötter, J. (2000). The molecularly-uncharacterized component of nonliving organic matter in natural environments. *Organic Geochemistry*, *31*(10), 945–958. https://doi.org/10.1016/S0146-6380(00)00096-6

Hedges, J. I., & Keil, R. G. (1995). Sedimentary organic matter preservation: An assessment and speculative synthesis. *Marine Chemistry*, *49*(2), 81–115. https://doi.org/10.1016/0304-4203(95)00008-F

Hoehler, T. M., Alperin, M. J., Albert, D. B., & Martens, C. S. (1998). Thermodynamic control on hydrogen concentrations in anoxic sediments. *Geochimica et Cosmochimica Acta*, *62*(10), 1745–1756. https://doi.org/10.1016/S0016-7037(98)00106-9

Hoffmann, K., Hassenrück, C., Salman-Carvalho, V., Holtappels, M., & Bienhold, C. (2017). Response of Bacterial Communities to Different Detritus Compositions in Arctic Deep-Sea Sediments. *Frontiers in Microbiology*, *8*, 266. https://doi.org/10.3389/fmicb.2017.00266

Howe, K. L., Seitz, K. W., Campbell, L. G., Baker, B. J., Thrash, J. C., Rabalais, N. N., Rogener, M.-K., Joye, S. B., & Mason, O. U. (2023). Metagenomics and metatranscriptomics reveal broadly distributed, active, novel methanotrophs in the Gulf of Mexico hypoxic zone and in the marine water column. *FEMS Microbiology Ecology*, *99*(2), fiac153. https://doi.org/10.1093/femsec/fiac153

Isaksen, M. F., & Teske, A. (1996). Desulforhopalus vacuolatus gen. nov., sp. Nov., a new moderately psychrophilic sulfate-reducing bacterium with gas vacuoles isolated from a temperate estuary. *Archives of Microbiology*, *166*(3), 160–168. https://doi.org/10.1007/s002030050371

Jia, M., Winkler, M. K. H., & Volcke, E. I. P. (2020). Elucidating the Competition between Heterotrophic Denitrification and DNRA Using the Resource-Ratio Theory. *Environmental Science & Technology*, *54*(21), 13953–13962. https://doi.org/10.1021/acs.est.0c01776

Jiang, W.-X., Li, P.-Y., Chen, X.-L., Zhang, Y.-S., Wang, J.-P., Wang, Y.-J., Sheng, Q., Sun, Z.-Z., Qin, Q.-L., Ren, X.-B., Wang, P., Song, X.-Y., Chen, Y., & Zhang, Y.-Z. (2022). A pathway for chitin oxidation in marine bacteria. *Nature Communications*, *13*(1), Article 1. https://doi.org/10.1038/s41467-022-33566-5

Jochum, L. M., Chen, X., Lever, M. A., Loy, A., Jørgensen, B. B., Schramm, A., & Kjeldsen, K. U. (2017). Depth Distribution and Assembly of Sulfate-Reducing Microbial Communities in Marine Sediments of Aarhus Bay. *Applied and Environmental Microbiology*, *83*(23), e01547-17. https://doi.org/10.1128/AEM.01547-17

Jones, S. E., Chiu, C.-Y., Kratz, T. K., Wu, J.-T., Shade, A., & McMahon, K. D. (2008). Typhoons initiate predictable change in aquatic bacterial communities. *Limnology and Oceanography*, *53*(4), 1319–1326. https://doi.org/10.4319/lo.2008.53.4.1319

Jørgensen, B. B. (1982). Mineralization of organic matter in the sea bed—The role of sulphate reduction. *Nature*, *296*(5858), Article 5858. https://doi.org/10.1038/296643a0

Jousset, A., Bienhold, C., Chatzinotas, A., Gallien, L., Gobet, A., Kurm, V., Küsel, K., Rillig, M. C., Rivett, D. W., Salles, J. F., van der Heijden, M. G. A., Youssef, N. H., Zhang, X., Wei, Z., & Hol, W. H. G. (2017). Where less may be more: How the rare biosphere pulls ecosystems strings. *The ISME Journal*, *11*(4), Article 4. https://doi.org/10.1038/ismej.2016.174

Kallscheuer, N., Jogler, M., Wiegand, S., Peeters, S. H., Heuer, A., Boedeker, C., Jetten, M. S. M., Rohde, M., & Jogler, C. (2020). Three novel Rubripirellula species isolated from plastic particles submerged in the Baltic Sea and the estuary of the river Warnow in northern Germany. *Antonie van Leeuwenhoek*, *113*(12), 1767–1778. https://doi.org/10.1007/s10482-019-01368-3

Kanzog, C., & Ramette, A. (2009). Microbial colonisation of artificial and deep-sea sediments in the Arctic Ocean. *Marine Ecology*, *30*(4), 391–404. https://doi.org/10.1111/j.1439-0485.2009.00290.x

Kanzog, C., Ramette, A., Quéric, N. V., & Klages, M. (2008). Response of benthic microbial communities to chitin enrichment: An in situ study in the deep Arctic Ocean. *Polar Biology*, *32*(1), 105. https://doi.org/10.1007/s00300-008-0510-4

Kerr, B., Riley, M. A., Feldman, M. W., & Bohannan, B. J. M. (2002). Local dispersal promotes biodiversity in a real-life game of rock–paper–scissors. *Nature*, *418*(6894), Article 6894. https://doi.org/10.1038/nature00823

Kleindienst, S., Ramette, A., Amann, R., & Knittel, K. (2012). Distribution and in situ abundance of sulfate-reducing bacteria in diverse marine hydrocarbon seep sediments. *Environmental Microbiology*, *14*(10), 2689–2710. https://doi.org/10.1111/j.1462-2920.2012.02832.x

Klouche, N., Fardeau, M.-L., Lascourrèges, J.-F., Cayol, J.-L., Hacene, H., Thomas, P., & Magot, M. (2007). Geosporobacter subterraneus gen. nov., sp. Nov., a spore-forming bacterium isolated from a deep subsurface aquifer. *International Journal of Systematic and Evolutionary Microbiology*, *57*(8), 1757–1761. https://doi.org/10.1099/ijs.0.64642-0

Köchy, M., Hiederer, R., & Freibauer, A. (2015). Global distribution of soil organic carbon – Part 1: Masses and frequency distributions of SOC stocks for the tropics, permafrost regions, wetlands, and the world. *SOIL*, *1*(1), 351–365. https://doi.org/10.5194/soil-1-351-2015

Kondrotaite, Z., Valk, L. C., Petriglieri, F., Singleton, C., Nierychlo, M., Dueholm, M. K. D., & Nielsen, P. H. (2022). Diversity and Ecophysiology of the Genus OLB8 and Other Abundant Uncultured Saprospiraceae Genera in Global Wastewater Treatment Systems. *Frontiers in Microbiology*, *13*, 917553. https://doi.org/10.3389/fmicb.2022.917553

Könneke, M., Kuever, J., Galushko, A., & Jørgensen, B. B. (2013). Desulfoconvexum algidum gen. nov., sp. Nov., a psychrophilic sulfate-reducing bacterium isolated from

a permanently cold marine sediment. *International Journal of Systematic and Evolutionary Microbiology*, *63*(Pt_3), 959–964. https://doi.org/10.1099/ijs.0.043703-0

Konopka, A., Lindemann, S., & Fredrickson, J. (2015). Dynamics in microbial communities: Unraveling mechanisms to identify principles. *The ISME Journal*, *9*(7), Article 7. https://doi.org/10.1038/ismej.2014.251

Koster, I. W., & Lettinga, G. (1984). The influence of ammonium-nitrogen on the specific activity of pelletized methanogenic sludge. *Agricultural Wastes*, *9*(3), 205–216. https://doi.org/10.1016/0141-4607(84)90080-5

Kubo, K., Lloyd, K. G., F Biddle, J., Amann, R., Teske, A., & Knittel, K. (2012). Archaea of the Miscellaneous Crenarchaeotal Group are abundant, diverse and widespread in marine sediments. *The ISME Journal*, *6*(10), Article 10. https://doi.org/10.1038/ismej.2012.37

Kurm, V., Geisen, S., & Gera Hol, W. H. (2019). A low proportion of rare bacterial taxa responds to abiotic changes compared with dominant taxa. *Environmental Microbiology*, *21*(2), 750–758. https://doi.org/10.1111/1462-2920.14492

Kurtz, J. C., Devereux, R., Barkay, T., & Jonas, R. B. (1998). Evaluation of sediment slurry microcosms for modeling microbial communities in estuarine sediments. *Environmental Toxicology and Chemistry*, *17*(7), 1274–1281. https://doi.org/10.1002/etc.5620170712

LaRowe, D. E., Arndt, S., Bradley, J. A., Estes, E. R., Hoarfrost, A., Lang, S. Q., Lloyd, K. G., Mahmoudi, N., Orsi, W. D., Shah Walter, S. R., Steen, A. D., & Zhao, R. (2020). The fate of organic carbon in marine sediments—New insights from recent data and analysis. *Earth-Science Reviews*, *204*, 103146. https://doi.org/10.1016/j.earscirev.2020.103146

LaRowe, D. E., & Van Cappellen, P. (2011). Degradation of natural organic matter: A thermodynamic analysis. *Geochimica et Cosmochimica Acta*, *75*(8), 2030–2042. https://doi.org/10.1016/j.gca.2011.01.020

Le Moigne, A., Randegger, F., Gupta, A., Petchey, O. L., & Pernthaler, J. (2023). Stochasticity causes high β-diversity and functional divergence of bacterial assemblages in closed systems. *Ecology*, *104*(4), e4005. https://doi.org/10.1002/ecy.4005

Lee, S.-H., Sorensen, J. W., Grady, K. L., Tobin, T. C., & Shade, A. (2017). Divergent extremes but convergent recovery of bacterial and archaeal soil communities to an ongoing subterranean coal mine fire. *The ISME Journal*, *11*(6), Article 6. https://doi.org/10.1038/ismej.2017.1

Lee, S.-Y., Lee, M.-H., Oh, T.-K., & Yoon, J.-H. (2012). Lutibacter aestuarii sp. Nov., isolated from a tidal flat sediment, and emended description of the genus Lutibacter Choi and Cho 2006. *International Journal of Systematic and Evolutionary Microbiology*, *62*(2), 420–424. https://doi.org/10.1099/ijs.0.030320-0

Leloup, J., Fossing, H., Kohls, K., Holmkvist, L., Borowski, C., & Jørgensen, B. B. (2009). Sulfate-reducing bacteria in marine sediment (Aarhus Bay, Denmark): Abundance

and diversity related to geochemical zonation. *Environmental Microbiology*, *11*(5), 1278–1291. https://doi.org/10.1111/j.1462-2920.2008.01855.x

Lennon, J. T., & Jones, S. E. (2011). Microbial seed banks: The ecological and evolutionary implications of dormancy. *Nature Reviews Microbiology*, *9*(2), Article 2. https://doi.org/10.1038/nrmicro2504

Letunic, I., & Bork, P. (2021). Interactive Tree Of Life (iTOL) v5: An online tool for phylogenetic tree display and annotation. *Nucleic Acids Research*, *49*(W1), W293–W296. https://doi.org/10.1093/nar/gkab301

L'Haridon, S., Chalopin, M., Colombo, D., & Toffin, L. (2014). Methanococcoides vulcani sp. Nov., a marine methylotrophic methanogen that uses betaine, choline and N,N-dimethylethanolamine for methanogenesis, isolated from a mud volcano, and emended description of the genus Methanococcoides. *International Journal of Systematic and Evolutionary Microbiology*, *64*(Pt_6), 1978–1983. https://doi.org/10.1099/ijs.0.058289-0

Liu, X., Sutter, J. L., de la Cuesta-Zuluaga, J., Waters, J. L., Youngblut, N. D., & Ley, R. E. (2021). Reclassification of Catabacter hongkongensis as Christensenella hongkongensis comb. Nov. Based on whole genome analysis. *International Journal of Systematic and Evolutionary Microbiology*, *71*(4), 004774. https://doi.org/10.1099/ijsem.0.004774

Losey, N. A., Stevenson, B. S., Busse, H.-J., Damsté, J. S. S., Rijpstra, W. I. C., Rudd, S., & Lawson, P. A. (2013). Thermoanaerobaculum aquaticum gen. nov., sp. Nov., the first cultivated member of Acidobacteria subdivision 23, isolated from a hot spring. *International Journal of Systematic and Evolutionary Microbiology*, *63*(Pt_11), 4149–4157. https://doi.org/10.1099/ijs.0.051425-0

Louca, S., Polz, M. F., Mazel, F., Albright, M. B. N., Huber, J. A., O'Connor, M. I., Ackermann, M., Hahn, A. S., Srivastava, D. S., Crowe, S. A., Doebeli, M., & Parfrey, L. W. (2018). Function and functional redundancy in microbial systems. *Nature Ecology & Evolution*, *2*(6), 936–943. https://doi.org/10.1038/s41559-018-0519-1

Lovley, D. R., & Phillips, E. J. P. (1987). Competitive Mechanisms for Inhibition of Sulfate Reduction and Methane Production in the Zone of Ferric Iron Reduction in Sediments. *Applied and Environmental Microbiology*, *53*(11), 2636–2641. https://doi.org/10.1128/aem.53.11.2636-2641.1987

Lundsten, L., Schlining, K. L., Frasier, K., Johnson, S. B., Kuhnz, L. A., Harvey, J. B. J., Clague, G., & Vrijenhoek, R. C. (2010). Time-series analysis of six whale-fall communities in Monterey Canyon, California, USA. *Deep Sea Research Part I: Oceanographic Research Papers*, *57*(12), 1573–1584. https://doi.org/10.1016/j.dsr.2010.09.003

Lynch, M. D. J., & Neufeld, J. D. (2015). Ecology and exploration of the rare biosphere. *Nature Reviews Microbiology*, *13*(4), Article 4. https://doi.org/10.1038/nrmicro3400

Marsland, R., III, Cui, W., Goldford, J., Sanchez, A., Korolev, K., & Mehta, P. (2019). Available energy fluxes drive a transition in the diversity, stability, and functional

structure of microbial communities. *PLOS Computational Biology*, *15*(2), e1006793. https://doi.org/10.1371/journal.pcbi.1006793

Mason, O. U., Scott, N. M., Gonzalez, A., Robbins-Pianka, A., Bælum, J., Kimbrel, J., Bouskill, N. J., Prestat, E., Borglin, S., Joyner, D. C., Fortney, J. L., Jurelevicius, D., Stringfellow, W. T., Alvarez-Cohen, L., Hazen, T. C., Knight, R., Gilbert, J. A., & Jansson, J. K. (2014). Metagenomics reveals sediment microbial community response to Deepwater Horizon oil spill. *The ISME Journal*, *8*(7), 1464–1475. https://doi.org/10.1038/ismej.2013.254

Matthews, A., Majeed, A., Barraclough, T. G., & Raymond, B. (2021). Function is a better predictor of plant rhizosphere community membership than 16S phylogeny. *Environmental Microbiology*, *23*(10), 6089–6103. https://doi.org/10.1111/1462-2920.15652

McClure, R., Naylor, D., Farris, Y., Davison, M., Fansler, S. J., Hofmockel, K. S., & Jansson, J. K. (2020). Development and Analysis of a Stable, Reduced Complexity Model Soil Microbiome. *Frontiers in Microbiology*, *11*. https://www.frontiersin.org/article/10.3389/fmicb.2020.01987

McDaniel, E. A., Scarborough, M., Mulat, D. G., Lin, X., Sampara, P. S., Olson, H. M., Young, R. P., Eder, E. K., Attah, I. K., Markillie, L. M., Hoyt, D. W., Lipton, M. S., Hallam, S. J., & Ziels, R. M. (2023). Diverse electron carriers drive syntrophic interactions in an enriched anaerobic acetate-oxidizing consortium. *The ISME Journal*, *17*(12), 2326–2339. https://doi.org/10.1038/s41396-023-01542-6

McMurdie, P. J., & Holmes, S. (2013). phyloseq: An R Package for Reproducible Interactive Analysis and Graphics of Microbiome Census Data. *PLOS ONE*, *8*(4), e61217. https://doi.org/10.1371/journal.pone.0061217

Milke, F., Wagner-Doebler, I., Wienhausen, G., & Simon, M. (2022). Selection, drift and community interactions shape microbial biogeographic patterns in the Pacific Ocean. *The ISME Journal*, *16*(12), Article 12. https://doi.org/10.1038/s41396-022-01318-4

Minh, B. Q., Schmidt, H. A., Chernomor, O., Schrempf, D., Woodhams, M. D., von Haeseler, A., & Lanfear, R. (2020). IQ-TREE 2: New Models and Efficient Methods for Phylogenetic Inference in the Genomic Era. *Molecular Biology and Evolution*, *37*(5), 1530–1534. https://doi.org/10.1093/molbev/msaa015

Moodley, L., Middelburg, J., Boschker, H., Duineveld, G., Pel, R., Herman, P., & Heip, C. (2002). Bacteria and Foraminifera: Key players in a short-term deep-sea benthic response to phytodetritus. *Marine Ecology Progress Series*, *236*, 23–29. https://doi.org/10.3354/meps236023

Mountfort, D. O., Rainey, F. A., Burghardt, J., Kaspar, H. F., & Stackebrandt, E. (1998). Psychromonas antarcticus gen. nov., sp. Nov., a new aerotolerant anaerobic, halophilic psychrophile isolated from pond sediment of the McMurdo Ice Shelf, Antarctica. *Archives of Microbiology*, *169*(3), 231–238. https://doi.org/10.1007/s002030050566

Na, H., Kim, S., Moon, E. Y., & Chun, J. (2009). Marinifilum fragile gen. nov., sp. Nov., isolated from tidal flat sediment. *International Journal of Systematic and*

Evolutionary Microbiology, *59*(9), 2241–2246. https://doi.org/10.1099/ijs.0.009027-0

Nobu, M. K., Narihiro, T., Kuroda, K., Mei, R., & Liu, W.-T. (2016). Chasing the elusive Euryarchaeota class WSA2: Genomes reveal a uniquely fastidious methyl-reducing methanogen. *The ISME Journal*, *10*(10), Article 10. https://doi.org/10.1038/ismej.2016.33

Nogales, B., Lanfranconi, M. P., Piña-Villalonga, J. M., & Bosch, R. (2011). Anthropogenic perturbations in marine microbial communities. *FEMS Microbiology Reviews*, *35*(2), 275–298. https://doi.org/10.1111/j.1574-6976.2010.00248.x

Oksanen, J., Blanchet, F. G., Friendly, M., Kindt, R., Pierre Legendre, Dan McGlinn, Peter R. Minchin, R. B. O'Hara, Gavin L. Simpson, Peter Solymos, M. Henry H. Stevens, Eduard Szoecs, & Helene Wagner. (2020). *vegan: Community Ecology Package* (2.5-7) [Computer software]. https://CRAN.R-project.org/package=vegan

Oremland, R. S., & Polcin, S. (1982). Methanogenesis and Sulfate Reduction: Competitive and Noncompetitive Substrates in Estuarine Sediments. *Applied and Environmental Microbiology*, *44*(6), 1270–1276. https://doi.org/10.1128/aem.44.6.1270-1276.1982

Osawa, R., & Koga, T. (1995). An investigation of aquatic bacteria capable of utilizing chitin as the sole source of nutrients. *Letters in Applied Microbiology*, *21*(5), 288–291. https://doi.org/10.1111/j.1472-765X.1995.tb01062.x

Park, S., Choi, J., Park, J.-M., & Yoon, J.-H. (2018). Aestuariimonas insulae gen. nov., sp. Nov., isolated from a tidal flat. *International Journal of Systematic and Evolutionary Microbiology*, *68*(4), 1365–1371. https://doi.org/10.1099/ijsem.0.002684

Pascoal, F., Costa, R., & Magalhães, C. (2021). The microbial rare biosphere: Current concepts, methods and ecological principles. *FEMS Microbiology Ecology*, *97*(1), fiaa227. https://doi.org/10.1093/femsec/fiaa227

Pel, R., & Gottschal, J. C. (1989). Interspecies interaction based on transfer of a thioredoxin-like compound in anaerobic chitin-degrading mixed cultures. *FEMS Microbiology Letters*, *62*(6), 349–357. https://doi.org/10.1111/j.1574-6968.1989.tb03390.x

Pelikan, C., Wasmund, K., Glombitza, C., Hausmann, B., Herbold, C. W., Flieder, M., & Loy, A. (2021). Anaerobic bacterial degradation of protein and lipid macromolecules in subarctic marine sediment. *The ISME Journal*, *15*(3), 833–847. https://doi.org/10.1038/s41396-020-00817-6

Pérez Castro, S., Borton, M. A., Regan, K., Hrabe de Angelis, I., Wrighton, K. C., Teske, A. P., Strous, M., & Ruff, S. E. (2021). Degradation of biological macromolecules supports uncultured microbial populations in Guaymas Basin hydrothermal sediments. *The ISME Journal*, *15*(12), 3480–3497. https://doi.org/10.1038/s41396-021-01026-5

Pester, M., Bittner, N., Deevong, P., Wagner, M., & Loy, A. (2010). A 'rare biosphere' microorganism contributes to sulfate reduction in a peatland. *The ISME Journal*, *4*(12), Article 12. https://doi.org/10.1038/ismej.2010.75

Peter, H., Beier, S., Bertilsson, S., Lindström, E. S., Langenheder, S., & Tranvik, L. J. (2011). Function-specific response to depletion of microbial diversity. *The ISME Journal*, *5*(2), Article 2. https://doi.org/10.1038/ismej.2010.119

Petriglieri, F., Kondrotaite, Z., Singleton, C., Nierychlo, M., Dueholm, M. K. D., & Nielsen, P. H. (2023). A comprehensive overview of the Chloroflexota community in wastewater treatment plants worldwide. *mSystems*, *8*(6), e00667-23. https://doi.org/10.1128/msystems.00667-23

Philippot, L., Griffiths, B. S., & Langenheder, S. (2021). Microbial Community Resilience across Ecosystems and Multiple Disturbances. *Microbiology and Molecular Biology Reviews*, *85*(2), 10.1128/mmbr.00026-20. https://doi.org/10.1128/mmbr.00026-20

Poulicek, M., & Jeuniaux, C. (1991). Chitin biodegradation in marine environments: An experimental approach. *Biochemical Systematics and Ecology*, *19*(5), 385–394. https://doi.org/10.1016/0305-1978(91)90055-5

Probandt, D., Eickhorst, T., Ellrott, A., Amann, R., & Knittel, K. (2018). Microbial life on a sand grain: From bulk sediment to single grains. *The ISME Journal*, *12*(2), 623–633. https://doi.org/10.1038/ismej.2017.197

Quast, C., Pruesse, E., Yilmaz, P., Gerken, J., Schweer, T., Yarza, P., Peplies, J., & Glöckner, F. O. (2013). The SILVA ribosomal RNA gene database project: Improved data processing and web-based tools. *Nucleic Acids Research*, *41*(D1), D590–D596. https://doi.org/10.1093/nar/gks1219

Reader, H. E., Thoms, F., Voss, M., & Stedmon, C. A. (2019). The Influence of Sediment-Derived Dissolved Organic Matter in the Vistula River Estuary/Gulf of Gdansk. *Journal of Geophysical Research: Biogeosciences*, *124*(1), 115–126. https://doi.org/10.1029/2018JG004658

Roden, E. E., & Wetzel, R. G. (2003). Competition between Fe(III)-Reducing and Methanogenic Bacteria for Acetate in Iron-Rich Freshwater Sediments. *Microbial Ecology*, *45*(3), 252–258. https://doi.org/10.1007/s00248-002-1037-9

Rodrigues, C., Núñez-Gómez, D., Silveira, D. D., Lapolli, F. R., & Lobo-Recio, M. A. (2019). Chitin as a substrate for the biostimulation of sulfate-reducing bacteria in the treatment of mine-impacted water (MIW). *Journal of Hazardous Materials*. https://doi.org/10.1016/j.jhazmat.2019.02.086

Rojas, C. A., De Santiago Torio, A., Park, S., Bosak, T., & Klepac-Ceraj, V. (2021). Organic Electron Donors and Terminal Electron Acceptors Structure Anaerobic Microbial Communities and Interactions in a Permanently Stratified Sulfidic Lake. *Frontiers in Microbiology*, *12*. https://www.frontiersin.org/article/10.3389/fmicb.2021.620424

Romesser, J. A., Wolfe, R. S., Mayer, F., Spiess, E., & Walther-Mauruschat, A. (1979). Methanogenium, a new genus of marine methanogenic bacteria, and characterization ofMethanogenium cariaci sp. Nov. andMethanogenium marisnigri sp. Nov. *Archives of Microbiology*, *121*(2), 147–153. https://doi.org/10.1007/BF00689979

Sahm, K., MacGregor, B. J., Jorgensen, B. B., & Stahl, D. A. (1999). Sulphate reduction and vertical distribution of sulphate-reducing bacteria quantified by rRNA slot-blot

hybridization in a coastal marine sediment. *Environmental Microbiology*, *1*(1), 65–74. https://doi.org/10.1046/j.1462-2920.1999.00007.x

Sass, A., Rütters, H., Cypionka, H., & Sass, H. (2002). Desulfobulbus mediterraneus sp. Nov., a sulfate-reducing bacterium growing on mono- and disaccharides. *Archives of Microbiology*, *177*(6), 468–474. https://doi.org/10.1007/s00203-002-0415-5

Schink, B. (1997). Energetics of Syntrophic Cooperation in Methanogenic Degradation. *MICROBIOL. MOL. BIOL. REV.*, *61*, 19.

Schnürer, A., Zellner, G., & Svensson, B. H. (1999). Mesophilic syntrophic acetate oxidation during methane formation in biogas reactors. *FEMS Microbiology Ecology*, *29*(3), 249–261. https://doi.org/10.1111/j.1574-6941.1999.tb00616.x

Shade, A. (2017). Diversity is the question, not the answer. *The ISME Journal*, *11*(1), 1–6. https://doi.org/10.1038/ismej.2016.118

Shade, A. (2018). Understanding Microbiome Stability in a Changing World. *mSystems*, *3*(2), e00157-17. https://doi.org/10.1128/mSystems.00157-17

Shade, A., Peter, H., Allison, S., Baho, D., Berga, M., Buergmann, H., Huber, D., Langenheder, S., Lennon, J., Martiny, J., Matulich, K., Schmidt, T., & Handelsman, J. (2012). Fundamentals of Microbial Community Resistance and Resilience. *Frontiers in Microbiology*, *3*. https://www.frontiersin.org/articles/10.3389/fmicb.2012.00417

Shade, A., Read, J. S., Youngblut, N. D., Fierer, N., Knight, R., Kratz, T. K., Lottig, N. R., Roden, E. E., Stanley, E. H., Stombaugh, J., Whitaker, R. J., Wu, C. H., & McMahon, K. D. (2012). Lake microbial communities are resilient after a whole-ecosystem disturbance. *The ISME Journal*, *6*(12), Article 12. https://doi.org/10.1038/ismej.2012.56

Shaffer, J. P., Nothias, L.-F., Thompson, L. R., Sanders, J. G., Salido, R. A., Couvillion, S. P., Brejnrod, A. D., Lejzerowicz, F., Haiminen, N., Huang, S., Lutz, H. L., Zhu, Q., Martino, C., Morton, J. T., Karthikeyan, S., Nothias-Esposito, M., Dührkop, K., Böcker, S., Kim, H. W., … Knight, R. (2022). Standardized multi-omics of Earth's microbiomes reveals microbial and metabolite diversity. *Nature Microbiology*, *7*(12), Article 12. https://doi.org/10.1038/s41564-022-01266-x

Shannon, P., Markiel, A., Ozier, O., Baliga, N. S., Wang, J. T., Ramage, D., Amin, N., Schwikowski, B., & Ideker, T. (2003). Cytoscape: A Software Environment for Integrated Models of Biomolecular Interaction Networks. *Genome Research*, *13*(11), 2498–2504. https://doi.org/10.1101/gr.1239303

Smith, C., Bernardino, A., Baco, A., Hannides, A., & Altamira, I. (2014). Seven-year enrichment: Macrofaunal succession in deep-sea sediments around a 30 tonne whale fall in the Northeast Pacific. *Marine Ecology Progress Series*, *515*, 133–149. https://doi.org/10.3354/meps10955

Smith, C. R., & Baco, A. R. (2003). Ecology of whale falls at the deep-sea floor. *Oceanography and Marine Biology: An Annual Review*, *41*, 311–354.

Sogin, M. L., Morrison, H. G., Huber, J. A., Welch, D. M., Huse, S. M., Neal, P. R., Arrieta, J. M., & Herndl, G. J. (2006). Microbial diversity in the deep sea and the

underexplored “rare biosphere.” *Proceedings of the National Academy of Sciences of the United States of America*, *103*(32), 12115–12120. https://doi.org/10.1073/pnas.0605127103

Sorokin, D. Y., Makarova, K. S., Abbas, B., Ferrer, M., Golyshin, P. N., Galinski, E. A., Ciordia, S., Mena, M. C., Merkel, A. Y., Wolf, Y. I., van Loosdrecht, M. C. M., & Koonin, E. V. (2017). Discovery of extremely halophilic, methyl-reducing euryarchaea provides insights into the evolutionary origin of methanogenesis. *Nature Microbiology*, *2*(8). https://doi.org/10.1038/nmicrobiol.2017.81

Souza, C. P., Almeida, B. C., Colwell, R. R., & Rivera, I. N. G. (2011). The Importance of Chitin in the Marine Environment. *Marine Biotechnology*, *13*(5), 823–830. https://doi.org/10.1007/s10126-011-9388-1

Speth, D. R., & Orphan, V. J. (2018). Metabolic marker gene mining provides insight in global mcrA diversity and, coupled with targeted genome reconstruction, sheds further light on metabolic potential of the Methanomassiliicoccales. *PeerJ*, *6*, e5614. https://doi.org/10.7717/peerj.5614

Speth, D. R., Yu, F. B., Connon, S. A., Lim, S., Magyar, J. S., Peña-Salinas, M. E., Quake, S. R., & Orphan, V. J. (2022). Microbial communities of Auka hydrothermal sediments shed light on vent biogeography and the evolutionary history of thermophily. *The ISME Journal*, 1–15. https://doi.org/10.1038/s41396-022-01222-x

Sprott, G. D., & Patel, G. B. (1986). Ammonia toxicity in pure cultures of methanogenic bacteria. *Systematic and Applied Microbiology*, *7*(2), 358–363. https://doi.org/10.1016/S0723-2020(86)80034-0

St. Pierre, K. A., Hunt, B. P. V., Giesbrecht, I. J. W., Tank, S. E., Lertzman, K. P., Del Bel Belluz, J., Hessing-Lewis, M. L., Olson, A., & Froese, T. (2022). Seasonally and Spatially Variable Organic Matter Contributions From Watershed, Marine Macrophyte, and Pelagic Sources to the Northeast Pacific Coastal Ocean Margin. *Frontiers in Marine Science*, *9*. https://www.frontiersin.org/articles/10.3389/fmars.2022.863209

Staley, J. T., & Konopka, A. (1985). Measurement of in Situ Activities of Nonphotosynthetic Microorganisms in Aquatic and Terrestrial Habitats. *Annual Review of Microbiology*, *39*(1), 321–346. https://doi.org/10.1146/annurev.mi.39.100185.001541

Steinegger, M., Mirdita, M., & Söding, J. (2019). Protein-level assembly increases protein sequence recovery from metagenomic samples manyfold. *Nature Methods*, *16*(7), Article 7. https://doi.org/10.1038/s41592-019-0437-4

Steinegger, M., & Söding, J. (2017). MMseqs2 enables sensitive protein sequence searching for the analysis of massive data sets. *Nature Biotechnology*, *35*(11), Article 11. https://doi.org/10.1038/nbt.3988

Stookey, L. L. (1970). Ferrozine—A new spectrophotometric reagent for iron. *Analytical Chemistry*, *42*(7), 779–781. https://doi.org/10.1021/ac60289a016

Szabo, R. E., Pontrelli, S., Grilli, J., Schwartzman, J. A., Pollak, S., Sauer, U., & Cordero, O. X. (2022). Historical contingencies and phage induction diversify bacterioplankton

communities at the microscale. *Proceedings of the National Academy of Sciences*, *119*(30), e2117748119. https://doi.org/10.1073/pnas.2117748119

Szeinbaum, N., Lin, H., Brandes, J. A., Taillefert, M., Glass, J. B., & DiChristina, T. J. (2017). Microbial manganese(III) reduction fuelled by anaerobic acetate oxidation. *Environmental Microbiology*, *19*(9), 3475–3486. https://doi.org/10.1111/1462-2920.13829

Talling, P. J., Hage, S., Baker, M. L., Bianchi, T. S., Hilton, R. G., & Maier, K. L. (2024). The Global Turbidity Current Pump and Its Implications for Organic Carbon Cycling. *Annual Review of Marine Science*, *16*(Volume 16, 2024), 105–133. https://doi.org/10.1146/annurev-marine-032223-103626

Thompson, L. R., Sanders, J. G., McDonald, D., Amir, A., Ladau, J., Locey, K. J., Prill, R. J., Tripathi, A., Gibbons, S. M., Ackermann, G., Navas-Molina, J. A., Janssen, S., Kopylova, E., Vázquez-Baeza, Y., González, A., Morton, J. T., Mirarab, S., Zech Xu, Z., Jiang, L., … Knight, R. (2017). A communal catalogue reveals Earth's multiscale microbial diversity. *Nature*, *551*(7681), Article 7681. https://doi.org/10.1038/nature24621

Tully, B. J., Wheat, C. G., Glazer, B. T., & Huber, J. A. (2018). A dynamic microbial community with high functional redundancy inhabits the cold, oxic subseafloor aquifer. *The ISME Journal*, *12*(1), 1–16. https://doi.org/10.1038/ismej.2017.187

Turkarslan, S., Raman, A. V., Thompson, A. W., Arens, C. E., Gillespie, M. A., von Netzer, F., Hillesland, K. L., Stolyar, S., López García de Lomana, A., Reiss, D. J., Gorman-Lewis, D., Zane, G. M., Ranish, J. A., Wall, J. D., Stahl, D. A., & Baliga, N. S. (2017). Mechanism for microbial population collapse in a fluctuating resource environment. *Molecular Systems Biology*, *13*(3), 919. https://doi.org/10.15252/msb.20167058

van den Berg, E. M., Boleij, M., Kuenen, J. G., Kleerebezem, R., & van Loosdrecht, M. C. M. (2016). DNRA and Denitrification Coexist over a Broad Range of Acetate/N-NO3− Ratios, in a Chemostat Enrichment Culture. *Frontiers in Microbiology*, *7*. https://www.frontiersin.org/journals/microbiology/articles/10.3389/fmicb.2016.01842

van den Berg, E. M., Elisário, M. P., Kuenen, J. G., Kleerebezem, R., & van Loosdrecht, M. C. M. (2017). Fermentative Bacteria Influence the Competition between Denitrifiers and DNRA Bacteria. *Frontiers in Microbiology*, *8*. https://www.frontiersin.org/journals/microbiology/articles/10.3389/fmicb.2017.01684

Van Vliet, D. M., Lin, Y., Bale, N. J., Koenen, M., Villanueva, L., Stams, A. J. M., & Sánchez-Andrea, I. (2020). Pontiella desulfatans gen. nov., sp. Nov., and Pontiella sulfatireligans sp. Nov., Two Marine Anaerobes of the Pontiellaceae fam. Nov. Producing Sulfated Glycosaminoglycan-like Exopolymers. *Microorganisms*, *8*(6), 920. https://doi.org/10.3390/microorganisms8060920

Vellend, M. (2010). Conceptual Synthesis in Community Ecology. *The Quarterly Review of Biology*, *85*(2), 183–206. https://doi.org/10.1086/652373

Wagner, M., Loy, A., Klein, M., Lee, N., Ramsing, N. B., Stahl, D. A., & Friedrich, M. W. (2005). Functional Marker Genes for Identification of Sulfate-Reducing Prokaryotes. In *Methods in Enzymology* (Vol. 397, pp. 469–489). Academic Press. https://doi.org/10.1016/S0076-6879(05)97029-8

Watts, S. C., Ritchie, S. C., Inouye, M., & Holt, K. E. (2019). FastSpar: Rapid and scalable correlation estimation for compositional data. *Bioinformatics*, *35*(6), 1064–1066. https://doi.org/10.1093/bioinformatics/bty734

Westbrook, A., Ramsdell, J., Schuelke, T., Normington, L., Bergeron, R. D., Thomas, W. K., & MacManes, M. D. (2017). PALADIN: Protein alignment for functional profiling whole metagenome shotgun data. *Bioinformatics*, *33*(10), 1473–1478. https://doi.org/10.1093/bioinformatics/btx021

Wirsen, C. O., & Jannasch, H. W. (1986). Microbial transformations in deep-sea sediments: Free-vehicle studies. *Marine Biology*, *91*(2), 277–284. https://doi.org/10.1007/BF00569444

Wisnoski, N. I., & Lennon, J. T. (2021). Stabilising role of seed banks and the maintenance of bacterial diversity. *Ecology Letters*, *24*(11), 2328–2338. https://doi.org/10.1111/ele.13853

Witte, U., Aberle, N., Sand, M., & Wenzhöfer, F. (2003). Rapid response of a deep-sea benthic community to POM enrichment: An in situ experimental study. *Marine Ecology Progress Series*, *251*, 27–36. https://doi.org/10.3354/meps251027

Wörner, S., & Pester, M. (2019). Microbial Succession of Anaerobic Chitin Degradation in Freshwater Sediments. *Applied and Environmental Microbiology*, *85*(18), e00963-19. https://doi.org/10.1128/AEM.00963-19

Wunder, L. C., Aromokeye, D. A., Yin, X., Richter-Heitmann, T., Willis-Poratti, G., Schnakenberg, A., Otersen, C., Dohrmann, I., Römer, M., Bohrmann, G., Kasten, S., & Friedrich, M. W. (2021). Iron and sulfate reduction structure microbial communities in (sub-)Antarctic sediments. *The ISME Journal*, *15*(12), Article 12. https://doi.org/10.1038/s41396-021-01014-9

Xu, S., Bu, J., Li, C., Tiong, Y. W., Sharma, P., Liu, K., Jin, C., Ma, C., & Tong, Y. W. (2024). Biochar enhanced methane yield on anaerobic digestion of shell waste and the synergistic effects of anaerobic co-digestion of shell and food waste. *Fuel*, *357*, 129933. https://doi.org/10.1016/j.fuel.2023.129933

Xun, W., Liu, Y., Li, W., Ren, Y., Xiong, W., Xu, Z., Zhang, N., Miao, Y., Shen, Q., & Zhang, R. (2021). Specialized metabolic functions of keystone taxa sustain soil microbiome stability. *Microbiome*, *9*(1), 35. https://doi.org/10.1186/s40168-020-00985-9

Yang, S.-H., Seo, H.-S., Woo, J.-H., Oh, H.-M., Jang, H., Lee, J.-H., Kim, S.-J., & Kwon, K. K. (2014). Carboxylicivirga gen. nov. In the family Marinilabiliaceae with two novel species, Carboxylicivirga mesophila sp. Nov. And Carboxylicivirga taeanensis sp. Nov., and reclassification of Cytophaga fermentans as Saccharicrinis fermentans gen. nov., comb. Nov. *International Journal of Systematic and Evolutionary Microbiology*, *64*(Pt_4), 1351–1358. https://doi.org/10.1099/ijs.0.053462-0

Yilmaz, P., Parfrey, L. W., Yarza, P., Gerken, J., Pruesse, E., Quast, C., Schweer, T., Peplies, J., Ludwig, W., & Glöckner, F. O. (2014). The SILVA and "All-species Living Tree Project (LTP)" taxonomic frameworks. *Nucleic Acids Research*, *42*(D1), D643–D648. https://doi.org/10.1093/nar/gkt1209

Yücel, M. (2013). Down the thermodynamic ladder: A comparative study of marine redox gradients across diverse sedimentary environments. *Estuarine, Coastal and Shelf Science*, *131*, 83–92. https://doi.org/10.1016/j.ecss.2013.07.013

Zakem, E. J., Mahadevan, A., Lauderdale, J. M., & Follows, M. J. (2020). Stable aerobic and anaerobic coexistence in anoxic marine zones. *The ISME Journal*, *14*(1), Article 1. https://doi.org/10.1038/s41396-019-0523-8

Zhang, C., Song, Z., Zhuang, D., Wang, J., Xie, S., & Liu, G. (2019). Urea fertilization decreases soil bacterial diversity, but improves microbial biomass, respiration, and N-cycling potential in a semiarid grassland. *Biology and Fertility of Soils*, *55*(3), 229–242. https://doi.org/10.1007/s00374-019-01344-z

Zhang, Y., Wang, X., Zhen, Y., Mi, T., He, H., & Yu, Z. (2017). Microbial Diversity and Community Structure of Sulfate-Reducing and Sulfur-Oxidizing Bacteria in Sediment Cores from the East China Sea. *Frontiers in Microbiology*, *8*. https://www.frontiersin.org/articles/10.3389/fmicb.2017.02133